



저작자표시-비영리-변경금지 2.0 대한민국

이용자는 아래의 조건을 따르는 경우에 한하여 자유롭게

- 이 저작물을 복제, 배포, 전송, 전시, 공연 및 방송할 수 있습니다.

다음과 같은 조건을 따라야 합니다:



저작자표시. 귀하는 원저작자를 표시하여야 합니다.



비영리. 귀하는 이 저작물을 영리 목적으로 이용할 수 없습니다.



변경금지. 귀하는 이 저작물을 개작, 변형 또는 가공할 수 없습니다.

- 귀하는, 이 저작물의 재이용이나 배포의 경우, 이 저작물에 적용된 이용허락조건을 명확하게 나타내어야 합니다.
- 저작권자로부터 별도의 허가를 받으면 이러한 조건들은 적용되지 않습니다.

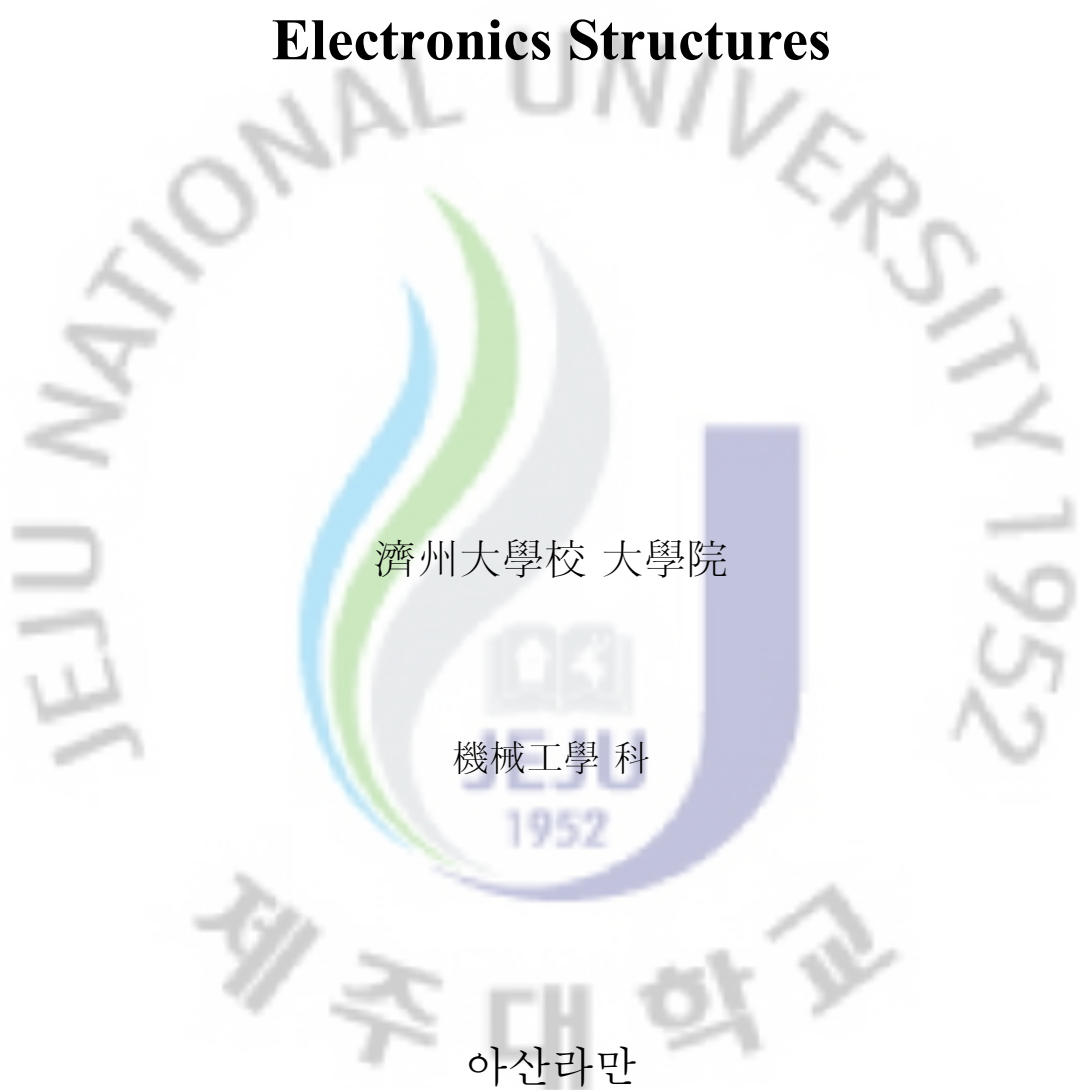
저작권법에 따른 이용자의 권리는 위의 내용에 의하여 영향을 받지 않습니다.

이것은 [이용허락규약\(Legal Code\)](#)을 이해하기 쉽게 요약한 것입니다.

[Disclaimer](#)

博士學位論文

**Development of Non-Contact Universal  
Platform Printing Technology for Micro-  
Electronics Structures**



濟州大學校 大學院

機械工學科

1952

아산라만

2011 年 2 月

# Development of Non-Contact Universal Platform Printing Technology for Micro-Electronics Structures

指導教授 최경현

아산라만

이 論文을 工學博士學位 論文으로 提出함

2011 年 2 月

아산라만의 工學博士學位 論文을 認准함

審査委員長

권기린



委員

배진호



委員

정동원



委員

조정래



委員

최경현



濟州大學校 大學院

2011 年 2 月

# Development of Non-Contact Universal Platform Printing Technology for Micro-Electronics Structures

Ahsan Rahman

(Supervised by Professor Kyunghyun Choi)

A thesis submitted in partial fulfillment of the requirement for the  
degree of Doctor of Philosophy

2011. 2

The thesis has been examined and approved.



Thesis Director, Kirin Kwon,

Professor, Jeju National University



Thesis Committee Member, Jinho Bae,

Professor, Jeju National University



Thesis Committee Member, Dongwon Jung,

Professor, Jeju National University



Thesis Committee Member, Dr. Jeongdai Jo, Korea Institute of Machinery and Materials

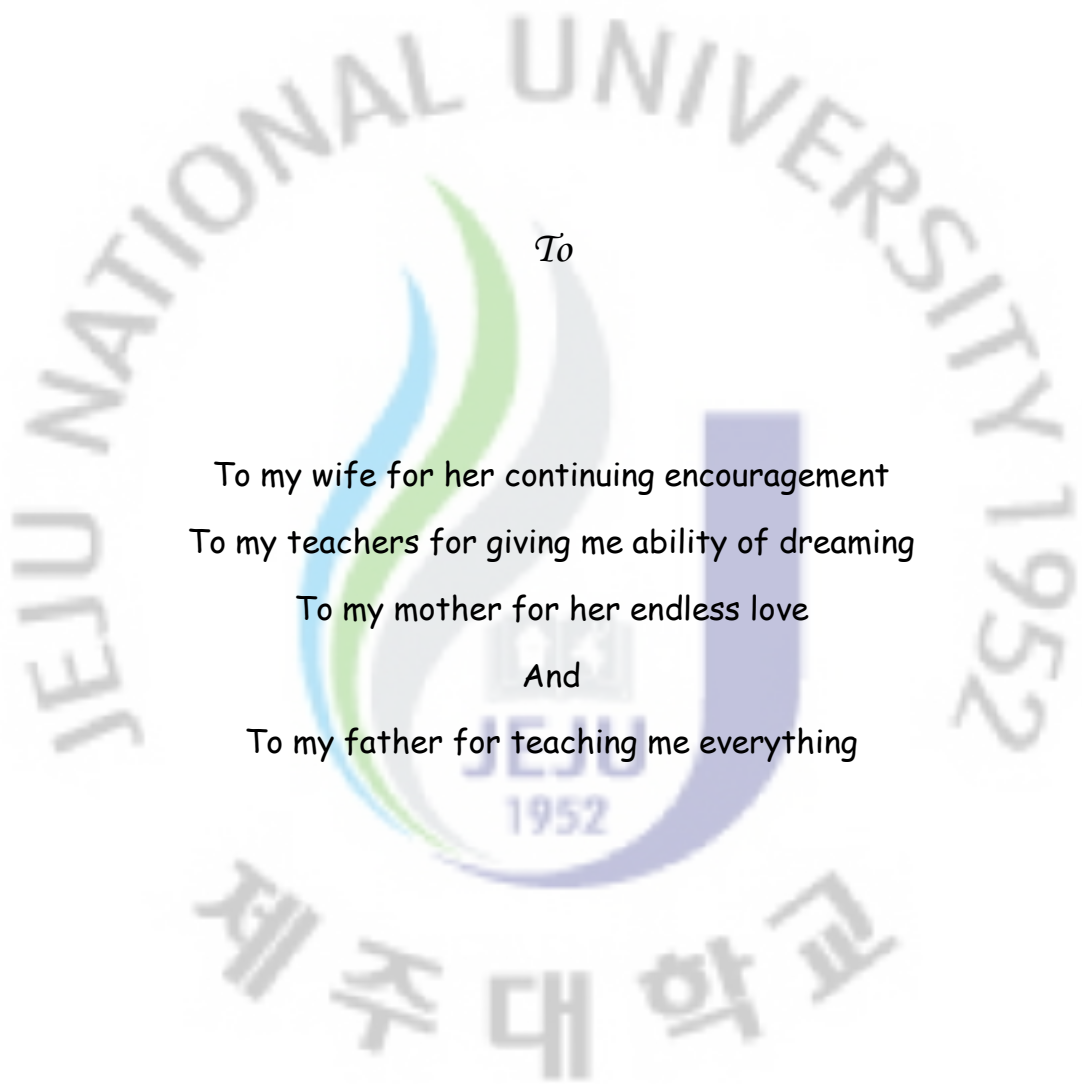


Thesis Committee Member, Kyunghyun Choi, Professor, Jeju National University

February, 2011

Date

**Department of Mechanical and System Engineering**  
**GRADUATE SCHOOL**  
**JEJU NATIONAL UNIVERSITY**  
**REPUBLIC OF KOREA**



*To*

To my wife for her continuing encouragement

To my teachers for giving me ability of dreaming

To my mother for her endless love

And

To my father for teaching me everything

## Acknowledgements

Shukar Alhamdulillah.

The work with this dissertation has been extensive and trying, but in the first place exciting, instructive, and fun. While working on doctorate, I had the pleasure of interacting with number of individuals from different professional and social backgrounds. All of them have one thing common: they have contributed constructively, directly, indirectly, to the manner in which my research as well as personality evolved. I got here because somebody - a parent, a teacher - bent down and helped me pick up my boots. It is a pleasant aspect that I have now the opportunity to express my gratitude for all of them.

Professor Choi, Kyung Hyun: Sir Issac Newton once said “If I have seen further it is only by standing on the shoulders of giants”. His conclusion is valid in my case too, as I was able to see further than I otherwise would have, by standing the shoulder of my supervisor Professor Choi, Kyung Hyun. I am thankful to you for your invaluable scientific inputs, and the entertaining chitchats on history and current affairs. I will surely miss our discussions o a wide range of topics. In spite of your high standing in academia, your down to earth demeanor and amiable personality even in the face of difficulties will be something I will always remember and try to emulate. Especially, providing me latest equipment to work on cutting edge technology and extracting the best out of me by allowing me to demonstrate my capabilities. I would also like to thank your wife whose affectionate support to my wife and kid were immeasurable.

Dissertation Committee: I would also like to thank my thesis committee Professor, Kirin Kwon, Professor Jinho Bae, Professor Dongwon Jung and Dr. Jeongdai Jo, Professor Kyunghyun Choi, for your guidance throughout the dissertation process.

AMM colleagues: Thanks are due to my all project mates at Advance Micro Mechatronics lab, Jeju. I have been fortunate enough to have had the support of so many people in the research group without them this thesis would not have been possible – Muhammad Asif Ali Rehmani, Khalid Rahman, Malik Nauman, Adnan Ali, Saleem Khan, Arshad Khan, Naeem Awais, Kim Chang Jong, Ko Jeong-beom,

Yang Bong Soo, Dang Hyun Hoo, Tran Trung Thanh, Lee Kyung Hyun, Kim Hyung Chan, Ganesh Thangaraj, Shridharan, Nguyeu minh and to our lab secretary Yoo Ji-Youne. I would like make a special mention of Khalid for insight in bridging research with industrial touch, and Nauman, Ko Jeong-beom and Yang Bong Soo for helping me out even in personal capacity.

Jeju Mates: Perhaps the most important outcome of my stay at Jeju National University is the number of friends I made. I am also thankful to the wonderful friends Ahmer Rashid & his family, Asif Ali & his family, Khalid & his family, Nauman & his family, Shafqat-ur-Rehman, Syed Murtaza Mehdi, Iskander, Shrikant and Dr. Anil who shared my high and lows of postgraduate studies. Especially, I am extremely grateful to Ahmer Rashid who not only introduced me to my supervisor for postgraduate studies but also paved my path in attaining the postgraduate studies. He was instrumental in guiding me to start my higher studies and helped me in settling down in Jeju. For want of space, I refrain from listing each and every one of them. But that does not diminish their importance by any means.

Family: My parents deserve a very special mention for all the hard work they have put in over the years, as well as for their support and confidence in me. I want to thank my father, who provided me motivation and supported me in my all edification career and my mother for her love and faith. I don't have words to thank you, but I love you lot Abu and Ami. I would also like to thank my brothers Zubair & Saqib and my sisters Sadaf, Dr. Saman, Irum & Sana who encouraged me throughout my studies and provided me the necessary moral support. Thank you all.

Afia Ahsan & Ajlal: Finally, I would like to pay my heartiest gratitude to my wife Afia who not only supported me throughout my postgraduate studies but also shared the responsibilities for taking care of my child when I was busy in my research. It is not an exaggeration to say that I would not have come to this far without her support, motivation, understanding, enthusiasm and love. And foremost, thank you Ajlal, the one who revive me, every day. But feel sorry for neglecting you during the course of my studies. I hope I will make up for the time you spent without me in future.

## Abbreviations and Notations

E	Electric field, V/m
I (t)	Current, A
$I_{\text{rms}}$	Current of root mean square, A
V(t)	Voltage, V
$V_{\text{rms}}$	Voltage of root mean square, V
t	Time, s
m	Mass of liquid, g/cm <sup>3</sup>
c	Damping coefficient, N.s/m
k	Spring constant, N/m
x	Liquid displacement, m
F(t)	Force, N
$f_c$	Oscillating frequency of liquid, Hz
$d_d$	Droplet diameter, m
Q	Flow rate, $\mu\text{l/hr}$
K	Conductivity of liquid, S/cm
Greek Symbols	
$\gamma$	Surface tension, N/m
$\epsilon_0$	Permittivity of free space, F/m
$\kappa$	Proportionality factor, 1/m
$\sigma_E$	Electrostatics stress, N/m <sup>2</sup>
$\sigma_\gamma$	Surface tension stress, N/m <sup>2</sup>
$\omega$	Frequency
$\theta$	Phase angle
$\rho$	Density of liquid, kg/m <sup>3</sup>
Subscript	
i, k	Variable numbers
rms	Root mean square



# Contents

요약-----	i
Abstract-----	iii
<b>1. Introduction</b>	<b>1</b>
1.1 Background and Motivation -----	1
1.2 Objective-----	3
1.3 Dissertation Outline-----	5
<b>2. Literature Review and Fundamentals of EHD</b>	<b>7</b>
2.1 Literature Survey-----	7
2.2 Working of Electrohydrodynamic Inkjet-----	9
2.3 Governing Equations-----	11
2.3.1 Electric Field Equations-----	11
2.3.2 Fluid Dynamic Equations-----	13
2.3.3 EHD Body Force-----	14
2.3.4 Dimensionless Form of Governing Equations-----	16
2.3.5 Equivalent Model-----	18
2.4 Parameters and its Effect-----	24
2.4.1 Surface Tension-----	24
2.4.2 Viscosity-----	25
2.4.3 Flow-rate-----	25
2.4.4 Charge Relaxation Time -----	26
2.4.5 Electric Reynolds Number-----	27
2.4.6 Current – Voltage Characteristic Curve-----	28
2.4.7 Onset Voltage-----	30
2.4.8 Effect of Electrode Spacing-----	30
2.4.9 Effect of Voltage Polarity-----	30
2.4.10 Nozzle Diameter-----	31
<b>3. Head Design and Fabrication</b>	<b>32</b>
3.1 Electrode Design and Geometry-----	32
3.2 Introduction of Silica Capillary and Flow channel -----	38
3.3 Numerical Analysis of Head-----	41
3.3.1 Simulation-----	43
3.4 Head Design-----	57
3.4.1 Head Design-----	57
3.4.2 Material Selection and Fabrication-----	58
<b>4 Head Results and Analysis</b>	<b>62</b>
4.1 Experiment Setup and Methodology-----	62
4.2 Experimental Analysis and Optimizing the Position of Silica----	64
4.3 Analysis of Deposition Process on Substrate-----	69
4.3.1 Patterning Analysis-----	69
4.3.2 Spray Deposition-----	72
4.4 Comparison Analysis-----	75

5.	<b>Literature Review and Fundamentals of Memristor</b>	<b>77</b>
5.1	Literature Survey-----	77
5.2	The Memristor as the Fourth Fundamental Circuit Element-----	79
5.2.1	Memristors : Theory and Properties-----	81
6.	<b>EHD Printed Memristor Results and Analysis</b>	<b>86</b>
6.1	Electrohydrodynamically Printed Memristor-----	86
6.1.1	Device Design-----	86
6.1.2	Ink Status and Optimization for Electrohydrodynamics	88
6.1.3	Analysis of Ink Behavior on Substrate-----	89
6.1.4	EHD Printed Memristor-----	93
6.1.5	Characterization-----	96
6.2	Comparison Analysis-----	99
7.	<b>Conclusion</b>	<b>101</b>
7.1	Concluding Remarks-----	101
7.2	Future work-----	102
	References-----	103
	Curriculum Vitae-----	109



## List of Figures

Figure 2.1: Shows schematic diagram of developing of meniscus on voltage increment-----	10
Figure 2.2: The basic concept of electric field-----	19
Figure 2.3: (a) The droplet mechanism in electrostatic system (b) the equivalent mechanical model and (c) representing equivalent electrical model-----	20
Figure 2.4: The effect of forces in the nozzle of electrostatic inkjet system---	21
Figure 2.5: (a) The droplet generation in electric field and (b) the equivalent electro-mechanical model representing electrostatic model-----	22
Figure 2.6: I-V Characteristic of a nonpolar liquid (Schmidt 1997)-----	28
Figure 3.1: (a) Pin to Pin setup and (b) Pin to Plate setup-----	33
Figure 3.2: Showing the results of placement of electrode under the nozzle while printing through the jet (a) simulation results (b) the complete picture of the physical setup (c) the high speed image and high zoom the nozzle above the nozzle and (d) the high speed and high zoom image of the camera under the counter electrode (ground)-----	35
Figure 3.3: Shows the effect of different placements and dimensions of counter electrodes (a) shows the effect of the counter electrode at height beside the nozzle, (b) shows the ring counter electrode beside the nozzle and above the nozzle (c) shows the effect of ground distance (d) shows the effect of ground thickness and; (e) and (f) shows the effect of the placement ground near the tip of the ground with close and open ground-----	37
Figure 3.4: (a) Showing the microscope image and (b) shows the high speed camera image of printing through proposed head-----	37
Figure 3.5: Schematic diagram of silica inside metallic capillary-----	38
Figure 3.6: Ink circulation mechanism at the meniscus-----	39
Figure 3.7. Ink and surface tension effect in metallic capillary and silica head	39
Figure 3.8: (a) Showing the effect of electric double layer in the nozzle and (b) showing the electric double layer in proposed model-----	40
Figure 3.9: (a) Shows the schematic diagram of the proposed head design and (b) shows the parameters-----	42
Figure 3.10: Finite Element model of the proposed head-----	43

Figure 3.11: Response analysis at different cases and position of ground electrode at 5kV (a) showing response of case 1,(b) response of case 2, (c) response of case 3, (d) response of case 4, (e) response of case 5, (f) response of case 6, (g) response of case 7, (h) response of case 8 and (i) response of case 9-----	50
Figure 3.12: Response analysis at different cases and position of ground electrode at 5kV at nozzle tip (a) showing response of case 1,(b) response of case 2, (c) response of case 3, (d) response of case 4, (e) response of case 5, (f) response of case 6, (g) response of case 7, (h) response of case 8 and (i) response of case 9-----	56
Figure 3.13: (a) Model diagram of head and (b) experimental model of head-----	57
Figure 3.14: (a), (b), (c) and (d) show the schematic diagram of the nozzle head and (e) shows the microscope image of the holder outlet-----	59
Figure 3.15 : (a) Showing the schematic diagram of the PDMS ink supply and silica holder and (b) showing the the final model of PDMS ink bank and silica holder mold-----	60
Figure 3.16: Showing the counter electrode manufacturing process-----	61
Figure 4.1: Experiment setup (a) schematic daiagram of the system and (b) physical system for the anlaysis of experimnets-----	63
Figure 4.2: (a) Experiment setup and (b) the meniscus, dripping and jetting analysis of the head-----	64
Figure 4.3: Showing (a) interaction and (b) perturbation graphs-----	65
Figure 4.4: Standard error design between voltage and Silica pos at (a) 2D and (b) 3D graphs-----	67
Figure 4.5: Region of stable and unstable jetting in (a) 2D and (b) 3D-----	68
Figure 4.6: (a) Showing image of printing on glass substrate through side camera (b) showing the image from the camera under the substrate while jetting before printing and (c) show the pattern developed on glass substrate from the camera under the substrate-----	70
Figure 4.7: Optimal range of cone jet-----	71
Figure 4.8: Different patterning results on the glass substrate through microscope-----	71

Figure 4.9: Flow distribution (a) concave, (b) convex, and (c) trapezoid-----	72
Figure 4.10: (a) Shows the spray image through camera eye (b) shows the spray results of commercially available Ag Ink (c) shows the results of TiO <sub>2</sub> results on edge and (d) shows the results in the center-----	73
Figure 4.11: (a) Shows the overall SEM image of the TiO <sub>2</sub> layer (b) at center and (c) at side (edge)-----	75
Figure 4.12: Voltage comparison chart-----	75
Figure 4.13: Comparison chart of shadowing effect-----	76
Figure 4.14: Resolution comparison chart-----	76
Figure 5.1: Relation between basic fundamental elements-----	82
Figure 6.1: Single layer Memristors (a) the layer by layer configuration (b) device design on glass substrate-----	87
Figure 6.2: Multiple layer multiple stack memory (a) layer by layer (b) device design on glass substrate -----	88
Figure 6.3: TiO <sub>2</sub> synthesis process-----	89
Figure 6.4: (a) Mesasuring terhnique used (b) measuring of surfce tension of TiO <sub>2</sub> through contact angle system-----	90
Figure 6.5: (a) Behavior of Ag ink on the glass and TiO <sub>2</sub> deposit layer (b) showing the schematic diagram of the contact angle-----	90
Figure 6.6: (a) Behavior of Ag ink on the glass and (b) behavior of Ag ink on the TiO <sub>2</sub> deposit layer-----	91
Figure 6.7: (a) Showing the printed memristors by using Electrohydrodynamic technique on glass substrate (b) showing 2 byte memory cells and (c) showing 6 nibble memory-----	95
Figure 6.8: Shows microscope image of the printed memristor (a) and (b) shows shows the 40x40 um cell-----	95
Figure 6.9: (a) Shows the schematic diagram of characterization of the memristors and (b) shows the schematic diagram of the characterization of the printed memristors-----	96
Figure 6.10: Shows pinch hysterical loop -----	97
Figure 6.11: Memory write and erase through pinch hysterical loop-----	97

## List of Tables

Table 2-1. Dimensionless parameters based on conservation equations (Tabulated in IEEE-DEIS EHD Technical Committee 2003)-----	16
Table 2-2. Charge relaxation times of typical materials-----	27
Table 3-1: The deflection of nano particles in Pin to Pin and Pin to Plate experiment-----	34
Table 3-2. The parameter of nozzle-----	42
Table 3-3: Showing the cases and values-----	45
Table 3-4: Response on different case at different potentials-----	51
Table 6-1: Material and deposition mechanism for Memristor-----	87
Table 6-2: Contact Angle measurements of Ag ink on glass and spray deposit TiO <sub>2</sub> glass-----	92
Table 6-3: The general values of the printing materials -----	93
Table 6-4: Complete Data-sheet for EHD Printed Memristor -----	98
Table 6-5: Comparison Analysis -----	99

## 요약

본 논문에서는 새로운 프린팅 장비 개발과 인쇄 전자 기술을 이용한 멤리스터 (Memristor) 소자 제작 기술에 대해 제안한다. 압전 소자 방식과 열 방식의 프린팅 방식과 비교하여, 전기수력학적 프린팅(EHD) 방식은 빠른 공정 속도와 프린팅 재료 및 소자의 다양성 그리고 공정의 단순성의 장점을 가지고 있다. 또한, 전기수력학적 프린팅 공정은 다른 프린팅 공정에서 나타나는 문제점인 흡착, 농도의 변화 및 냉각에 따른 안정성에 대하여 크게 구애 받지 않는다. 전기수력학적 시스템이 갖는 3가지 토출 모드인 액적토출, 연속토출 및 분무로 인하여 균일한 박막층 제어와 고 생산효율 및 고 정밀도를 제공할 수 있다. 전기수력학적 프린팅 시스템은 유무기반도체 재료, 금속 전도성 재료, 나노 재료 등이 포함된 다양한 용매기반 잉크를 사용 한다.

본 논문에서는 링 타입 카운터 전극을 포함한 EHD 패터닝 접근법과 단점들을 자세히 기술하였으며, 이 단점들은 실험적 설계기술(DOE)의 적용을 통해 보완하고 새로운 전기수력학적 프린팅 헤드 기술을 개발하였다. 먼저 링 카운터 전극 헤드는 노즐 오리피스 보다 위쪽에 설치되는 형태로 안정된 전기력선 제어를 통해 젯팅 길이를 짧게 가져갈 수 있으며, 안정적인 프린팅을 가능하게 한다. 시뮬레이션 분석 기법을 도입하여 각 헤드별 전기장의 형태와 성능을 비교 및 실험 결과를 예측하였다. 또한, DOE 분석에 기반으로 금속 모세관이 내부에 삽입되어 있는 형태인 실리카 재질의 헤드를 제시하였다. 실리카 헤드는 이중구조의 전극을 가지며, 메니스커스 (meniscus) 내의 방전된 입자의 역순환 메커니즘 제어가 용이하다. 이러한

특징들은 안정된 젯팅 모드와 균일한 패터닝을 얻기 위해 필요한 전압을 낮추는데 유리하다. 이러한 연구를 통해 전기수력학적 헤드 내의 잉크 순환 메커니즘 분석의 필요성을 논의하였으며, 실험적 결과를 비교하기 위해 동일한 유리기판 상에서 전도성 패터닝과 분무 증착 실험을 진행하였다. 또한 메니스커스 모양과 인가된 전압에 의한 전기수력학적 헤드의 토출 현상을 분석하였고, 낮은 전압에서의 메니스커스 형성과 토출의 안정화 대해 논의하였다.

새로운 메모리 형태인 멤리스터를 전기수력학적 인쇄방식 사용하여 제작할 수 있는 방법을 제시하였다. 멤리스터의 제작 실험에서는 실버 나노 입자 기반의 전도성 잉크와  $\text{TiO}_2$  잉크 및, 유리 기판으로 전기수력학적 프린팅 및 분무 메커니즘을 통해 전도성 잉크 패터닝과  $\text{TiO}_2$  증착을 시도하였다. 본 논문에서는 전기수력학적 기법에 의해 제조된 멤리스터를 통해 보다 수명이 긴 메모리 형태를 제안하였으며, 인쇄전자분야에서 생산비용을 절감하는 기술을 제안하였다. 향후 본 논문은 유연 기판기반의 기술로 발전하는데 기여 할 것으로 기대한다.



## Abstract

This manuscript introduces a novel design for Electrohydrodynamics (EHD) inkjet head for Printed Electronics. The goal of the research is to study and enable the printing through cone jet mode from EHD based single nozzle integrated counter electrode head. For head analysis purpose, experiments are performed on conductive and dielectric ink. And for authentication purpose of the printing tool for Printed Electronics, Memristor are printed on glass substrate.

In the first section, the manuscript detailed different EHD patterning approaches including ring type counter electrodes and their drawbacks. And after elaborating the drawbacks, this study will introduce a new approach for EHD patterning of conductive ink supported by Design of Experiment (DOE) techniques. The counter electrode is kept above the nozzle orifice and patterning is done by maneuvering contour of electric field in such a way that even with the smaller length of jet, stable printing can be done. For better understanding and evaluation of phenomenon, simulations and comparisons are performed. For the formation and stabilization of electrohydrodynamics jet printing, a non conductive silica capillary is used inside the metallic capillary. The silica capillary is used to control electric double layer distribution and the black flow in liquid meniscus. This also allows ink circulation mechanism to be applied to uncharged particles. The above factors also helped to reduce the potential needed to obtain stable cone-jet mode and uniform patterning. Moreover, this study also discusses the need for ink circulation mechanism in EHD head and also proposed the circulation mechanism by stabilizing the jet. The head is also tested on the glass substrate. Furthermore, the meniscus shape and response on applied voltage is studied and analyzed. Manuscript also elaborates and addresses issues like the meniscus generation and ejections at low voltage with stability problems.

The second section of the book covers the Electrohydrodynamically printed Memristor. For the deposition particle based silver (Ag) based conductive ink and  $\text{TiO}_2$  is used. Ag ink is used for patterning and  $\text{TiO}_2$  deposit through electro-spray

mechanism of the head. The Electrohydrodynamically developed Memristor can revolutionize the printed electronics by providing long lasting memory to printed circuits. This will also helps to transfigure discrete electronics in the world of printed electronics computationally and due to its cost effectiveness.



# 1. Introduction

This chapter introduces the readers with the motivation and need for this research. Moreover, this chapter also compares the competing technologies and their drawbacks and need for new printing tool. And at the end of the chapter a brief outline of the thesis is elaborated.

## 1.1 Background and Motivation

Today micro/nano-electronics is characterized by migration of research from pure down-scaling to new functionality and combined technology-system innovation. This is mainly required in order to manage power dissipation, variability and complexity issues that exploit nano-technology. While this new functionality and technology-system innovation will exploit the properties of future nano-scaled technologies, the aggressive scaling will also play a fundamental, but not an exclusive role. New research drivers, such as ultra-low power technologies, bio-inspired circuit and system design and ambient intelligence applications are expected to play an increasingly important role in the next years.

The generally accepted view of micro and nano-electronics identifies three main research domains: (i) More Moore, (ii) More than Moore and (iii) Beyond CMOS.

The More Moore domain is essentially dealing with technologies related to the nanometer CMOS; prevailing business directions together with continuing scalability have determined the evolution of silicon CMOS as the technology with the highest added value. CMOS technology will be considered as a key platform to supply the massive computing power and communication capability needed for the realization of Ambient Intelligence applications at an affordable cost and a power efficiency exceeding today's leading-edge examples.

The Beyond CMOS domain deals with disruptive technology and device principles (from charge to non-charge based devices, from semiconductor to molecular technology), compared to CMOS, to exploit atomic-scale technology and novel functionality. Novel switches, architectures for universal memory and new

interconnect approaches are some of the identified challenges. In addition to technologies such as nanowires and nanotubes, particular attention will be devoted to the development of disruptive technologies such as molecular electronics, over a longer time horizon. In this perspective, partial (hybridization) or total replacement solutions for silicon CMOS are foreseen.

The More than Moore field deals with true engineering of complex systems that combine, by heterogeneous integration techniques, various technologies (Rao R. Tummala. 2006, Andrew B. Kahng. 2010). The More than Moore technology platform also gives particular attention to MEMS/NEMS and sensor technologies that are combined to silicon or non-silicon computing, information storage and encryption and wireless / RF communication technologies.

One of the new emerging technologies includes Printed Electronics. Printing scheme is very appealing technique to fabricate different micro and nano electronics and electrical patterns due to its advantage over conventional photolithography techniques in source dissipation, energy level and material wastage with liberty and flexibility of using different substrates ( J. Heinzl et al.1991, H.P.Le. 1998) . Printed electronics has revolutionized the electronics world with low-cost, low-performance electronics useful for applications not typically associated with conventional high performance (*i.e.*, silicon-based) electronics, such as flexible displays, smart labels, decorative and animated posters, and active clothing. Furthermore, limitations exist in the range of materials that may be incorporated using these lithographic methods, particularly in the combination of a broad range of organic and inorganic materials (Coatanea et al. 2009, Roth et al). In Printed electronics, instead of printing graphic arts inks, families of electrically functional electronic or optical inks are used to print active or passive devices, such as thin film transistors or resistors. With the advancement and progress in areas of science, different techniques and procedures for the deposition of the nano particles are needed which can work under low temperature. Earlier, Moore's predication is basic law behind the modern research and development in electronics and semiconductor electronics industry. The accuracy of the law proved to be uncannily accurate, expanding with exponential rate. Futurists such as Ray Kurzweil, Bruce Sterling, and Vernor Vinge believe that the

exponential improvement described by Moore's law will ultimately lead to a technological singularity (Kurzweil Ray. 2005, Ray. 2001, Yang 2000, Malone 2003). With the advancement and progress in areas of science, different techniques and procedures for the deposition of the nano particles are needed which can work under low temperature to utilize different substrates. Furthermore, another biggest challenge in patterning to current industrial system is the integration of bottom-up self-assembly producing useful, complex architectures with a top-down approach, in one step. Therefore, novel methods for the patterning process of organic and inorganic materials are needed and essential for the success of these developments.

But lack of an ideal printing system at industry level makes it one of the hot topics in modern research for patterning and material deposition system. One of the most successful techniques for the low-cost patterning of polymeric materials is undoubtedly nano-imprint lithography (NIL) proposed by Chou *et al.* The process is typically carried out at high temperatures ( $50\text{--}100\text{ }^{\circ}\text{C}$  above the glass transition temperature ( $T_g$ ) of the polymer) and high pressures ( $\sim 40\text{ bar}$ ). However, there are a number of issues associated with NIL like life time of the mold, the high differences in the thermal expansion coefficients of the materials involved, thermal degradation of the resist and fast aging of the anti adhesive layers of the mold which restrict it to be implemented in low temperature substrate at industrial level. Among the traditional industrial printing methods mainly inkjet and screen printing as well as the so-called mass-printing methods gravure, offset and flexographic printing are used in printed electronics. Out of all these, inkjet is more popular due to its contactless deposition mechanism, flexibility and versatile digital printing methods, and ability to be setup in current industry with relatively low effort. Therefore it is probably the most admired printing method for printed electronics.

## 1.2 Objective

There are different inkjet depositing systems but electrohydrodynamic approach emerged as the leading system due to its faster speed, ability of variable printing and involves less mechanical efforts as compared to its competitor system like piezo and thermal technologies (Esinenco *et al.* 2006, Choi *et al.* 2010). Electrostatic

mechanism also prevents the absorption, density loss and colorant-related stability problems found in other contactless fabrication apparatus. Through electrohydrodynamic system, due to the ability of variable (drop-wise, continuous (cone jet) and spray) printing and deposition, can provide better control of the homogenization of layer, productivity and resolution. Electrohydrodynamic printing can be used for organic semiconductors, organic field-effect transistors (OFETs) and organic light-emitting diodes (OLEDs). Furthermore, front planes and backplanes of OLED-displays, integrated circuits, organic photovoltaic cells (OPVCs) and other devices can be prepared by means of electrohydrodynamic inkjet printing. Electrohydrodynamic inkjet system utilizes any solution-based material, including organic semiconductors, inorganic semiconductors, metallic conductors, nanoparticles, etc for deposition.

But this technology is in its age of infancy and needs work to increase and understand the reliability of the printing. In this research those problems addressed and new strategy for the improvement and printing is proposed and experimentally verified. This manuscript, proposed a novel approach on integrated terminal single nozzle electrostatic inkjet system for the fabrication and patterning of conductive pattern. The reason of integrating nozzle with ring counter electrode is to use the head in one package and reduce the effect and dependence of substrate on stable meniscus, dripping and jetting. The counter electrode attracts the droplet and before printing droplet changes its direction towards the ground instead of leading to substrate. To overcome this imperfection of printing, drop on demand and larger size of the counter electrode is proposed. But aforementioned technologies has its drawbacks as it lacks speed, accuracy of drop size from meniscus, placement on substrate and hurdle in designing of multi nozzle head to make possible for the direct writing at the industrial level. Since the components must be integrated to form a functional system in order to provide desired services, system-level complexities in both architecture. For patterning and deposition of contents, so far, pin to pin and pin to plate setup is been used (Ahsan et al, 2008). Due to this setup, the drop extraction potential is substrate dependent. But for industrial use and applications, it's important that charged nozzle and counter ground terminal can be connected in a single

package to minimize the effect of substrate. Thus, one of the critical design issues is the electrode shape and configuration to achieve desired electric field gradient of the dielectrophoresis driven axon migration. The control of electric field contour through different configuration makes this classical problem of electric field. The position of counter electrode/s has to be setup in such a way that electric field should lead the path to the substrate. Moreover, (depending of the placement of the substrate) a very homogenous layer of spay can also be developed. Another problem resolved is to deposit the nano particles on substrate without the solvent and to reduce the effect of back flow. To subsided and enhanced the ability of the head a circulation mechanism at the tip of the nozzle is proposed. This also helps to reduce the surface tension of the inks and in the end decrease the applied voltage and increase the jet length. And finally to authenticate the ability of the head, a revolutionary memory device Memristor are printed and characterized.

### **1.3 Dissertation Outline**

This dissertation is divided into 6 chapters. Chapter 2 reviews the fundamental operation mechanism of the Electrohydrodynamic inkjet printing. This chapter also summarizes the EHD phenomena mathematically by using analytical and equivalent model. And then at the end of the chapter effect of different parameters on EHD is evaluated found by mathematical analysis.

Chapter 3 explains the step by step development of the electrostatic head based upon the pervious chapter analysis. The chapter also introduce the drawback of the pervious heads and developed a new one based on the improving the head formation. In this chapter, based upon the different parameters and equations (analyzed in last chapter), an idea of the head design is proposed and analyzed. For counter electrode, a ring type ground is being used. The reason of integrated the nozzle with ring ground is to use the head in one package and reduce the effect and dependence of substrate on stable meniscus, dripping and jetting. And then for more optimizing the head, patterning on substrate, removing the back flow and minimizing the effect of the disturbance at the nozzle orifice, silica capillary is proposed and analyzed.

Simulation is also performed for in detail analysis. And based on theoretical and simulated analysis a head is proposed and fabricated.

Chapter 4 analyzes the experiment setup and the behavior of the head on different silica position. And based on the findings introduce new head design for patterning supported by DOE techniques. The head is also tested on the glass substrate for high aspect conductive pattern and nano-level with equilibrium spray deposition.

Chapter 5 reviews fundamentals of Memristors. This chapter also includes different details of Memristors including historical point of view, equations to current state (HP developed) Memristors. And on the basis of literature survey, choose one model for printed Memristors.

Chapter 6 explains the step by step development of Electrohydrodynamically Printed Meritor to authenticate the ability of spray and patterning of the head on glass substrate. Both dielectric ( $\text{TiO}_2$ ) and conductive ink used. This chapter also summarizes different steps needed for the development of the printed device by inkjet including device design, ink fabrication to optimization and analyzing techniques. To authenticate the results, 6 nibble and 2 byte printed memories are also developed.

And finally, chapter 7 summarizes the approach, results and overall achievement of the work listed in this manuscript. And at the end of chapter, also lists some suggestions and directions for future work.



## 2. Literature Review and Fundamentals of EHD

This chapter briefly explains the EHD working. The EHD is reviewed in detail and divided into four sections namely theoretical review of EHD, analytical analysis of EHD, equivalent model of EHD and effects of different parameters on EHD. This study is decomposed into different sections, to build foundation for the head design, explained in next chapter.

### 2.1 Literature Survey

Printing technologies can be divided into two basic categories namely, contact and non-contact printing. Chinese were first to introduce the printing technology to world in second century by printing text and images via woodblock (Hind 1935). And in 19<sup>th</sup> century, idea of non contact printing was introduced. Prior to that, all printing methods used physical transfer parts to make an image. Moreover, most methods invented to date use different physical phenomena to deposit material on a substrate. Flexography and gravure use a relief method, offset lithography relies on surface energy, screen printers require masking, embossing uses high force and pressure to replace material, laser ablation removes material, and laser transfer uses excessive force and energy to release material (Khan 2006). Inkjet technology is the only method that directly dispenses material, without contact, to the receiving material. Furthermore, inkjet technology is the only method that uses remotely amount of material and has the potential to be a high-throughput, low-cost process.

Inkjet printing is a simple method in theory, but is rather involved in many areas. Some of the main things that need to be controlled during the printing process are drop volume, drop shape and formation, printing distance and its impact on print quality, evaporation kinetics of the droplet, surface energy of the substrate and surface tension of the droplet, penetration or spreading parameters and film thickness. Inkjet printing is also referred as digital printing technique, as printed image and deposition position can be controlled by using electronic control circuitry. The dispensing method divides inkjet technologies into two groups: continuous and drop-

on-demand (DOD). Most commercial and industrial ink-jet printers use a DOD (Gamota et al. 2004). The printers use piezoelectric element or heating elements to produce drop-on-demand droplets to print desired image or conductive lines. When voltage is applied to the element, the element generates pressure pulse in the fluid forcing a droplet of ink to eject from the nozzle. The continuous method use forced force like ink flow or air pressure and for the stabilization the jet, jet is charged electrically by using high-voltage deflection plates. Droplets that will not be deposited are collected by a gutter and re-circulated. The application of these technologies varies from the image to text printing and resolution needed.

But with different emerging technologies like printed electronics (PE), new trends are rising. Printed electronics is being driven by electronics industry. The idea to print and develop low cost electronics and on different substrates has revolutionized printing technologies. The attraction of printing technology for the fabrication of electronics mainly results from the possibility to prepare stacks of micro-structured layers (and thereby thin-film devices) in a much more simple and cost-effective way compared to conventional electronics. Beside this, also the possibility to implement new or improved functionalities (e.g. mechanical flexibility) plays a role. The selection of used printing methods is determined by requirements concerning printed layers, by properties of printed materials as well as economic and technical considerations in terms of printed products. Therefore different printing strategies are reinvestigated and inkjet technology gain advantages due to its contact less nature. But the aforementioned inkjet technologies have certain commercial bottlenecks with regard to printing frequency, clogging, maintenance and resolution. But Electro hydrodynamic (EHD) inkjet technology seems to be a promising technology as EHD inkjet printing system has advantages over other types of the inkjet (piezo, thermal) printing techniques in size of fabricated device and precision in extraction. The electrostatic forces enable the system to overcome the mechanical actuation which is often require high fabrication cost, actuation limitation and integration problems to produce printed electronics and electrical patterns at higher frequencies rate.

## 2.2 Working of Electrohydrodynamic Inkjet

Since the inception of printed electronics and micro fluidics, the electric force has been exploited as one of the leading mechanisms for driving and controlling the movement of the operating fluid (electrohydrodynamics) and the charged suspensions (electrokinetics) (Jun Zeng. 2009). Electrostatic approach is faster, capable of variable printing and involves less mechanical efforts as compared to its competitor system like piezo and thermal technologies (J.S. Lee. 2008). Electrostatic mechanism also prevents the absorption, density loss, and colorant-related stability problems found in other contact less fabrication apparatus (K. H.Choi. 2009, D.B. Chrisey, 2000). The first scientific observation of this phenomenon was reported by Zeleny (Zeleny. 1914) and the physics of interaction of a liquid in capillaries with electrified was established by Taylor (Taylor. 1964). As the name implies electrostatic use electrostatic attraction of particles to create an image. Electrostatic forces can generate droplet sizes of under  $10\mu\text{m}$  even when using a nozzle size of over  $100\mu\text{m}$  in diameter (H.F. Poon. 2002, D.Y.Lee. 2007). The main purpose is to produce drops of materials at a high rate in a controlled manner with the ability of replication in such way the final size and position of the dot on the substrate is predictable (Ahsan Rahman et al. 2008). Electric force also has an intrinsic advantage in miniaturized devices. Because the electrodes are placed cross a small distance, from sub-millimeter to a few microns, a very high electric field is rather easy to obtain. The electric force can be highly localized with its strength rapidly decaying away from the peak. This makes the electric force an ideal candidate for spatial precision control. The geometry and placement of the electrodes can be used to design electric fields of varying distributions, which can be readily realized by micro machining and fabrication methods. This geometry depends upon the application of the electrostatic system which varies from medical, micro fluids to inkjet printers. Electrohydrodynamics (also referred to as electrostrictive hydrodynamics) is the conversion of electrical energy into kinetic energy, and vice versa. It is a field of science that deals with the motions of ionized particles or molecules under the influence of electric field (Wikipedia, accessed October 2007).

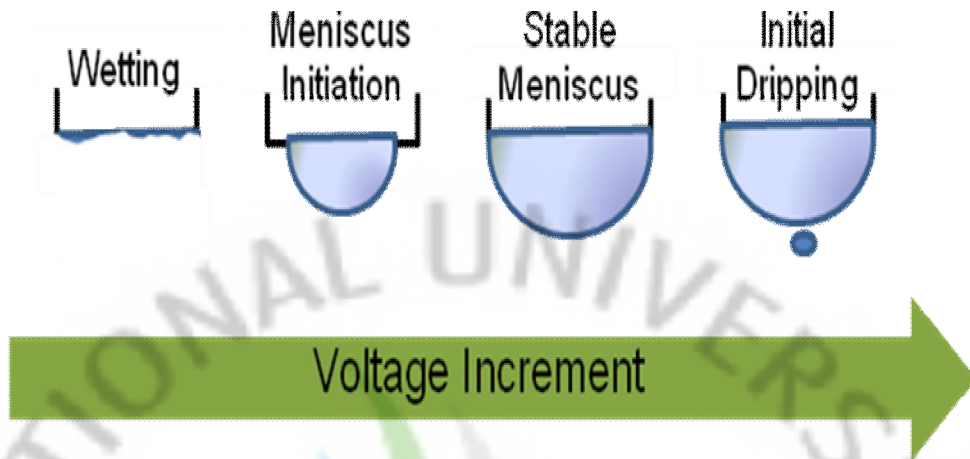


Figure 2.1: Shows schematic diagram of developing of meniscus on voltage increment.

The drop generation mechanism in the electrostatic system is different as compared to the piezo and the thermal based inkjet system. In piezo or the thermal based system, a complete drop from the orifice of the drop emerges due to applied force. Whereas, in electrostatic case, firstly, the meniscus is generated, then the field is applied on the meniscus. The drop comes from the surface of the meniscus and the droplet is much smaller as compared to the diameter of the orifice. The drop size depends on the field applied field on the surface of the meniscus. Therefore, it is important that the meniscus surface is charged adequately to produce the droplet. When the surface of a meniscus is subjected to an electric field, the field cause a deformation of the meniscus and eventually a stable drop is formed (Ahsan Rahman et al. 2010) as shown in the Figure 2.1. Figure 2.1 a shows schematic diagram of developing of meniscus on voltage increment.

### 2.3 Governing Equations

The EHD phenomenon is a direct result of the interaction between electric and fluid flow fields. When an electric potential difference is applied to a dielectric fluid, an electric field is formed within the fluid. If the field sets the liquid into motion, the distributions of both charge density and electric field change. This complicated and nonlinear behavior of the electric force and liquid motion makes EHD difficult to quantify. In order to better understand the phenomenon, the first step is to develop a theoretical model in which the liquid behavior under the influence of an electric field can be analyzed. For this study, we start with two basic series of governing equations which describe the electric field and the flow field. Later, the electric body force is formalized and these equations are non-dimensionalized, and the importance of dimensionless parameters is discussed. And finally, the equivalent model is summarized to develop understanding with the phenomena.

### 2.3.1 Electric Field Equations

Melcher (1981) in his book has explained extensively that the electromagnetic field in a system can be considered as a quasi-static electric field system. Since dielectric fluids exhibit a very low conductivity, the conduction current becomes so small that the magnetic induction will be negligible. Therefore in a simplified system, such as a parallel plate electrodes system, Maxwell's equations (a set of four basic equations) are reduced to only electrostatic laws. Gauss's law relates the free charge density,  $\rho_e$ , to the electric field intensity  $E$

$$\nabla \cdot E = \frac{\rho_e}{\varepsilon} \quad (2.1)$$

Where  $\varepsilon$  is the permittivity of dielectric liquid.

Since the magnetic field is negligible, Faraday's law reduces to

$$\nabla \times E = 0 \quad (2.2)$$

And therefore, the electric field can be expressed as the gradient of a potential field

$$E = -\nabla \phi \quad (2.3)$$

$$\nabla \cdot J + \frac{\partial \rho_e}{\partial t} = 0 \quad (2.4)$$

where  $J$  is the electric current density. And different mechanisms for the current flow: convection, migration and conduction can be given as:

$$J = \sigma_e E + \mu \rho_e E + \rho_e u \quad (2.5)$$

Where  $\mu$ ,  $\rho_e$  and  $\sigma_e$  are the mobility, unipolar charge density and bipolar conductivity of the bulk fluid respectively (Melcher and Taylor 1969).

The terms in equation represents the conduction term, which refers to the bipolar conduction and is given by the Ohmic constitutive law. When, an electric potential difference is applied to a dielectric fluid (with resistivity usually above 107  $\Omega$ -m and permittivity below 20), the electrical conduction process starts as a result of dissociation of either impurity molecules inside the liquid or the liquid molecules themselves. Dissociation always creates an equal number of positive and negative ions which under the influence of electric field does not affect the net force on the liquid but only appears as additional input power requirements (Crowley et al. 1990). In most areas of EHD for dielectric liquids of high enough resistivity, Ohm's law and electroneutrality often fail to be valid. An excellent review on the electrohydrodynamics of liquids in the ohmic regime and subjected to coulomb forces has been written by Melcher and Taylor (1969), and more recently by Ohadi et al. (2001).

The second and last terms, the so-called migration and convection currents, represent the motion of the net space charges, which are always free to move inside the fluid. In a stationary fluid, electric force applied to the charges tends to pull them through the fluid at the velocity  $\mu_e E$  relative to the fluid (Crowley et al. 1990). If the fluid is set into motion, the distribution of charge density changes (via the charge conservation law), which in turn changes the velocity field (via the Navier-Stokes equation) (Castellanos 1991).

### 2.3.2 Fluid Dynamic Equations

The equations of motion for an incompressible Newtonian fluid are continuity

$$\nabla \cdot u = 0 \quad (2.6)$$

and Navier-Stokes equations with an electric body force

$$\rho \left[ \frac{\partial u}{\partial t} + (u \cdot \nabla) u \right] = -\nabla p + \eta \nabla^2 u + \rho g + f_e \quad (2.7)$$

Electric body force, as will be explained further in detail, represents the interaction between electric and flow fields. Equation represents the energy equation for an incompressible fluid

$$\frac{\partial T}{\partial t} + u \cdot \nabla T = \nabla \cdot (\alpha \nabla T) + \frac{v}{c_p} \phi + \frac{S_j}{\rho c_p} \quad (2.8)$$

where  $S_j$  is the Joule heating source term. Joule heating or ohmic heating refers to the increase in temperature of the bulk liquid as a result of resistance to an electrical current flowing through it. For a fluid with unipolar charge migration and ohmic conduction, the Joule heating term is defined by Equation (Castellanos 1998).

$$S_j = \sigma_e E^2 + \mu_e \rho_e E^2 \quad (2.9)$$

In ion-drag, the power consumption is very low; as a result, the amount of heat generation in the bulk liquid is very low, which results in no apparent temperature variation as observed during the experiments. Therefore, the energy equation and the joule heating terms are often negligible except in the numerical modeling case, in which an additional variable  $T$  is added to the system of equations.

### 2.3.3 EHD Body Force

As explained earlier, the influence of the electric field on the fluid field is expressed by the electric body force. The body force cannot be determined using the molecular thermodynamic principles due to the complexity of the problem. Instead, an energy balance method is used to derive the equation by Stratton (1941) and Panofsky and Phillips (1962). A comprehensive review of the derivation of the body force is also presented by Darabi (1999). Equation below expresses the electric body force acting on the fluid:

$$f_e = \rho_e E - \frac{1}{2} E^2 \nabla \varepsilon - \frac{1}{2} \nabla \left[ \rho E^2 \left( \frac{\partial \varepsilon}{\partial \rho} \right)_T \right] \quad (2.10)$$

Where  $\rho_e E$  represents electrophoresis force (Coulomb force),

$\frac{1}{2} E^2 \nabla \varepsilon$  represents dielectrophoresis force and

$\frac{1}{2} \nabla \left[ \rho E^2 \left( \frac{\partial \varepsilon}{\partial \rho} \right)_T \right]$  represents electrostrictive force

This effect is summarized in Parisa Foroughi's thesis (Parisa Foroughi, 2008). The three terms on the right hand side of the equation represent different types of electrical forces acting on the fluid, which are known as the electrophoretic, dielectrophoretic, and electrostrictive forces, respectively. Electrophoretic force represents the Coulomb force and is the force that acts upon free charges within the fluid. As the Coulomb's law states, the magnitude of the electrostatic force between two charged particles is directly proportional to the magnitudes of each charge and inversely proportional to the square of the distance between the charges. It also indicates that when a DC potential difference is applied to free charges within a fluid (dipoles are not free charges), charged particles move along the electric field according to their charge sign and generate fluid motion. In an incompressible single phase flow, the Coulomb force is expected to be responsible for most of the fluid motion. In the first term,  $f_e$  is the force density and  $\rho_e$  is the charge density which represents the sum of all charge densities including positive and negative.



It therefore defines only one direction for fluid motion under the DC electric field and oscillation under AC fields. The Coulomb force requires the existence of free charges within the working fluid. There are different methods by which free charges can be generated in a liquid. In ion-drag, charge injection is the dominant process of free charge generation. Charge injection is initiated at or close to the electrode/fluid interface if a sufficient voltage potential is applied across the electrode pairs.

The second and third terms, known as polarization forces, are more important in two-phase and/or compressible fluids. The dielectrophoretic force, implemented as the interaction of a non-uniform electric field with the dipole moments induced in the neutral molecules of the fluid. In a uniform electric field, the forces acting on two charges of a dipole molecule cancel out, however in a non-uniform field; the polarization force on the side located at a more intense electric field exceeds the force on the other side and moves the dipole toward the direction of increasing electric field strength. As it is expanded and shown by equation, the dielectrophoretic force is generated as a result of permittivity gradient at the liquid-vapor interface in the two-phase flow or due to a temperature gradient in the non-isothermal fluids.

The last term in Equation 2.10 is a gradient term called electrostrictive force which similar to dielectrophoretic forces, acts upon the dipoles in liquid. A single-phase dielectric liquid becomes polarized when the permittivity (or dielectric constant) changes with position or density. In cases where the liquid becomes elastically deformed by electrostrictive field, the fluid flow is not generally affected, and only the pressure changes. In an isothermal single-phase flow, the effect of polarization forces can generally be neglected as  $\nabla \epsilon$  vanishes.

The main goal of this study is to characterize the EHD ion-drag mechanism as applied to micro flowing of liquid nitrogen. Ion-drag is designed to employ a single-phase incompressible liquid with a large dielectric constant as the working

liquid. Therefore, the major driving force in an ion-drag EHD is the Coulomb force, which requires the existence of free charges within the working liquid.

### 2.3.4 Dimensionless Form of the Governing Equations

To make the EHD governing equations independent of the measured units, the EHD governing equations are rewritten in terms of dimensionless parameters. Dimensionless parameters are chosen according to the recommendations of the IEEE-DEIS EHD Technical Committee (2003). The system of equations, which was developed, based on a unipolar charge injection assumption is mainly adapted from Shoostari's work (2004).

Table 2-1. Dimensionless parameters based on conservation equations (Tabulated in IEEE-DEIS EHD Technical Committee 2003).

Symbol	Expression	Name
Re	$LU_0/v$	Reynolds number
E <sub>hd</sub>	$\rho_e E_0 L^3 / \rho v^2$	EHD number
Md	$\epsilon_0 E_0^2 L^2 / \rho v^2$	Masuda number
Sc <sub>i</sub>	$v/D$	Ion Schmidt number
F <sub>E</sub>	$\mu_e E_0 L / D$	Ion drift number
Re <sub>e</sub> *	$\epsilon U_0 / \sigma_e L$	Electric Reynolds number

To nondimensionalize the governing equations, the following terms are used

$$\nabla^* = L\nabla, \rho_e^* = \frac{\rho_e}{\rho_{e0}}, E^* = \frac{E}{E_0}, u^* = \frac{u}{U_0} \quad (2.11)$$

The dimensionless parameters used in this study are tabulated in Table 2-1. Thus equation can now be expressed as

$$\nabla^* \cdot (\varepsilon_r E^*) = \frac{E_{hd}}{Md} \rho_e^* \quad (2.12)$$

The charge conservation law, can be change to

$$\frac{\partial \rho_e^*}{\partial t^*} + \frac{FE}{E_{hd} \cdot \text{Re} \cdot \text{Sc}_i} \nabla^* \cdot J^* = 0 \quad (2.13)$$

where the dimensionless current density is defined as

$$J^* = \frac{L^3}{\rho \nu^2 \mu_e} J \quad (2.14)$$

Therefore, further equation can be nondimensionalize as

$$J^* = \frac{\text{Re} \text{Sc}_i \text{Md}}{\text{Re}_e F_E} E^* + E_{hd} \rho_e^* E^* + \frac{\text{Re} \text{Sc}_i E_{hd}}{F_E} \rho_e^* u^* \quad (2.15)$$

The momentum equation, equation, can be rewritten as

$$\left[ \frac{\partial u^*}{\partial t^*} + (u^* \cdot \nabla^*) u^* \right] = -\nabla^* p^* + \frac{1}{\text{Re}} \nabla^{*2} u^* + g^* + f_e^* \quad (2.16)$$

where the dimensionless electrohydrodynamic body force is defined as

$$f_e^* = \frac{L f_e}{\rho U_0^2} \quad (2.17)$$

And finally, the EHD body force for a non-compressible single-phase flow can be expressed as in equation

$$f_e^* = \frac{E_{hd}}{\text{Re}^2} \rho_e^* E^* \quad (2.18)$$

### 2.3.5 Equivalent Model

Another way of understanding the behavior of electrostatic inkjet mechanism is to use numerical simulation based and equivalent model (Ahsan Rahman, 2009). In case of numerical simulation, flow fields inside inkjet nozzles are difficult to simulate using CFD because of the complex boundary conditions associated with the problem. For instance, it is difficult to properly model the inkjet phenomenon precisely. To overcome aforementioned problems analytical techniques have been used to analyze the fluid flow. To analysis the phenomena, equivalent electromechanical model is also suggested for more simplification of the process. With no electric field and magnetic field; a constant electric field can be approximated as given:

$$\vec{\nabla} * \vec{E} = 0 \quad (2.19)$$

By keeping curl of the electric field zero; maintaining:

$$\frac{\partial B}{\partial t} = 0 \quad (2.20)$$

The equation (from faraday's law) indicates that the electrostatic doesn't require absence of magnetic field; rather it says that the field should be kept constant. As the electric field is irrotational as shown in the Figure 2.2, it is possible to express the electric field as the gradient of a scalar function, called the electrostatic potential. The electrostatic potential at a point can be defined as the amount of work per unit charge required to move a charge from infinity to the given point, mathematically can be expressed as :

$$\vec{E} = -\vec{\nabla}\phi \quad (2.21)$$

Where, E is the electric field, points from regions of high potential,  $\phi$ , to regions of low potential.

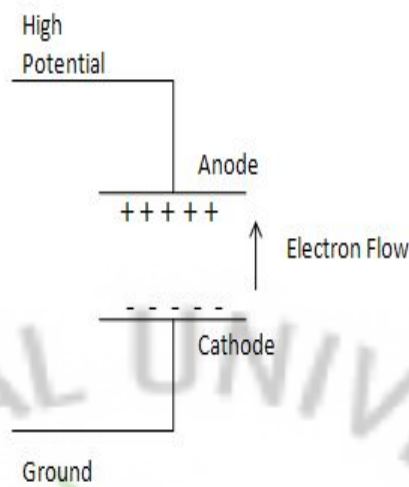


Figure 2.2: The basic concept of electric field

The force on any charge particle in the presences of electric field can be given as :

$$F = Eq \quad (2.22)$$

Where  $q$  is the charge particle and  $E$  is the electric field and can be given as :

$$E = \frac{q}{4\pi\epsilon_0 r^2} \quad (2.23)$$

Where  $Q$  is the charge and  $\epsilon_0$  is the dielectric constant and  $r$  is the distance.

In equivalent model, the stable meniscus can be visualized as the mass on the surface of the orifice of the nozzle. The model and the equivalent model are shown in the Figure2.3. Mathematical, the equivalent model can be expressed as:

$$F_{net} = m\ddot{x} + Kx + B\dot{x} \quad (2.24)$$

Where  $F$  is the force applied on the droplet,  $m$  is the mass of the droplet having metallic contents and solvent, and spring ( $K$ ) and damper ( $B$ ) elements depends upon the ink properties like surface tension, viscosity and intermolecular forces. The droplet emission only starts when the net force on the mass greater than the force other all forces on meniscus.

$$F_{net} > m\ddot{x} + Kx + B\dot{x} \quad (2.25)$$

The vibration and development of cone shape in the meniscus can be given as:

$$F_{0 \rightarrow \max} = m\ddot{x} + Kx + B\dot{x} \quad (2.26)$$

At equilibrium state, when no droplet is being generated the equation can be given as:

$$F_{net} = 0 = m\ddot{x} + Kx + B\dot{x} \quad (2.27)$$

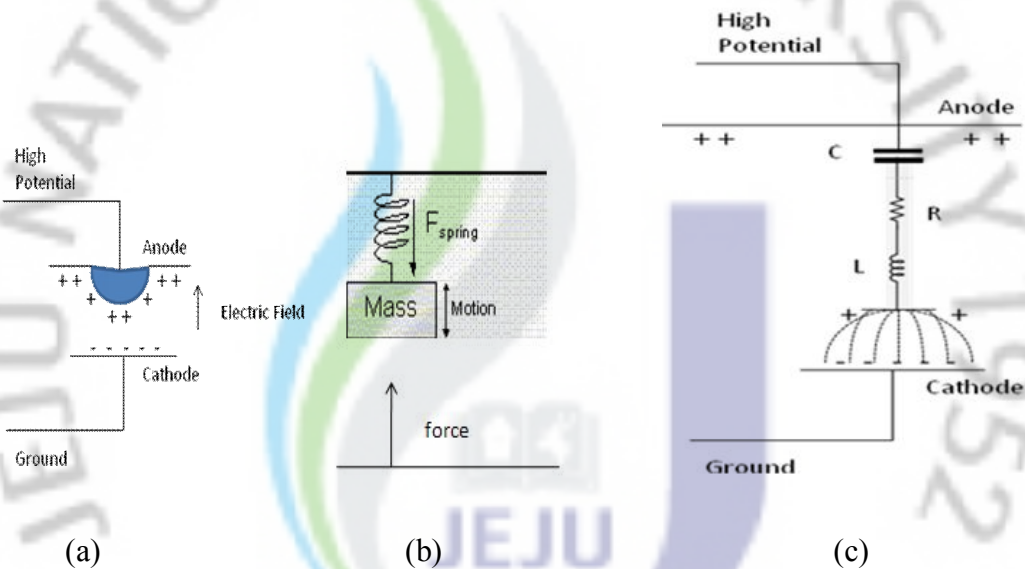


Figure 2.3: (a) The droplet mechanism in electrostatic system (b) the equivalent mechanical model and (c) representing equivalent electrical model

And equivalent electrical model expression can be given as:

$$Applied\ Potential = L\ddot{q} + R\dot{q} + \frac{1}{C}q \quad (2.28)$$

Where L is inductance, R is the resistance due to the other forces, C indicates the fluid resistance and properties and q is the charge transferred between time  $t_o$  and  $t_f$  can be given as:

$$q = \int_{t_o}^{t_f} Idt \quad (2.29)$$

This equation is representing not only the stable meniscus phase but also the when one droplet per force being generated.

In general terms, for the stable meniscus and stable drop-on-demand generation through nozzle head, (inter and intra) molecular forces should be equal to molecular forces of the system values. In this problem, it can be divided this into two cases, namely stable meniscus and stable drop generation behavior. For obtaining the stable meniscus shape, the main parameters include surface tension of fluid which is countering the effect of the pressure applied by the flow of the ink and gravity. Whereas, the stable on- demand behavior needs the study of the electrical forces as shown in the Figure 2.4.

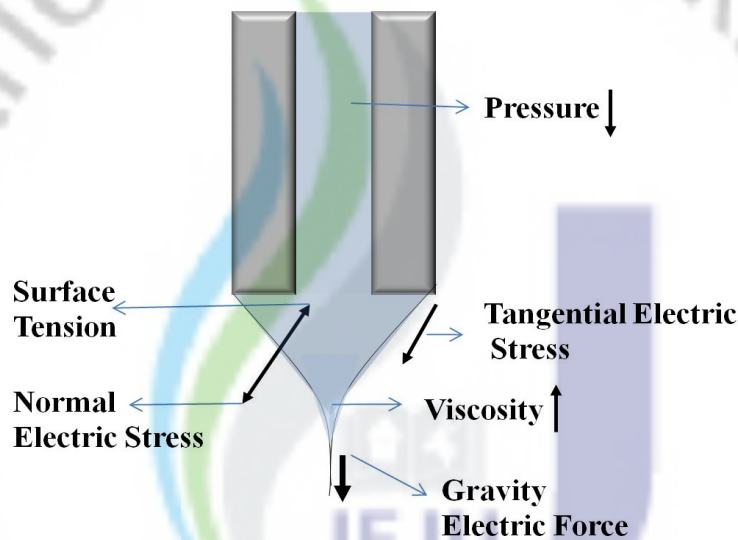


Figure 2.4: The effect of forces in the nozzle of electrostatic inkjet system

But to predict the meniscus shapes both theoretically and experimentally under the influence of given electric pressure and hydrostatic pressure, the electrostatic and hydrostatic equations should be solved simultaneously. The Figure 2.5 shows complete model diagram, superimposing both the models.

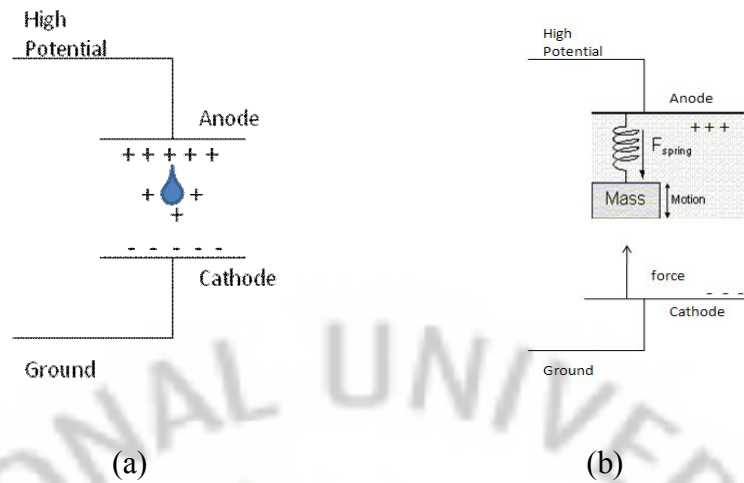


Figure 2.5: (a) The droplet generation in electric field and (b) the equivalent electro-mechanical model representing electrostatic model.

The maximum meniscus extension is presented as a function of voltage, surface tension, hydrostatic pressure, orifice diameter, material and electrode spacing for tube-plane geometry, surface of nozzle and its relation to fluid properties. When the system is in equilibrium the net force applied on the ink droplet is equal to surface tension and can be given as:

$$F_g - F_{st} + F_e = 0 \quad (2.29)$$

Where  $F_g$  is the force due to gravity,  $F_{st}$  is force due to the surface tension and  $F_e$  is the electrostatic force. Electrostatic (capacitive) energy relies on the changing capacitance, duty cycle and energy transformed each time. The energy required to generate the drop should be characterized by their power density, rather than energy density. After the generation of droplet the force on the model can be represented as:

$$F_{\max \rightarrow 0} = m\ddot{x} \quad (2.30)$$

Thus, the electrical potential energy also can be changed by changing distance between two charges. Electric potential energy equals to the electric potential energy divided by charge.

$$PE = qEd \quad (2.31)$$

Where,  $q$  is the charge of drop,  $E$  is electric field produced and  $d$  is the distance between the two charges. But voltage can be given as:



$$V = Ed \quad (2.32)$$

Thus equation (13) can be reduced to:

$$PE = Vq \quad (2.33)$$

But above mentioned case is applicable when the electric field and gravity is the only force on the nozzle orifice. If the flow rate is also applied on the nozzle then the net force can be given as:

$$F_g - F_{st} + F_e + F_q = F_{net} \quad (2.34)$$

Where, the  $F_q$  is the applied flow rate on the system. Due to electrical forces the Maxwell effect will be applied on the nozzle orifice. Due to effect of the Maxwell forces on the nozzle orifice, the effect of the gravity is negligible, as the other forces on the meniscus (like surface tension, electrical stress, viscosity, pressure and electric field) will overcome it. Thus the above equation may reduce to:

$$F_e + F_q - F_{st} = F_{net} \quad (2.35)$$

When the surface of a meniscus is subjected to an electric field, the field causes a deformation of the meniscus and eventually a stable liquid meniscus is formed again. The surface of the liquid meniscus is subjected to surface tension  $\sigma_s$ , hydrostatic pressure  $\sigma_h$  and electrostatic pressure  $\sigma_e$  is valid at each point on the liquid surface, given as:

$$\sigma_h + \sigma_e + \sigma_s = 0 \quad (2.36)$$

$$\sigma_h = \rho g \Delta h \quad (2.37)$$

$$\sigma_e = E_n^2 / 2\epsilon_r \quad (2.38)$$

Where  $\rho$  is the density of liquid,  $g$  the acceleration due to gravity,  $\Delta h$  the liquid level difference between the container and the free end of the nozzle,  $\epsilon_r$  is the relative permittivity of the liquid to vacuum permittivity, and  $E_n$  the electric field strength normal to the liquid surface. Li et al has explained this behavior, that in the Electro-

hydro dynamics spraying process, the normal electric stress is likely to produce a dripping mode while the tangential electric stress will move liquid from the meniscus surface to the apex of the meniscus to form a jet. And thus flow rate is required to compensate fluid in the meniscus is directly proportional to the backflow of fluid due to the electrical stress. Thus, the governing force for the ejection of the droplet is electrostatic force since the flow rate is provided to maintain the steady level of ink at the orifice outlet. Whereas the gravitational force has little contribution due to the high fluidic resistance in the micro channel.

## **2.4 Effects of Parameters**

Effects of different parameters are summarized here from literature. The aim of this section is to develop the basis for the head design based on equations analyzed in last sections and research. This section summarizes the findings and details of others researcher.

### **2.4.1 Surface Tension**

The drop on demand and cone jet formation occurs only when the surface tension is overcome by the applied force. Thus, with higher surface tension the critical voltage required to generate the drop from the meniscus also increase. As experimentally verified by Smith by using water with different concentrations of nonionic surfactants, the square-root dependence between the surface tension and the onset voltage is anticipated. The stronger the required electric field, the more chance that electrical discharges will occur in the air surrounding the cone. Stronger electric fields will also result in a higher free surface charge at the cone surface. This results in a higher electric current through the cone and jet. A higher current results in a higher droplet charge. The droplet size is often considered to be independent of the surface tension. But Poon also establishes that surface tension force can be utilized to counteract Brownian motion of submicron jets and improve the deployment accuracy.

### **2.4.2 Viscosity**

Viscosity was found to have little influence on the current, and the droplet size, as long as the radial profile of axial liquid velocity in the jet was almost flat. With increasing viscosity, the wavelength at jet break-up increases as can be expected from jet break-up theory. However, with increasing viscosity, the jet break-up also becomes slower. As a result the jet becomes longer, and has more time to be accelerated by the electric field. So, at jet break-up the jet diameter has decreased. As a result the increase in droplet size due to a longer wavelength is largely compensated by a decrease in the jet diameter. So, the droplet size is almost not affected by viscosity. When the liquid properties are kept constant, then there is a threshold value for the influence of the viscosity. When the viscosity is below this threshold value, then the radial profile of the axial liquid velocity is not flat anymore. The velocity at the jet surface is larger than in the jet center. As a result, the charge convection current is larger, and the total current is larger. A larger current means also a smaller droplet size. The threshold value for the influence of the viscosity depends on the jet diameter. This jet diameter depends mainly on the liquid flow rate and the liquid conductivity. The fluid viscosity can be increased to enhance the jet stability. Viscosity enhances the jet stability directly by damping the growth of disturbance and indirectly by decreasing the radial electric field strength at the jet surface.

### 2.4.3 Flow-rate

The overall flow rate is an important parameter in electrostatic jet printing; it involves the balance of electrical stress, capillary pressure, and applied pressure. Chen et al. suggested a Poiseuille-type flow rate relation for this type of system, according to

$$Q \approx \frac{\pi d_N^4}{128\mu L} \left( \Delta p + \frac{1}{2} \varepsilon_0 E^2 - \frac{4\gamma}{d_N} \right) \quad (2.39)$$

Where  $Q$  is the flow rate,  $\Delta p$  is the pressure drop,  $\mu$  is the viscosity of the liquid,  $d_N$  and  $L$  is the diameter and the length of the nozzle, respectively,  $\varepsilon_0$  is permittivity

of free space,  $\gamma$  is the surface tension of the air ink interface and  $E$  is the magnitude of electric field.

Flow rate also has significant effect on the jet diameter in the cone-jet transition. Jet diameter can be varied by two order of magnitude of jet diameter. Flow rate also affects the shape of the cone jet. Liquid flow-rate affects the critical potential required for the formation of steady cone-jet transition and resulting the shape of cone-jet. High the flow-rate, the lower required electric field strength and the smoother the transition near the conical apex. High flow-rate usually leads to a high entrance momentum and dynamic pressure within the cone, which affect the shape of the cone and flow pattern.

#### 2.4.4 Charge Relaxation Time

According to Panofsky and Phillips (1962), in a stationary homogeneous medium, the continuity equation can be combined with the conductivity equation  $J = \sigma_e E$  and the source equation to find a differential equation for  $\rho_e$ :

$$\frac{\partial \sigma_e}{\partial t} + \frac{\sigma_e \rho_e}{\varepsilon} = 0 \quad (2.40)$$

Above equation are an ordinary differential equation and its solution can be found by integrating with respect to time:

$$\rho_e = \rho_e e^{-t/\tau} \quad (2.41)$$

where the characteristic time,  $\tau_e$ , is

$$\tau_e = \frac{\varepsilon}{\sigma_e} \quad (2.42)$$

The characteristic time,  $\tau_e$  is usually known as the charge relaxation time of the medium. It is the time it takes for the stationary condition to take place after the initiation (or injection) of an electric charge flow. Charge relaxation time has the typical values illustrated in Table 2-2 (Haus and Melcher 1998).

Table 2-2. Charge relaxation times of typical materials

Substance	$\sigma$ (S/m)	$\frac{\epsilon}{\epsilon_0}$	$\tau_e$
Copper	$5.8 \times 10^7$	1	$1.5 \times 10^{-19}$
Water, distilled	$5.8 \times 10^{-4}$	81	$3.6 \times 10^{-6}$
Corn oil	$5.8 \times 10^{-11}$	3.1	0.55
Mica	$10^{-11} - 10^{-15}$	5.8	$5.1 - 5.1 \times 10^4$

As shown in Table 2-2, the relaxation time in conductive media is much less than in insulators because it takes less time for the charges to dissipate in a conductive media. It should also be noted that the above discussion only applies to homogenous media. If the medium is not homogenous, the spatial dependence of the conductivity and the dielectric constant must be taken into account in the integration of equation.

#### 2.4.5 Electric Reynolds Number

Electric Reynolds number,  $Re_e$ , is a well-established number which reflects the efficiency of the energy conversion process within an EHD. It is defined as the ratio of two characteristic times: the charge relaxation time of the fluid,  $\tau_e$ , and the mechanical transport time,  $\tau_m$ :

$$Re_e = \frac{L/U}{\epsilon/\sigma_e} = \frac{\tau_m}{\tau_e} \quad (2.43)$$

In EHD with dielectric working liquids, the liquid phenomenon takes place when the charge relaxation time is much shorter than the mechanical transport time or, according to Crowley et al. (1990), when the fluid passes from one electrode to the other before the charge has time to flow backward. They showed that for high

efficiency, the Reynolds number should be low. That requires a longer charge relaxation time,  $\tau_e$ , or a high-speed flow:

$$U > \sigma_e L / \varepsilon \quad (2.44)$$

That also indicates that during actual EHD phenomenon within a liquid, the conduction current,  $\sigma_e E$ , is negligible compared to the convection current,  $\rho_e u$ . Because of its very small conductivity, liquid nitrogen has a pretty high charge relaxation time ( $\varepsilon/\sigma_e$ ) compared to more conductive liquids such as HFE-7100.

#### 2.4.6 Current – Voltage Characteristic Curve

In nonpolar liquids, the electric current displays a dependence on the electric potential difference. Generally, four regions can be distinguished in the trend shown in Figure 2.6 (Schmidt 1997).

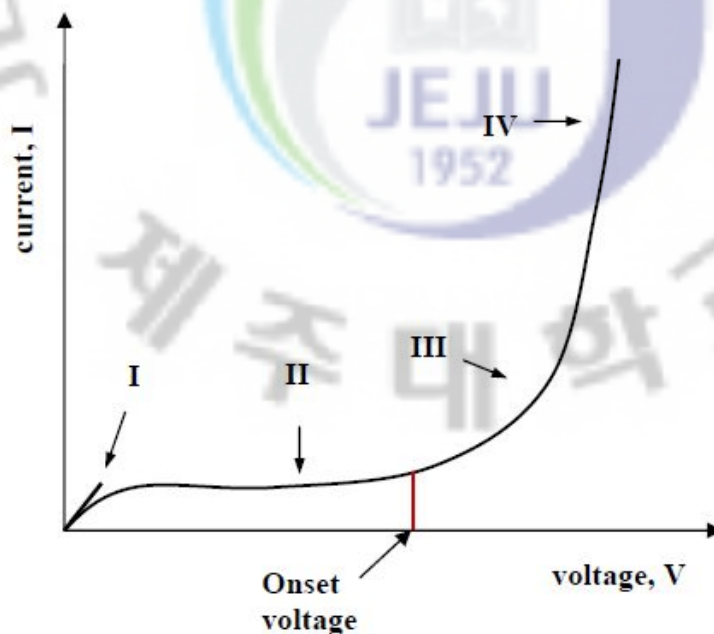


Figure 2.6: I-V Characteristic of a nonpolar liquid (Schmidt 1997).

In Region I, where the electric field is at its lowest, the conduction mechanism is Ohmic. The slope in this region represents the conductivity of the liquid. In insulating liquids, this is associated with the dissociation of the impurity molecules existing in the working fluid.

$$V = IR \quad (2.45)$$

Region II is established as we move to higher voltages. In this regime, the current remains nearly constant with the voltage as it reaches a saturation state or the so-called space charge limited current (SCLC). The space charge limit sets in at relatively low electric fields when the ion generation rate is faster than the rate at which ions reach the opposite-side electrodes. In this situation, each additional unipolar charge weakens the electric field. When the electric field becomes too low, charges can no longer be removed from the electrodes, as the charges already present in the liquid repel them. That is why it is not always possible to inject a large amount of ions into a medium (Crowley et al. 1990).

At higher voltages, a sharp increase of current with voltage begins (Region III). This is due to either charge injection at the electrodes or charge multiplication in the bulk. In simple molecular liquids, the dissociation of the bulk liquid molecules is weak, and the charge carriers are mainly injected at the electrode/liquid interface. If the voltage is further increased, the dielectric strength of the liquid can be exceeded. This eventually leads to dielectric breakdown of the liquid and causes a destructive short circuit between electrodes (Region IV).

In going from Region I to II, the ions generated from dissociation of impurity molecules within the liquid are often accumulated and absorbed by the electrodes. This can change the electrodes' work function and thus change the voltage required for the emission process in the ion-injection regime (Region III). Therefore, care must be taken in handling the working liquid and the test rig properly, as any level of impurity changes the ionization process and even leads to dielectric breakdown of the liquid. In dealing with EHD, the goal is to limit the operation regime in Region

III to prevent a possible breakdown, and thus to ensure a repeatable and stable performance. The voltage at which the transition from Region II to III begins is called the onset voltage.

#### **2.4.7 Onset Voltage**

One of the determining factors in selecting the proper design is the onset voltage. As with most microelectromechanical devices, the trend is to lower the electricity consumption of these devices to make them compatible with microelectronic devices and to save electricity. Therefore, it is necessary to have a clear estimation of onset voltages. Onset voltage could not be calculated theoretically due to the complexity of the EHD nature; therefore, a mathematical approach is needed to estimate its value from experimental data for every single design.

#### **2.4.8 Effect of Electrode Spacing**

The onset values are believed to be a function of the local electric field and the energy barrier at the metal/liquid interface. The energy barrier at the metal/liquid interface is a function of only the metal work function and liquid ionization energy, and is therefore independent of electrode geometry and distance. The local electric field, on the other hand, is a function of the electrode geometry and the emitter-collector distance.

#### **2.4.9 Effect of Voltage Polarity**

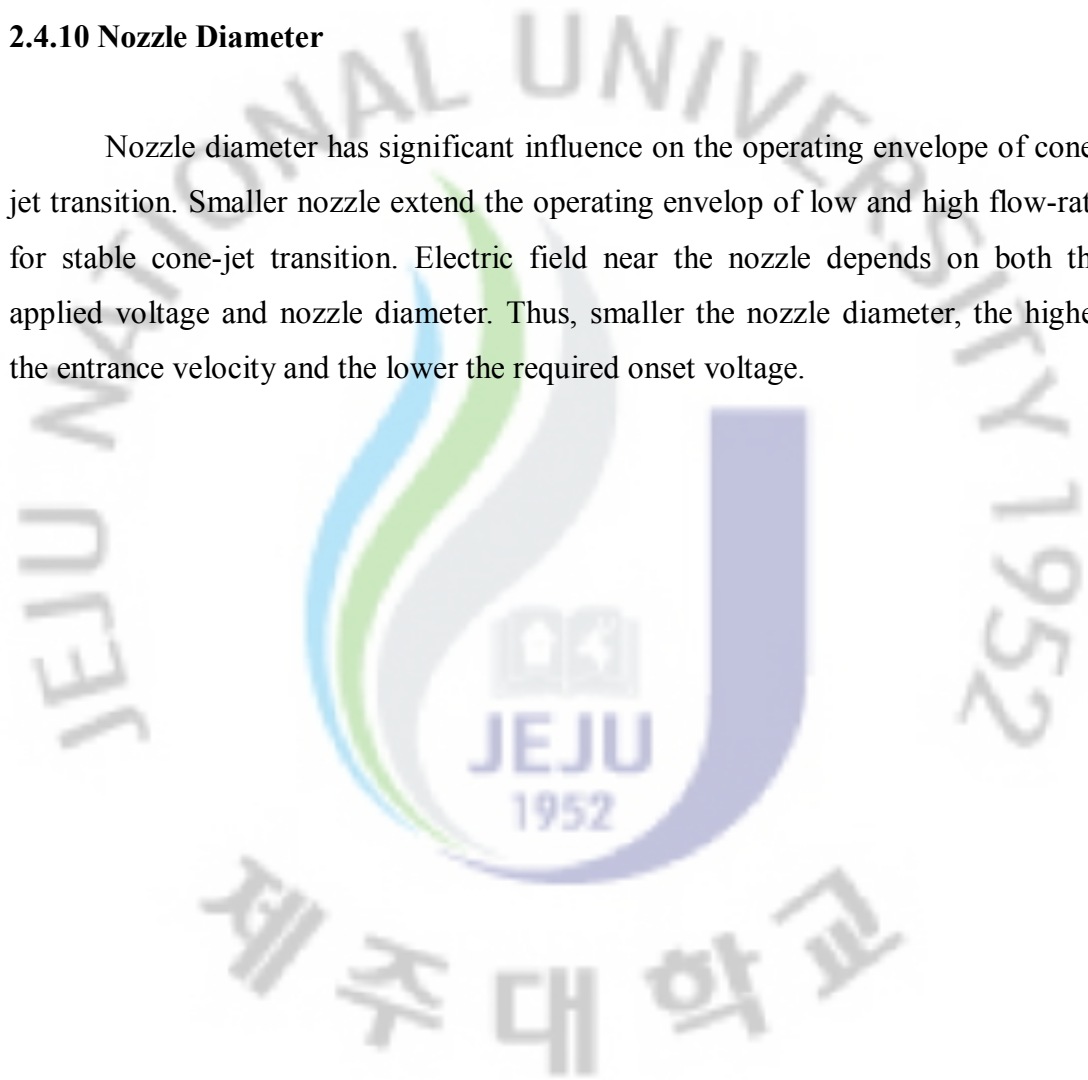
In most liquids, the onset voltage of the EHD pressure generation is lower with a certain polarity. That polarity can be either positive or negative, depending on the work function of the metal electrode and the ionization energy of the dielectric liquid. Schmidt (1997) on the energy barriers for fieldionization (the primary ion generation process at the positive electrode) and fieldemission (the primary ion or electron generation process at the negative electrode) phenomena at the metal electrode/liquid interface was discussed extensively. Schmidt indicated that for most



non-polar liquids the energy barrier of field emission is less than that of field ionization. DC voltage with positive polarity was used for most of the tests in this study, in part because scientists such as Krahenbuhl et al. (1994) have shown that the breakdown with (+) polarity is less aggressive than that with (-) polarity at the same voltage level.

#### **2.4.10 Nozzle Diameter**

Nozzle diameter has significant influence on the operating envelope of cone-jet transition. Smaller nozzle extend the operating envelop of low and high flow-rate for stable cone-jet transition. Electric field near the nozzle depends on both the applied voltage and nozzle diameter. Thus, smaller the nozzle diameter, the higher the entrance velocity and the lower the required onset voltage.



## 3. Head Design and Fabrication

In this chapter, based upon the different parameters and equations (analyzed in last chapter), an idea of the head design is proposed and analyzed. First of all placing of electrode is analyzed. For counter electrode, a ring type ground is being used. The reason of integrated the nozzle with ring ground is to use the head in one package and reduce the effect and dependence of substrate on stable meniscus, dripping and jetting. And optimization of the head, removing the back flow and minimizing the effect of the disturbance at the nozzle orifice, silica capillary is proposed and analyzed. Simulation is also performed for in-detail analysis. And based on theoretical and simulated analysis a head is proposed and fabricated.

### 3.1 Electrode Design and Geometry

Different types of electrode geometry are under investigation for drop generation through electrostatic inkjet head. But the key feature is to minimize the effect of the substrate on drop generation which in turn decreases the applied potential and precise drop position. Therefore in this section we will summarize the effects of the different position of electrodes for generating precise printing.

For analysis of different electric field different patterning techniques are studied. The Figure 3.1 shows the simulations of basic patterning setup. In electric field simulations, red portion represents the nozzle and the bottom blue portions represent the ground portion. Figure 3.1 shows the effect of different placements of counter electrodes where arrow indicates the direction of the field and the color indicates the strength, where black is the strongest and blue is the weakest. The Figure 3.1(a) shows pin to pin (P2pin) and Figure 3.1 (b) shows the pin to plate (P2plate) setup (Ahsan Rahman, 2008). It can be seen from the simulations, that electric field is more focused and directed in the case of P2pin setup. For further verification of phenomena, experiments were also conducted and the results are summarized in Table 3-1. For experiment purpose, particle based conductive ink is used.

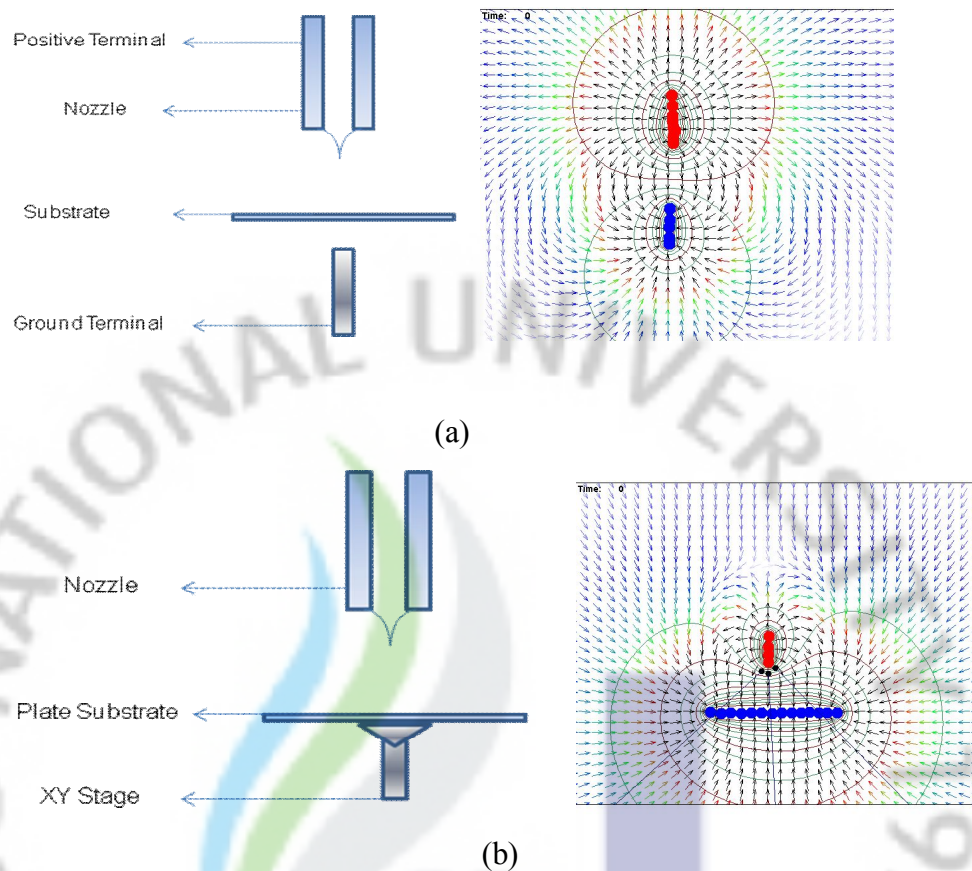
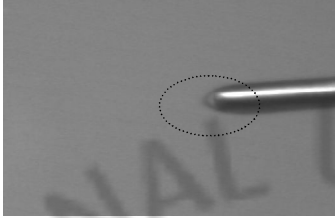
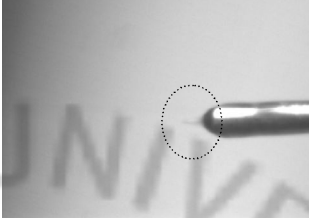
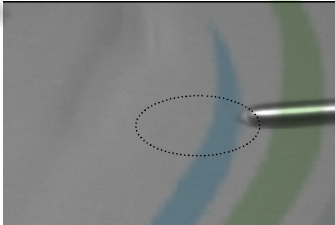
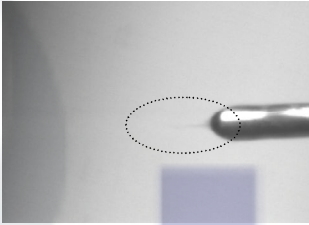
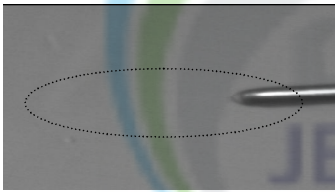
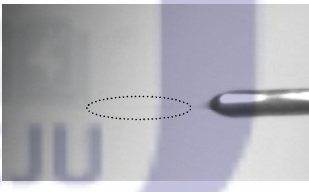
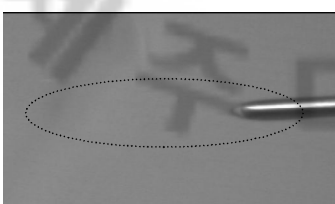
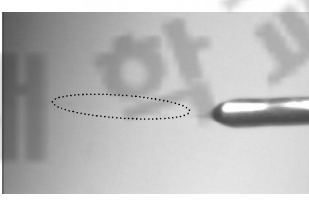


Figure 3.1: (a) Pin to Pin setup and (b) Pin to Plate setup

From the experiment results, it can be observe that keeping all the other parameters same Pin to pin give more better results, as the electric field is only coming from the one specific nozzle point whereas in the case of pin to plate a uniform electric field is supplied to the base terminal and drop will be attracted by each point with equal force so more random drops. From above it can be evaluated that the effect of electric field on the nozzle and droplet, which in resultant shows more spreading and splashing along the printed line. But there is also a drawback in the case of P2pin set is the alignment of the electrodes. And another important factor is the position of substrate. The substrate is placed between the nozzle and the counter electrode which make onset voltage and onset electric field depending upon the dielectric constant of substrate.

Table 3-1: The deflection of nano particles in Pin to Pin and Pin to Plate experiment

<b>Pin to pin</b>		<b>Pin to plate</b>	
<b>Experiment stage and Remarks</b>		<b>Experiment stage and Remarks</b>	
1: At the start of experiment			1: At the start of experiment when cone shape is available on the nozzle
2: At the time "t" after starting of ejection of drop			2: At the time "t" after starting of ejection of drop
3: At slow speed the drop is following the path			3: At slow speed the drop is following the path
4: Even at relatively high speed the drop is following the pattern			4: At relatively high speed the drop is changing path as at ground uniform field is available

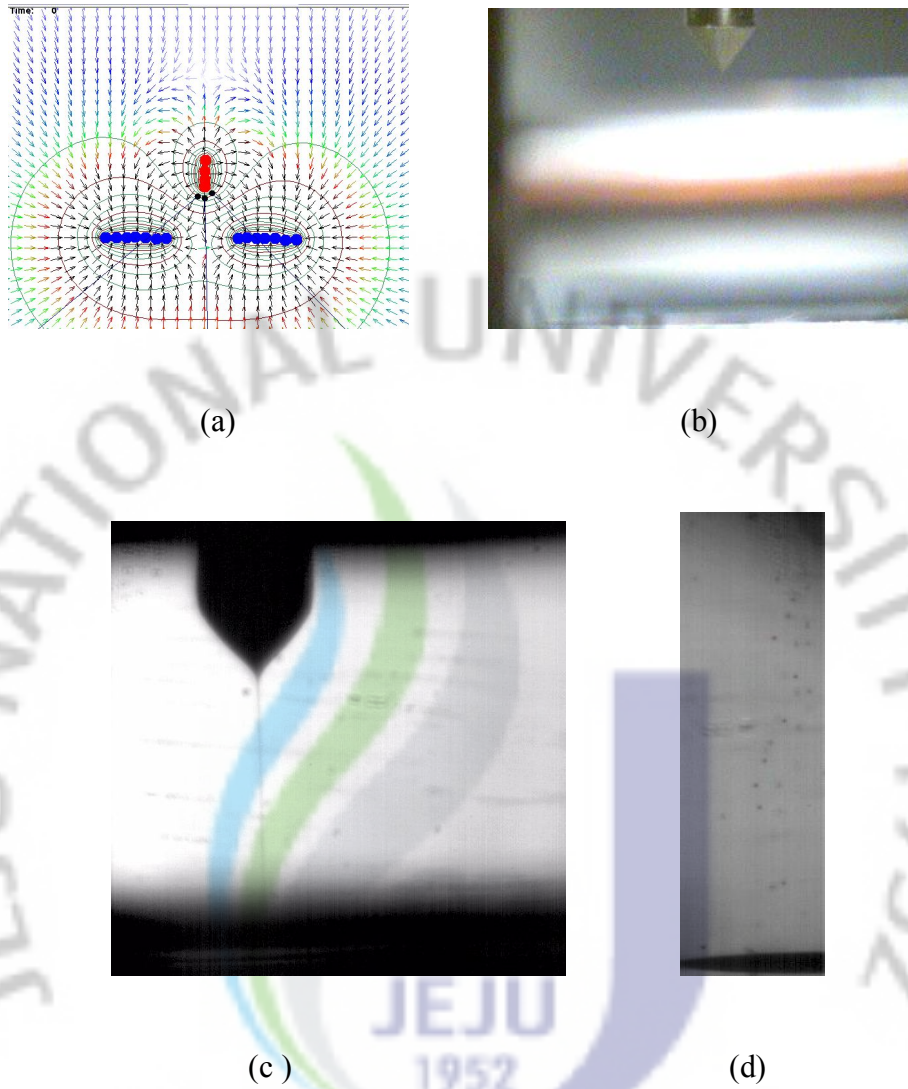


Figure 3.2: Showing the results of placement of electrode under the nozzle while printing through the jet (a) simulation results (b) the complete picture of the physical setup (c) the high speed image and high zoom the nozzle above the nozzle and (d) the high speed and high zoom image of the camera under the counter electrode (ground)

To overcome and reduce the effect of substrate, in literature and research different types of geometries, materials are used for the nozzle heads and even different attempts are made to integrate nozzle with the counter electrode. The reason of integrating nozzle with ring counter electrode is to use the head in one package and reduce the effect and dependence of substrate on stable meniscus, dripping and

jetting. But these techniques have flaw, the counter electrode attracts the droplet and before printing droplet changes its direction towards the ground instead of leading to substrate. To overcome this imperfection of printing, drop on demand and larger size of the counter electrode is proposed. But aforementioned technologies has its drawbacks as it lacks speed, accuracy of drop size from meniscus, placement on substrate and hurdle in designing of multi nozzle head to make possible for the direct writing at the industrial level. Since the components must be integrated to form a functional system in order to provide desired services, system-level complexities in both architecture. Even some researcher also used multiple counter electrodes to elongate the jet, but that also make printing very difficulty due to complex nature of geometry and electrodes. Figure 3.2 shows the effect of counter electrode below the nozzle. It also summarized the high speed image of the nozzle and effect on jet after it passes through the ground.

But to overcome the above affects this manuscript proposed a new novel idea of patterning through ring counter electrode to resolve the problem of printing through cone jet. The ring counter electrode is kept above the nozzle orifice. Patterning is done by maneuvering contour of electric field in such a way that even with the smaller length of jet, stable printing can be done. For better understanding and evaluation of this phenomenon, simulations were also performed. From literature, it has been found that radial effects of electric field produce more instability. To analysis the radial effects of electric field, simulations are performed. Figure 3.3 shows the effect of different placements of counter electrodes. And it's found that thicker the ground and away from the nozzle better the direction of the electric field for printing. For further verification, experiments were conducted. For experiment, a new head design is designed, with the ability of moving ground terminal at different position as shown in Figure 3.4.

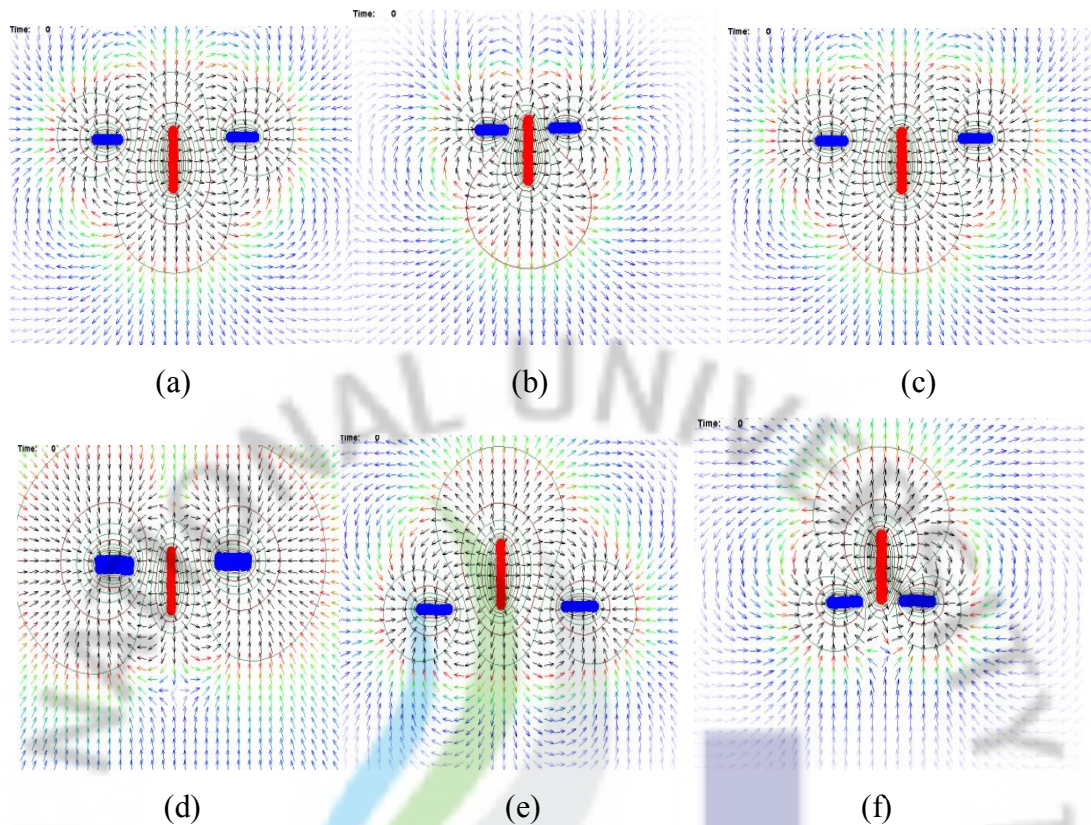


Figure 3.3: Shows the effect of different placements and dimensions of counter electrodes (a) shows the effect of the counter electrode at height beside the nozzle, (b) shows the ring counter electrode beside the nozzle and above the nozzle (c) shows the effect of ground distance (d) shows the effect of ground thickness and; (e) and (f) shows the effect of the placement ground near the tip of the ground with close and open ground.

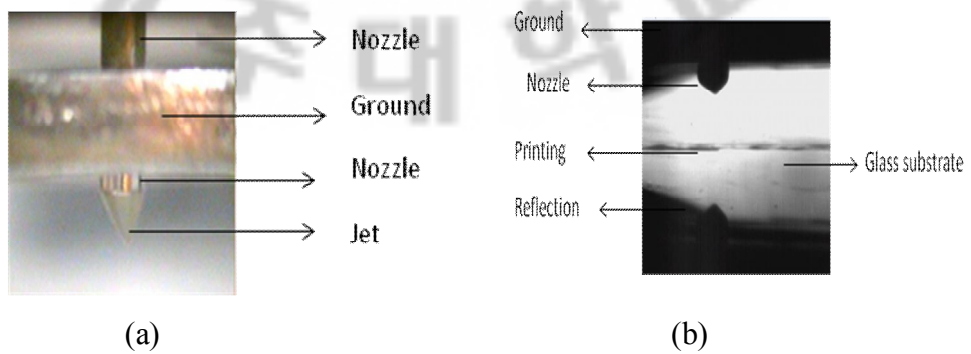


Figure 3.4: (a) Showing the microscope image and (b) shows the high speed camera image of printing through proposed head

And it's found that even very high conductive solution can be printed by using this technique as high conductive ink has very short jet length. But at the tip of the nozzle two main problems were observed: firstly at the nozzle tip stagnation were observed due to back flow problem of the solution. The suspended fluid at the orifice is very hard to control due to backflow problem. This back flow depends upon the conductivity and relaxation time of the ink solution. And secondly, the fluid, however, the vectors of the electric field are not focused near the cone, which may cause instability in the cone jet or push positively charged droplets outward. And which in resultant causes unstable jetting on substrate. Therefore, to remove this problem a silica capillary is inserted in the metallic capillary which is discussed in next section. On the applied side, the process can be used in paint spraying, electrostatic printing, electrostatic emulsification, fuel atomization in combustion systems and in space vehicle propulsion systems.

### 3.2 Introduction of Silica Capillary and Flow Channel

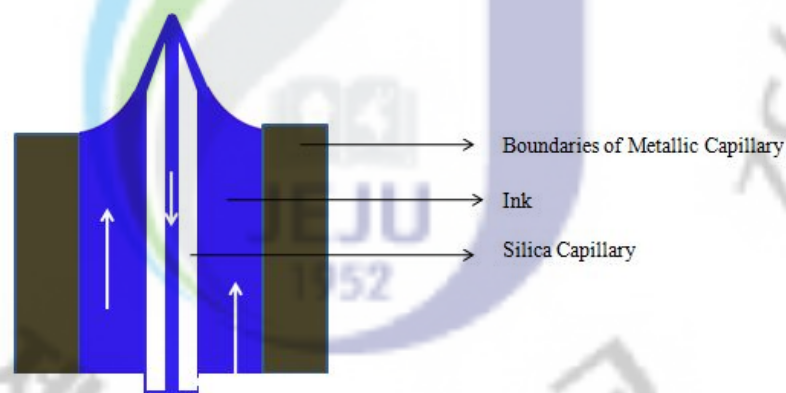


Figure 3.5: Schematic diagram of silica inside metallic capillary

The above technique is able to generate the jetting but it was observed experimentally that the jet was disintegrate and may cause instability in the cone jet or push positively charged droplets outward. Therefore, for stability of the jet a silica capillary is introduced in the head. Moreover, electrostatic inkjet have the backflow problem due to unionization and relaxation of the ink. Ink circulation mechanism in the printed electronics is very important for continues process of the printing through solvent. Solvent produces the coffee ring effect on the substrate; therefore it's very



important to deposit only nano particles on the surface of the substrate. Therefore, in this section an ink circulation mechanism is studied. The head works on extraction of droplets from the meniscus. Therefore the ink circulation mechanism is proposed on the meniscus as shown in the Figure 3.5 where arrows show the direction of fluid. The new novel idea is the ink circulation direction from bottom to up, the nozzle and head shape and the extraction technique of the fluid for printing. This technique can also be used to control the stable meniscus. The ink is supplied at the side. Figure 3.6 summarize the complete schematic diagram of the head. And for circulation purpose the ink is lead to upside. Stable meniscus can also be achieved by controlling ink regulator.

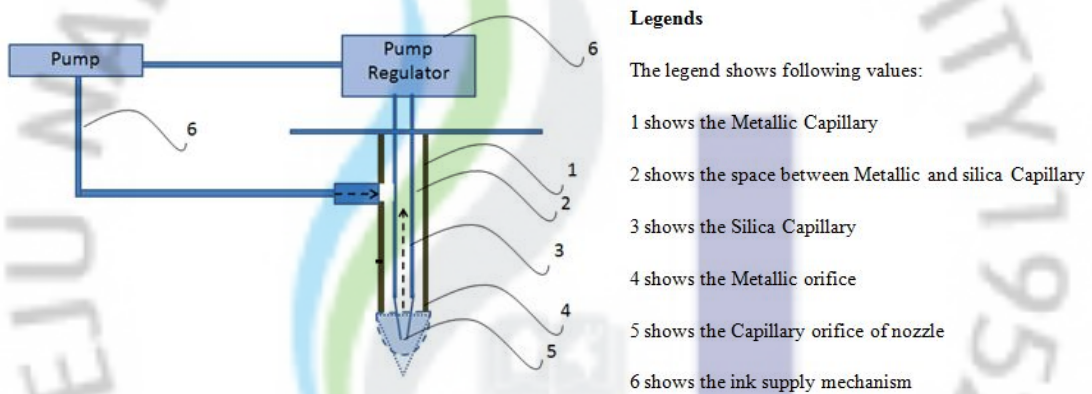


Figure 3.6: Ink circulation mechanism at the meniscus

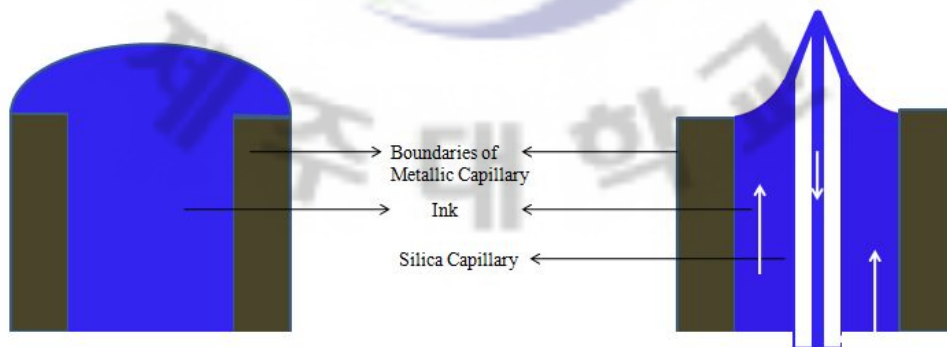


Figure 3.7. Ink and surface tension effect in metallic capillary and silica head

Moreover, the fiber position also helps to reduce the surface tension and allows using the higher surface tensions inks at low potentials. Figure 3.7 shows the ink and surface tension effect in metallic capillary and silica head. It can be seen that the silica head breaks the overall surface tension of the head and which in turn reduce the potential for making jet. The experimental and simulation study of this case is analyzed in later half of the chapter.

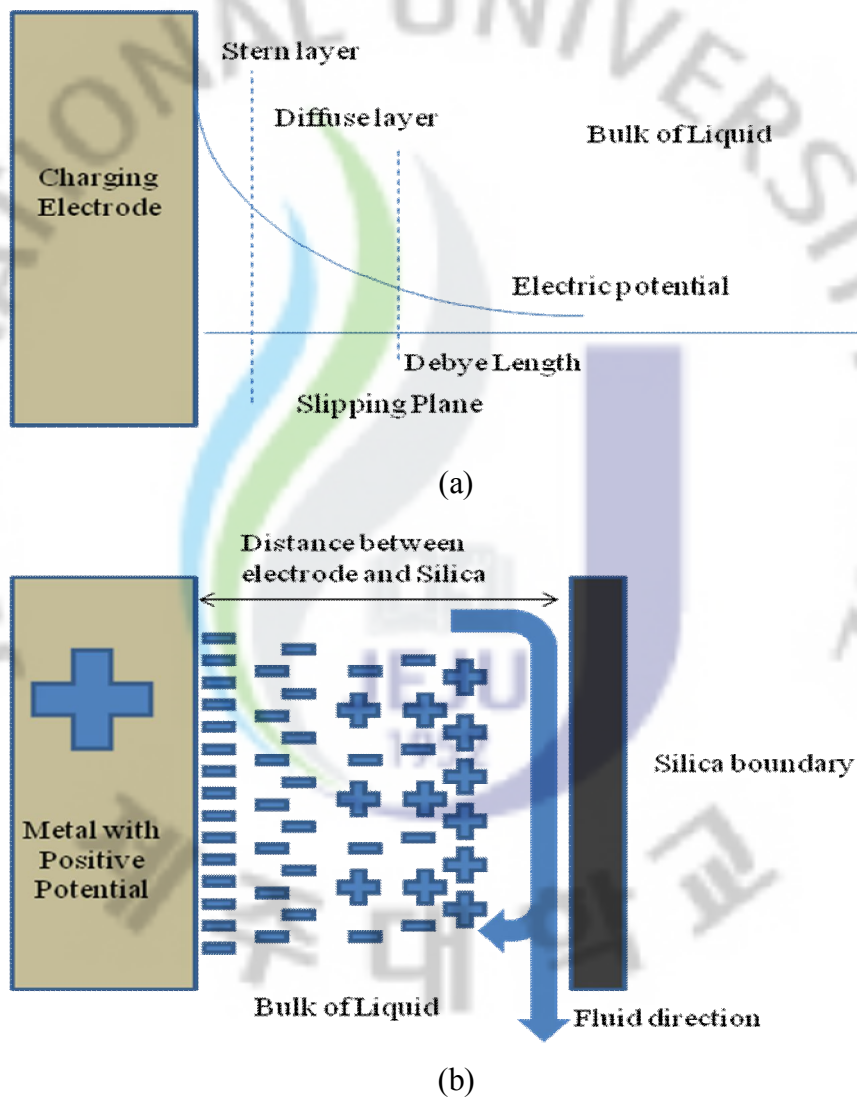


Figure 3.8: (a) Showing the effect of electric double layer in the nozzle and (b) showing the electric double layer in proposed model

The effective passage area for the ink is between the metallic and silica capillary is 50 $\mu$ m in this case. But this parameter can be varied depending upon ink properties like viscosity and particle size. This factor also helps to control the electric double layer (DL). The DL refers to two parallel layers of charge surrounding the object. The first layer, the surface charge (either positive or negative), comprises ions adsorbed directly onto the object due to a host of chemical interactions. The second layer is composed of ions attracted to the surface charge via the Coulomb force, electrically screening the first layer. This second layer is loosely associated with the object, because it is made of free ions which move in the fluid under the influence of electric attraction, thermal motion and the flow rate pressure rather than being firmly anchored. It is thus called the diffuse layer. And as shown in the Figure 3.8, electric potential decreases exponentially away from the surface to the fluid bulk.

The diffuse layer, or at least part of it, can move under the influence of tangential stress. There is a conventionally introduced slipping plane that separates mobile fluid from fluid that remains attached to the surface. Electric potential at this plane is called electrokinetics potential or zeta potential. It is also denoted as  $\zeta$ -potential. It's important to mention here that this is very critical to find an optimized distance between the electrode and the silica boundary, to reduce the DL effect in the nozzle less distance is preferable but this will make difficult to use the high viscous ink. Therefore it's very important to choose the optimized model for the head.

### 3.3 Numerical Analysis of Head

In this section the final design of the head is optimized for jetting as explained in the previous sections. For the circulation at the meniscus and breaking the effect of the surface tension, a silica based capillary is introduced in the metallic capillary. The metallic capillary is used for the charging of the ink. The parameters of the head design are tabulated in Table 3-2. Figure 3.9 (a) shows the schematic diagram of the proposed head design and Figure 3.8 (b) shows different parameters of the head.

Table 3-2. The parameter of nozzle

S/n	Parameters	Values
1	Metallic nozzle orifice	410um
2	Silica Capillary orifice	30um
3	Silica Capillary thickness	360um

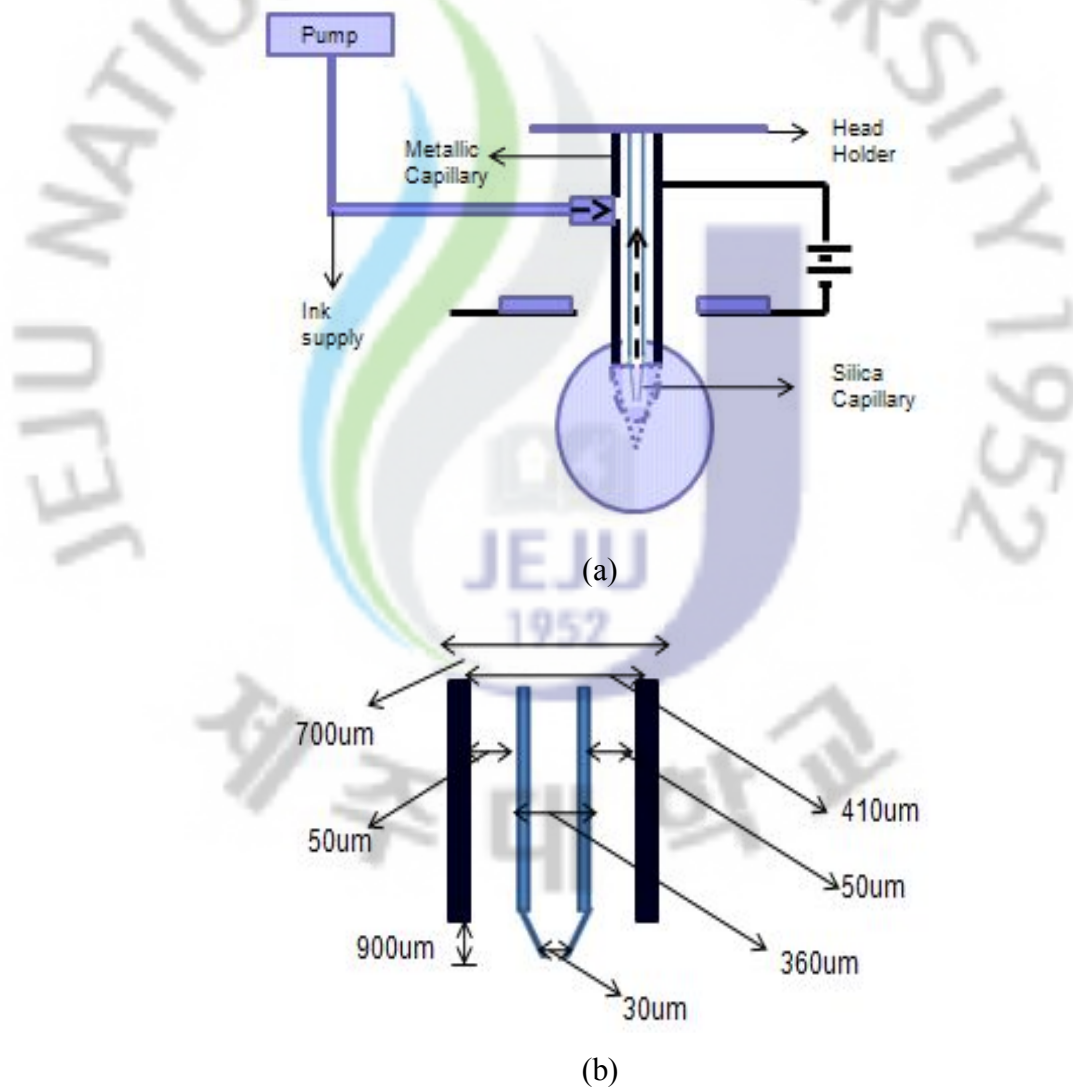


Figure 3.9: (a) Shows the schematic diagram of the proposed head design and (b) shows the parameters

### 3.3.1 Simulation

Electrostatic Inkjets system is a multi physical system, consists of many variables like voltage, frequency, distance and shapes of electrodes, capillary nozzle designs and orifice, ink parameters, etc. So, to analyses and study the behavior of each parameter in detail the benefit of simulation analysis (or numerical analysis) can be used. Therefore, for the further analysis of the head, simulations are done to deeply investigate the electrostatic inkjet process in this proposed head by using commercial available software COMSOL®. Figure 3.10 shows the model diagram of the head. The head model is designed to analysis the behavior of the head at different parameters. The ground is raised at different heights to analysis the behavior of the head. The various parameters are also summarized in the Figure 3.10.

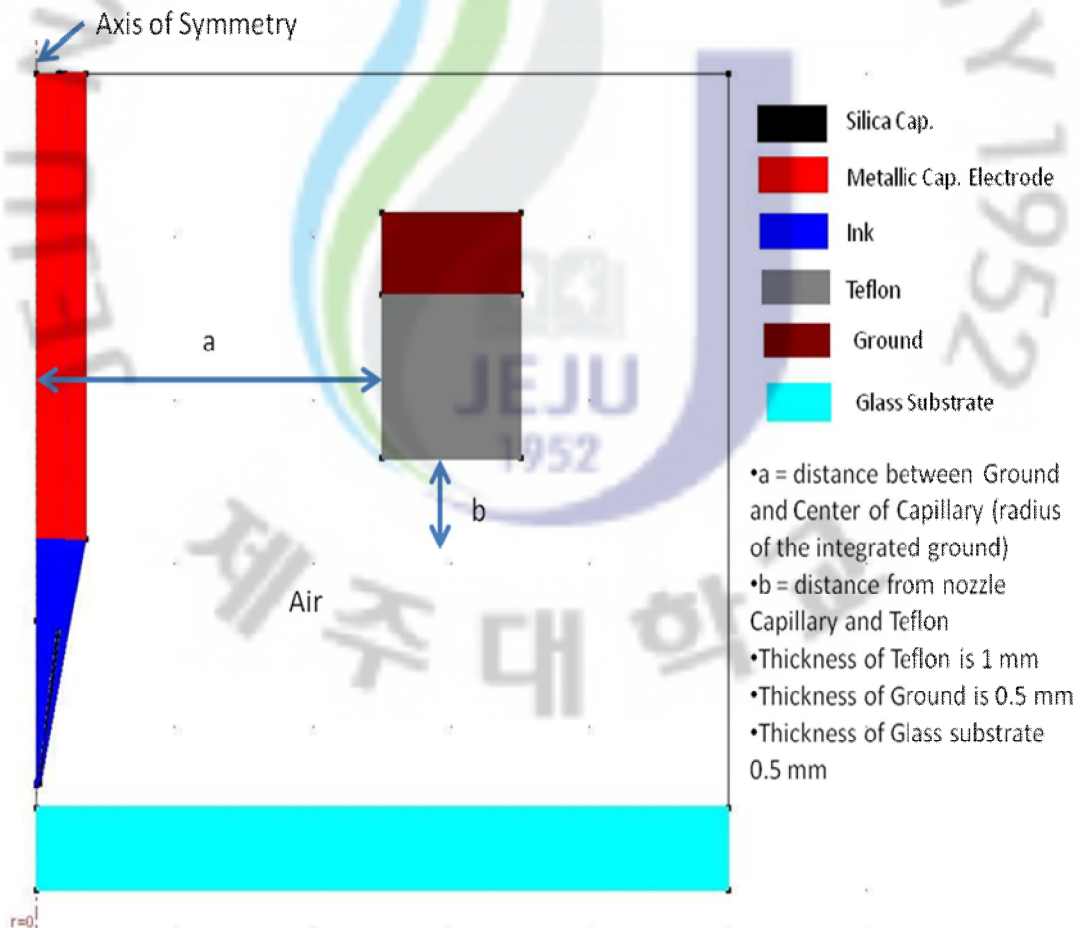


Figure 3.10: Finite Element model of the proposed head

In numerical simulation, in order to solve the complete behavior of EHD inkjet system the fluid dynamic and electric equation used is (Bruce R. Munson et al, 2002):

$$\rho \frac{du}{dt} = \nabla \cdot (T^m + T^e) \rho g \quad (3.1)$$

Where

$$T^m = -\nabla P + \eta \nabla^2 u$$

$$T^e = qE$$

And the effect of the polarization forces are neglected because in isotropic and incompressible fluid the permittivity has no gradient and the dielectric force is also equals to zero (R. J. Melcher, 1981).

$$\rho \frac{du}{dt} = \nabla P + \eta \nabla^2 u + qE + \rho g \quad (3.2)$$

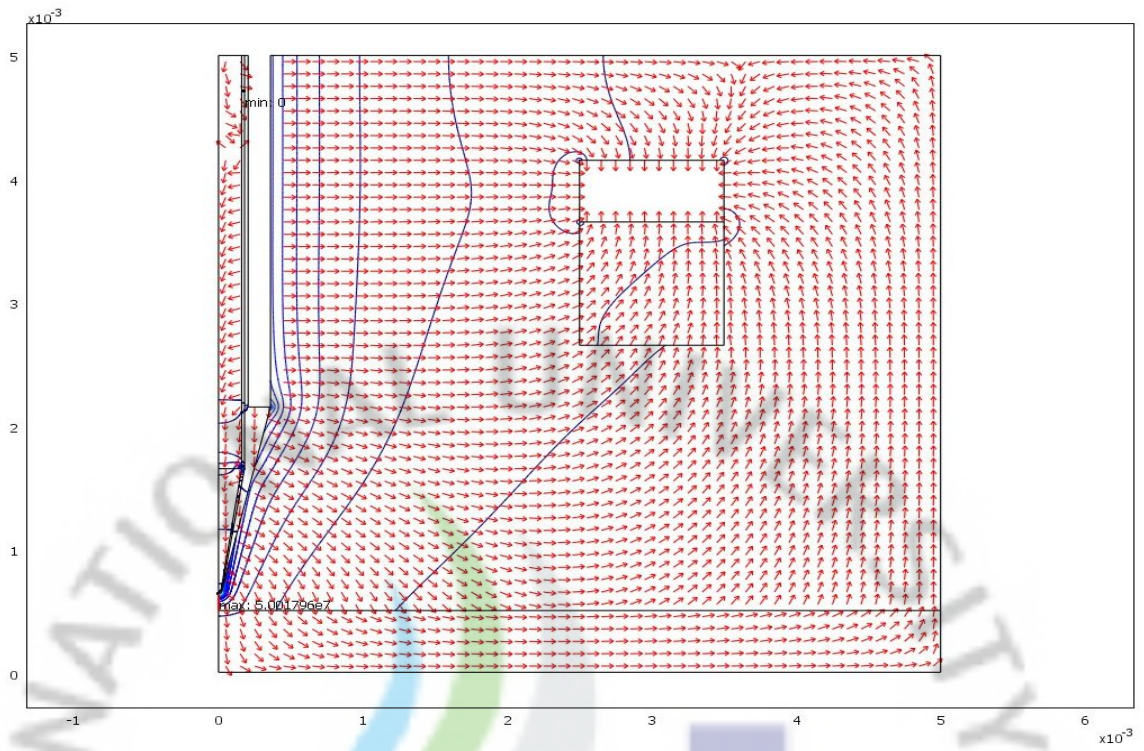
In order to simplify the problem axis symmetric model is used for the analysis purpose. The region near to the nozzle and the path of the drop was allotted large number of cells to capture the behavior of the problem. Total number of elements for 410 $\mu$ m diameter capillary case was 65700. Moreover, for simulation, areas of higher intensity of electric field at positive and negative terminals are also highlighted. And the contour and field vectors of electric field is analyzed. The electric field is estimated for each case, shown in the Tables by keeping all other parameters constant like the distance between the electrodes, ink and temperature. Thus, for the evaluation of the electrode experiment is conducted. Electric field is estimated at each point to find the optimal distance and voltage of each head to avoid corona discharge and the breakdown of the medium (air) between the positive and negative terminals.

For in detail study, the simulations were performed at different ground and nozzle position to estimate the behavior of the head. Also simulations are performed on different potentials. Table 3-3 summarizes the different cases. The study is divided in to nine different cases. The different values of a and b indicates the

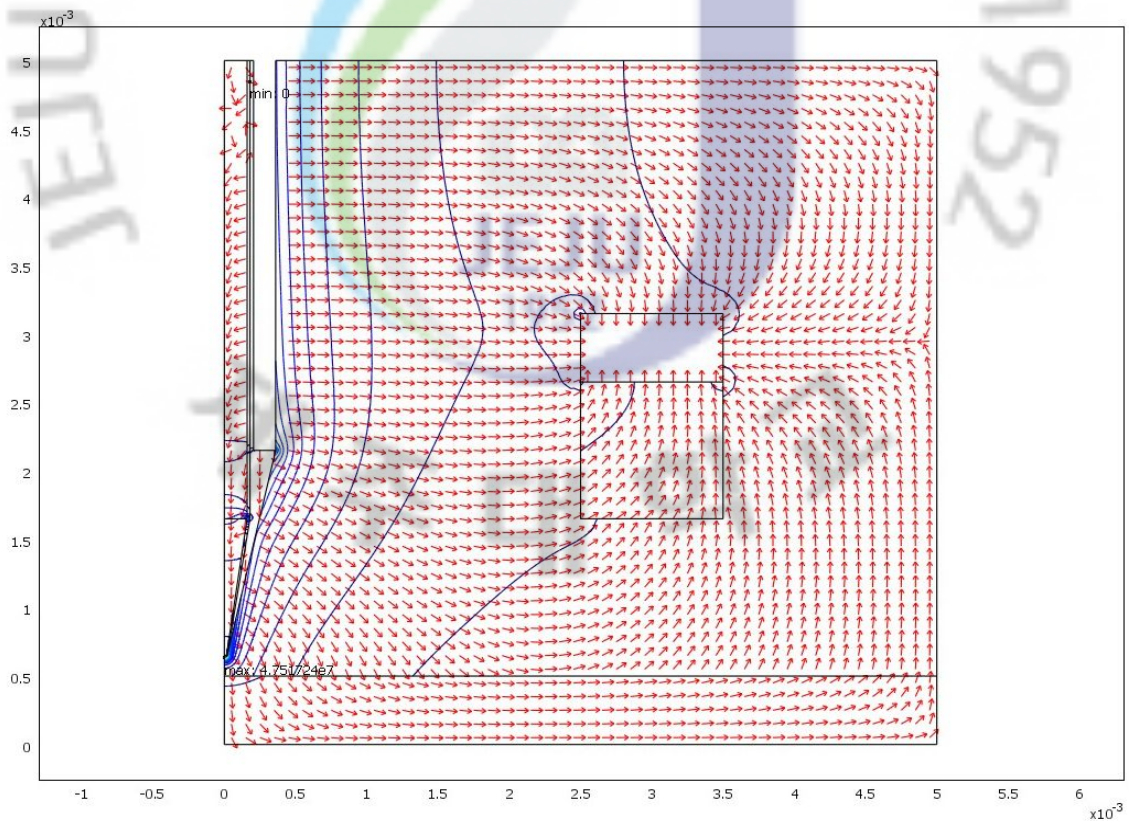
different placement of the ground for in detail analysis of contour of electric field, strength of electric field and estimation of electric field on the nozzle. For each case different potential is applied from 1kV to 5kV to estimate the behavior. Each Figure in Figure 3.11 shows the results at different ground position at 5kV. In simulations and Figure 3.11, the effect of different placements of counter electrodes where arrow indicates the direction of the field and solid lines indicates the contour directions and different randomly selected point. Table 3-4 also show the estimated electric field estimated in each geometry case.

Table 3-3: Showing the cases and values

Case	a	b
1	2.5 mm (radius)	3 mm
2	2.5 mm (radius)	1.5 mm
3	2.5 mm (radius)	0 mm
4	1.5 mm (radius)	3 mm
5	1.5 mm (radius)	1.5 mm
6	1.5 mm (radius)	0 mm
7	0.5 mm (radius)	3 mm
8	0.5 mm (radius)	1.5 mm
9	0.5 mm (radius)	0 mm



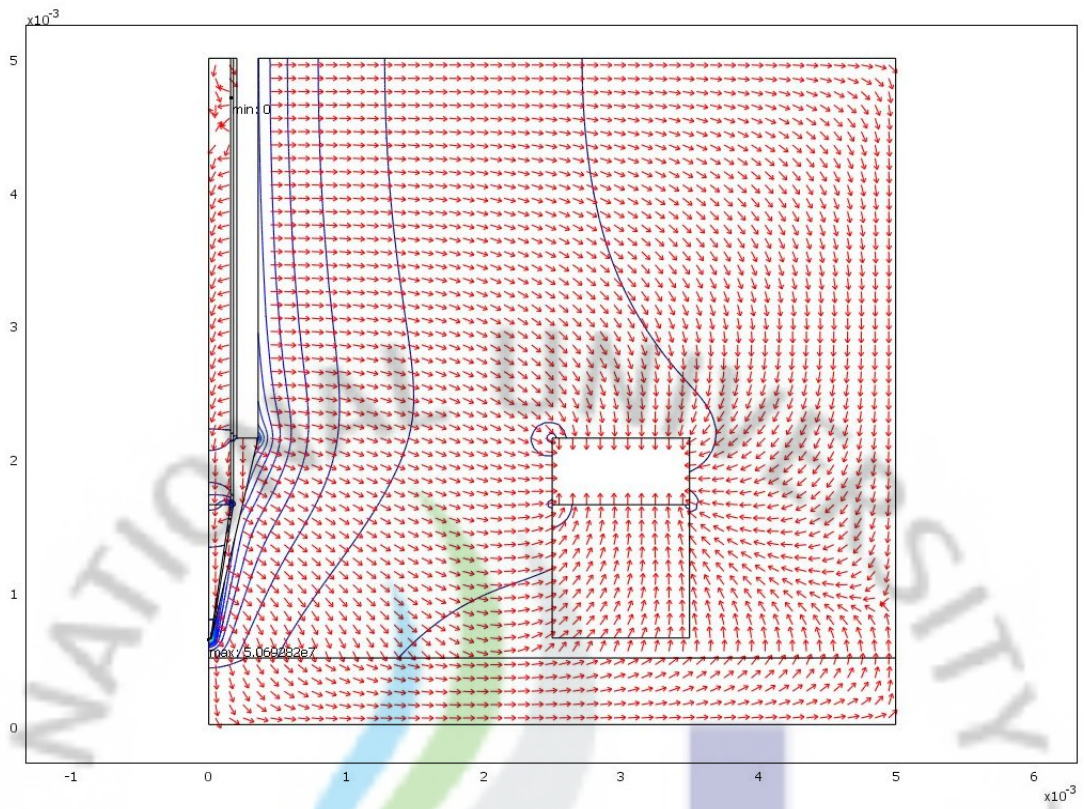
(a)



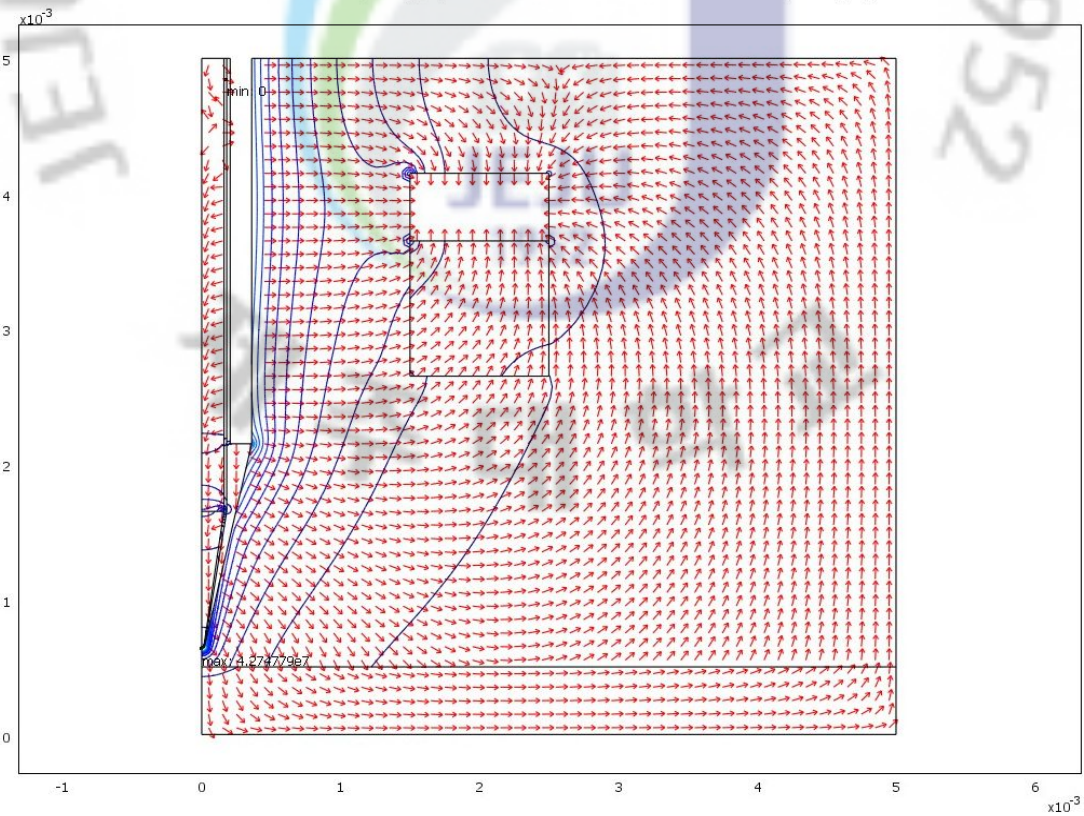
(b)

(continue)



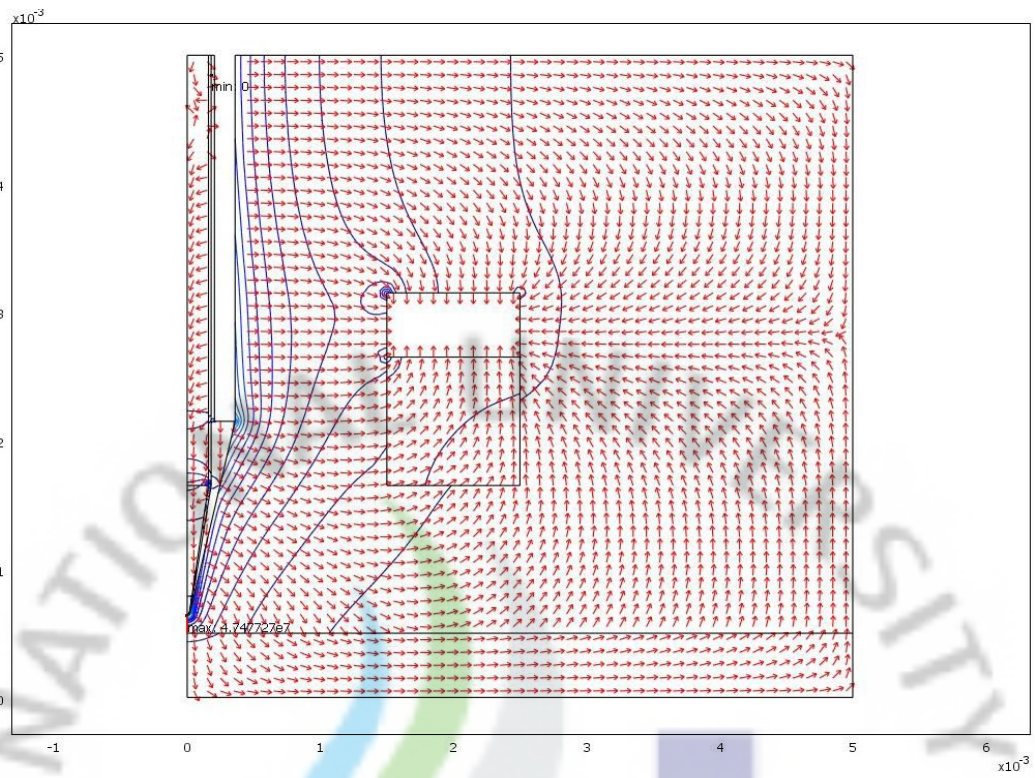


(c)

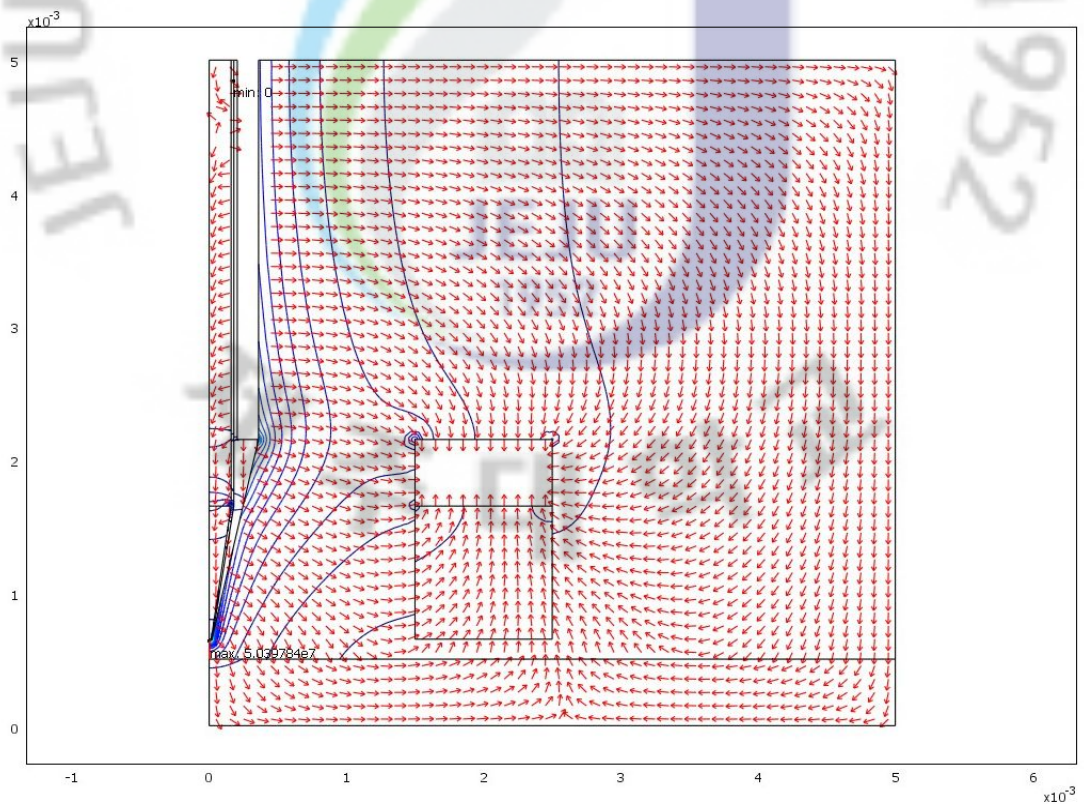


(d)

(continue)

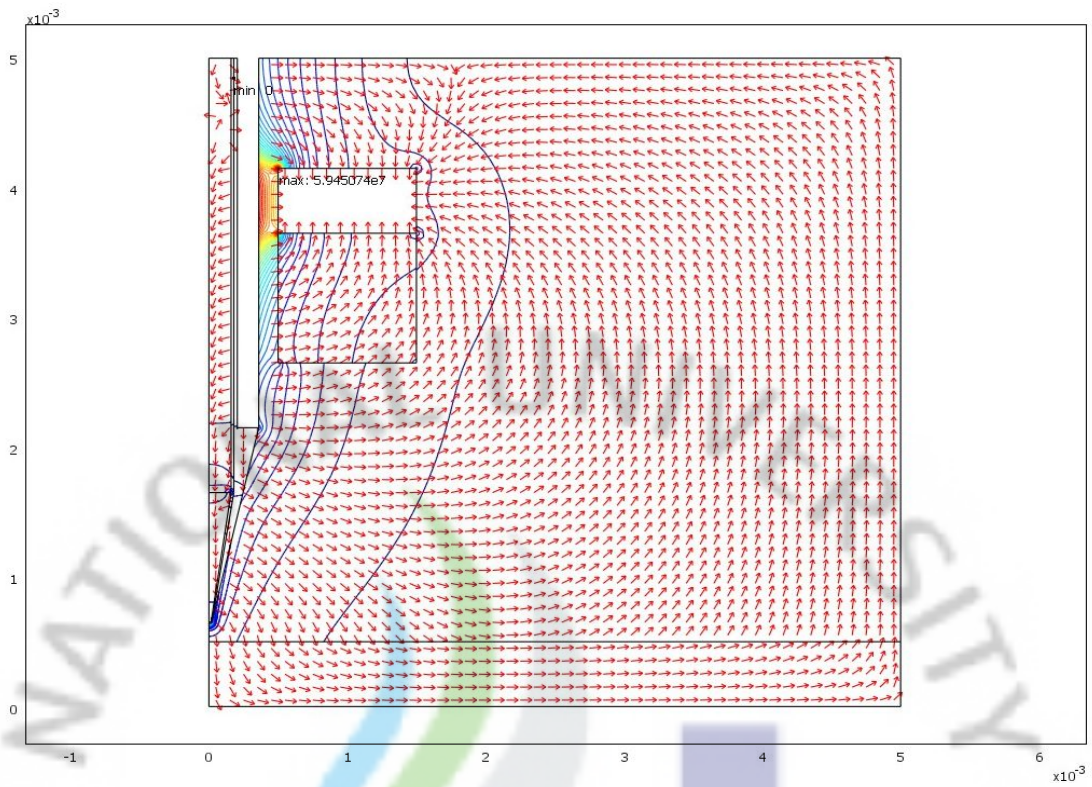


(e)

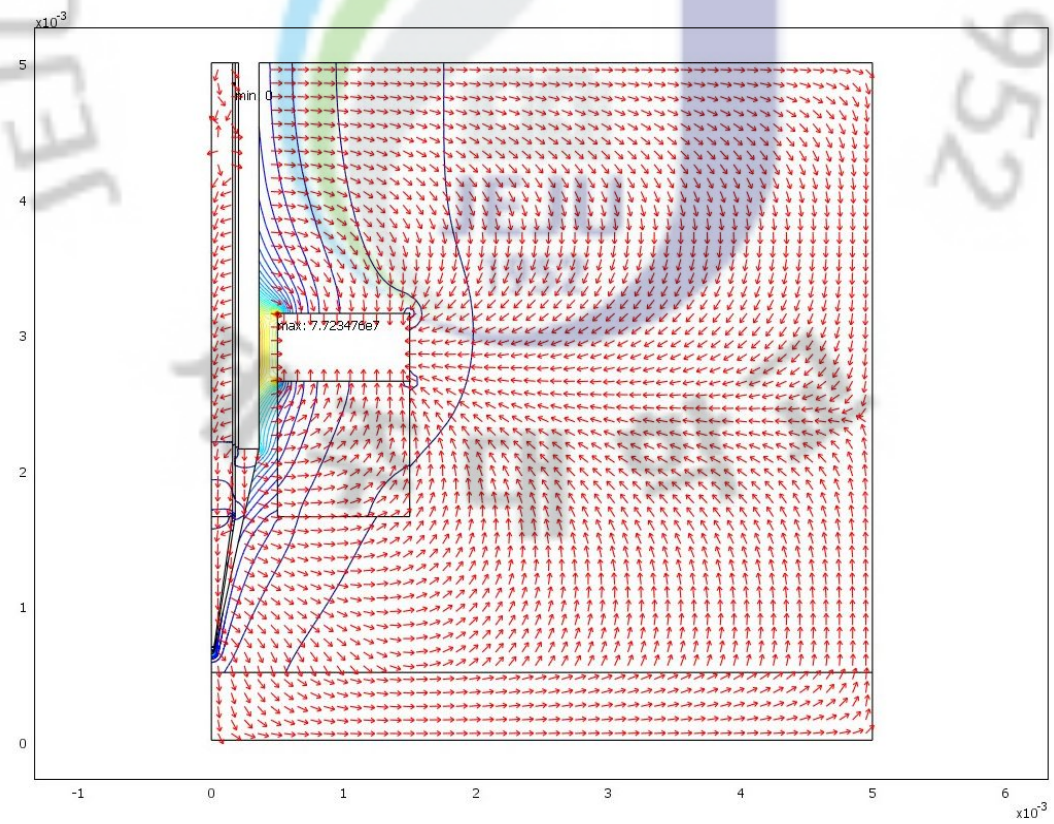


(f)

(continue)

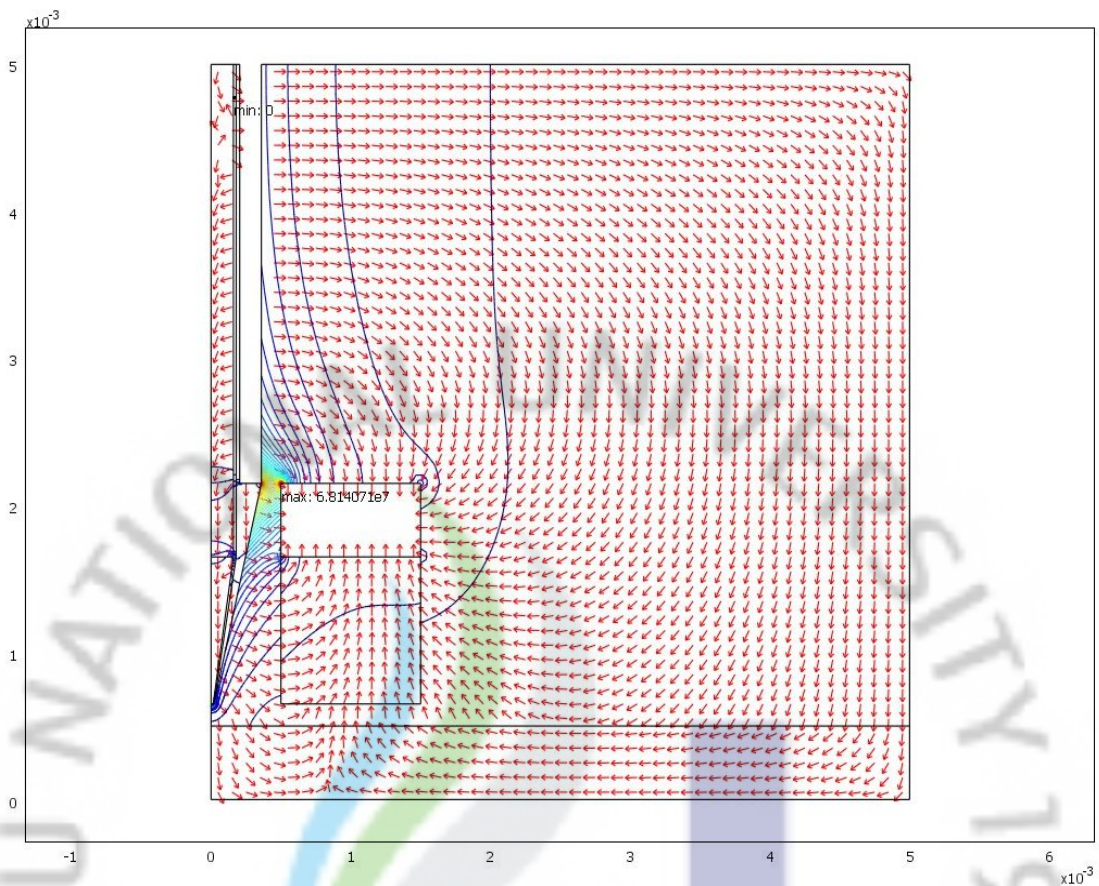


(g)



(h)

(continue)



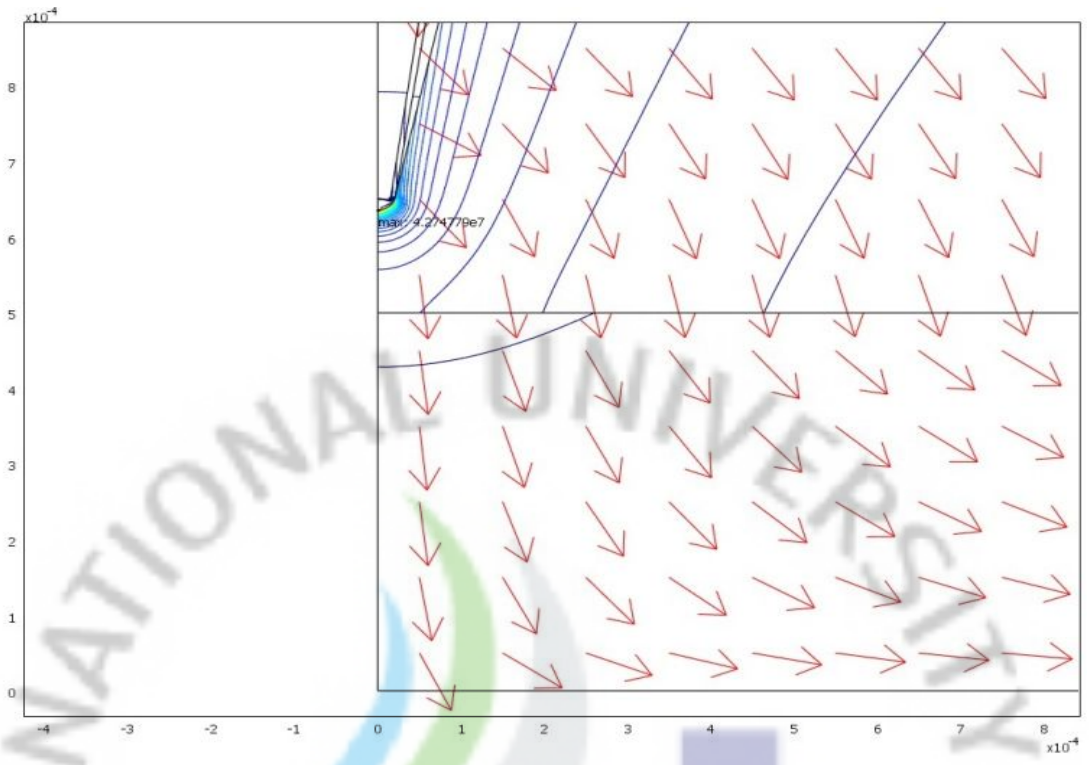
(i)

Figure 3.11: Response analysis at different cases and position of ground electrode at 5kV (a) showing response of case 1, (b) response of case 2, (c) response of case 3, (d) response of case 4, (e) response of case 5, (f) response of case 6, (g) response of case 7, (h) response of case 8 and (i) response of case 9

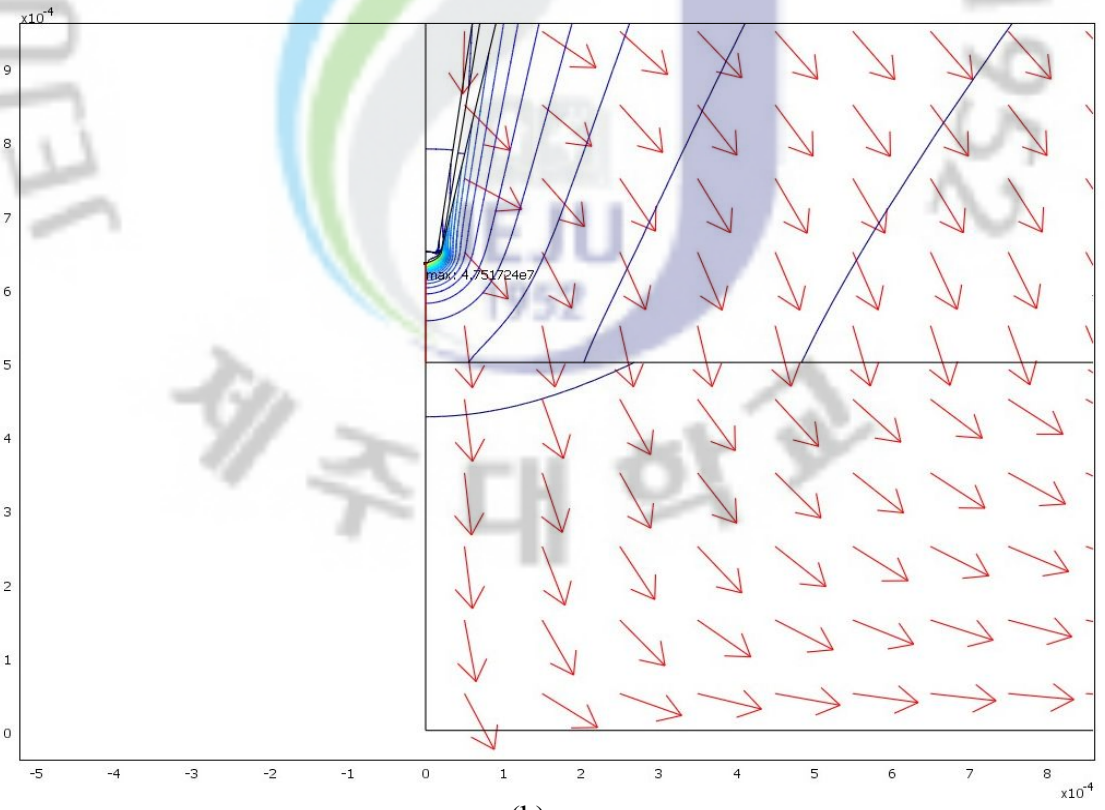
To analyse head with further details simulations are also performed on the tip of the nozzle. The results are shown in Figure 3.12. Electric field is estimated at each point to find the optimal distance and voltage of each head to avoid corona discharge and the breakdown of the medium (air) between the positive and negative terminals. In first four 6 cases, no corona discharge was found even up to 5kV as shown in the figure. But in last three cases the corona discharge is predicted. The simulation is performed at highest voltage to predict the performance of the head.

Table 3-4: Response on different case at different potentials

Voltage (kV)	Electric field (V/m)	Voltage (kV)	Electric field (V/m)	Voltage (kV)	Electric field (V/m)
Case-1		Case-2		Case-3	
1	1.003e7	1	9.503e6	1	1.01e7
2	2.007e7	2	1.9006e7	2	2.027e7
3	3.001e7	3	2.85e7	3	3.0415e7
4	4.0014e7	4	3.801e7	4	4.055e7
5	5.0017e7	5	4.751e7	5	5.069e7
Case-4		Case-5		Case-6	
1	8.8549e6	1	9.496e6	1	1.0017e7
2	1.709e7	2	1.899e7	2	2.012e7
3	2.564e7	3	2.84e7	3	3.023e7
4	3.419e7	4	3.79e7	4	4.03e7
5	4.274e7	5	4.747e7	5	5.039e7
Case-7		Case-8		Case-9	
1	1.189e7	1	1.544e7	1	1.36e7
2	2.378e7	2	3.089e7	2	2.727e7
3	3.567e7	3	4.634e7	3	4.088e7
4	4.756e7	4	6.178e7	4	5.45e7
5	5.945e7	5	7.723e7	5	6.814e7

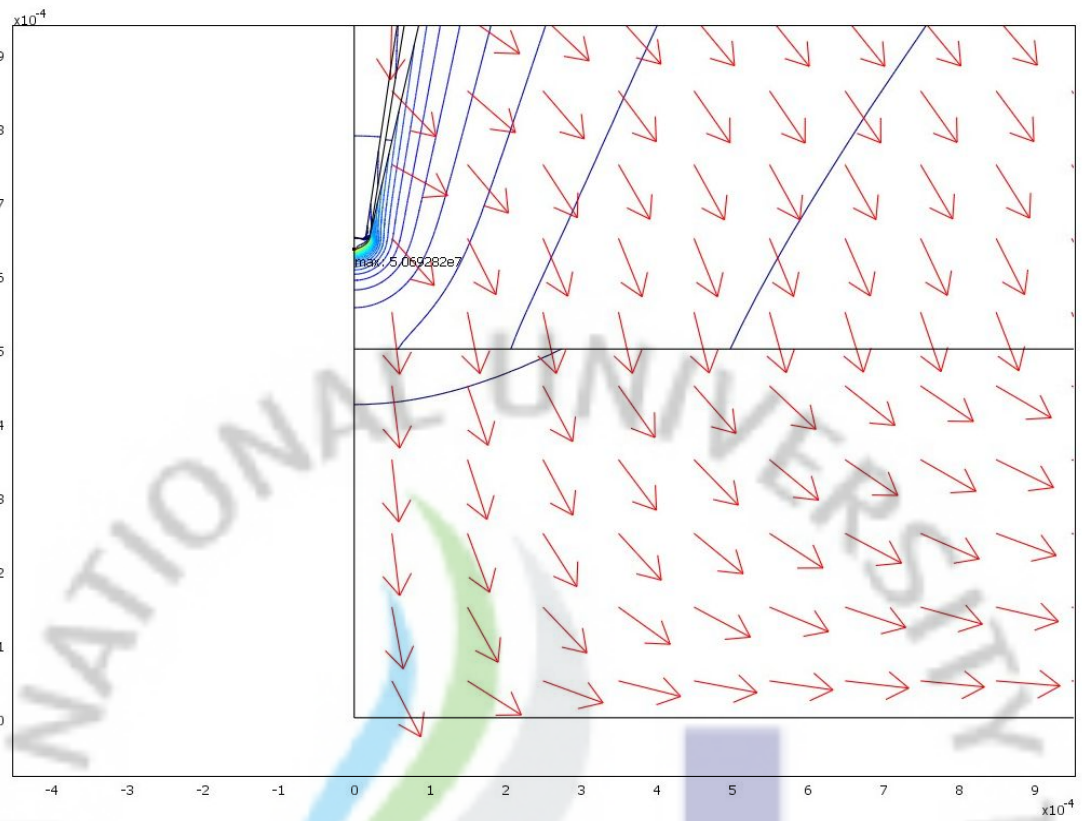


(a)

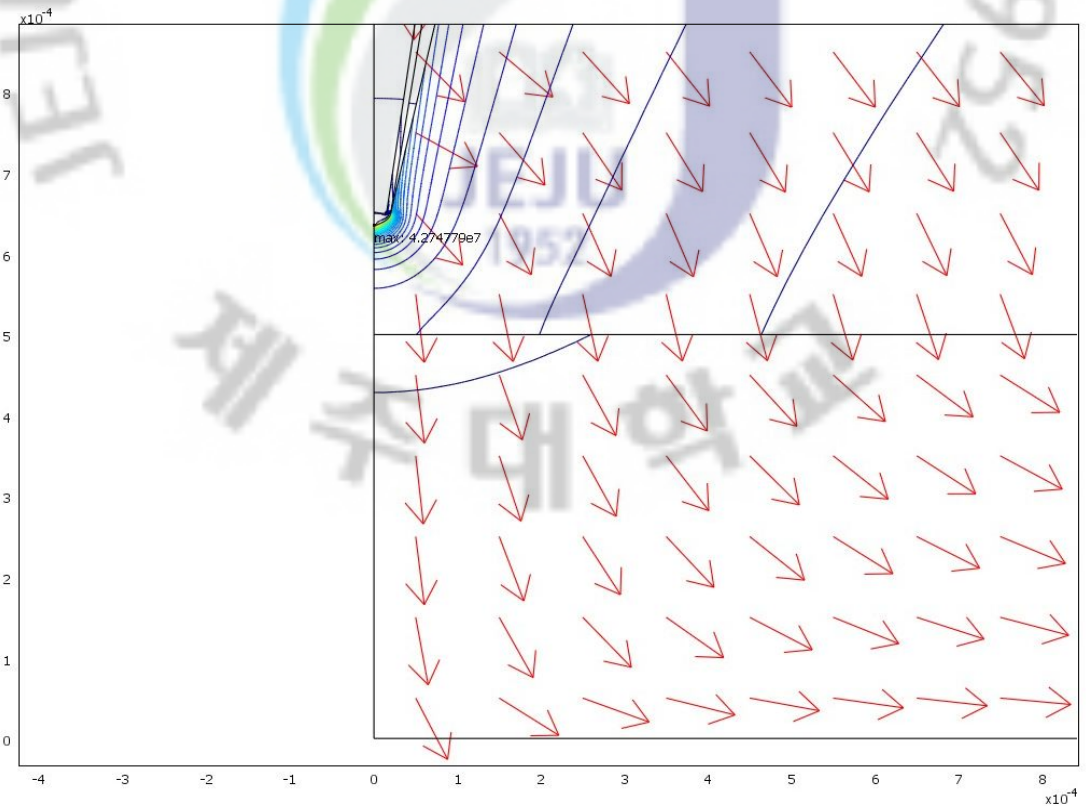


(b)

(continue)

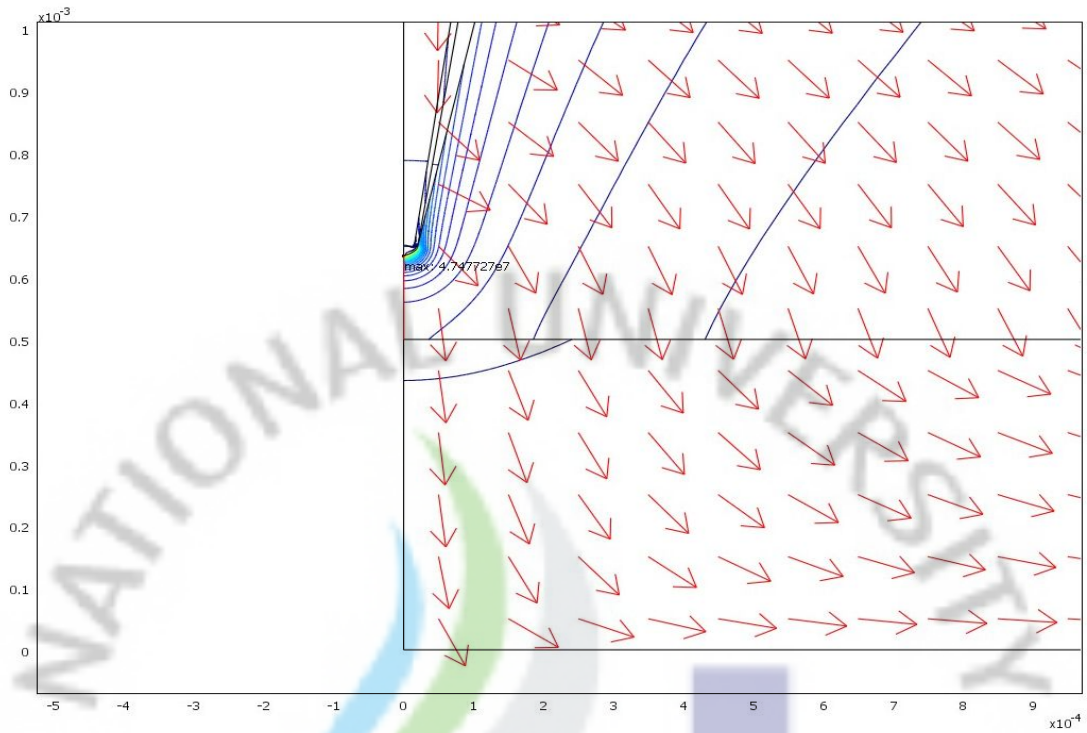


(c)

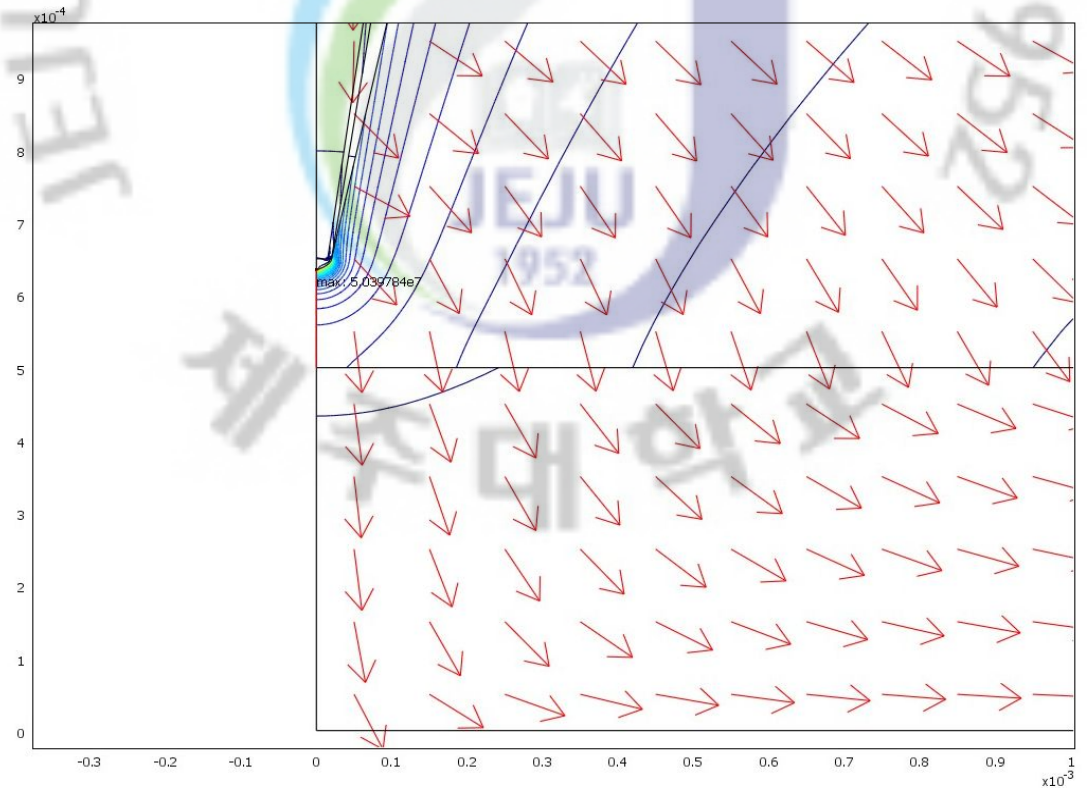


(d)

(continue)



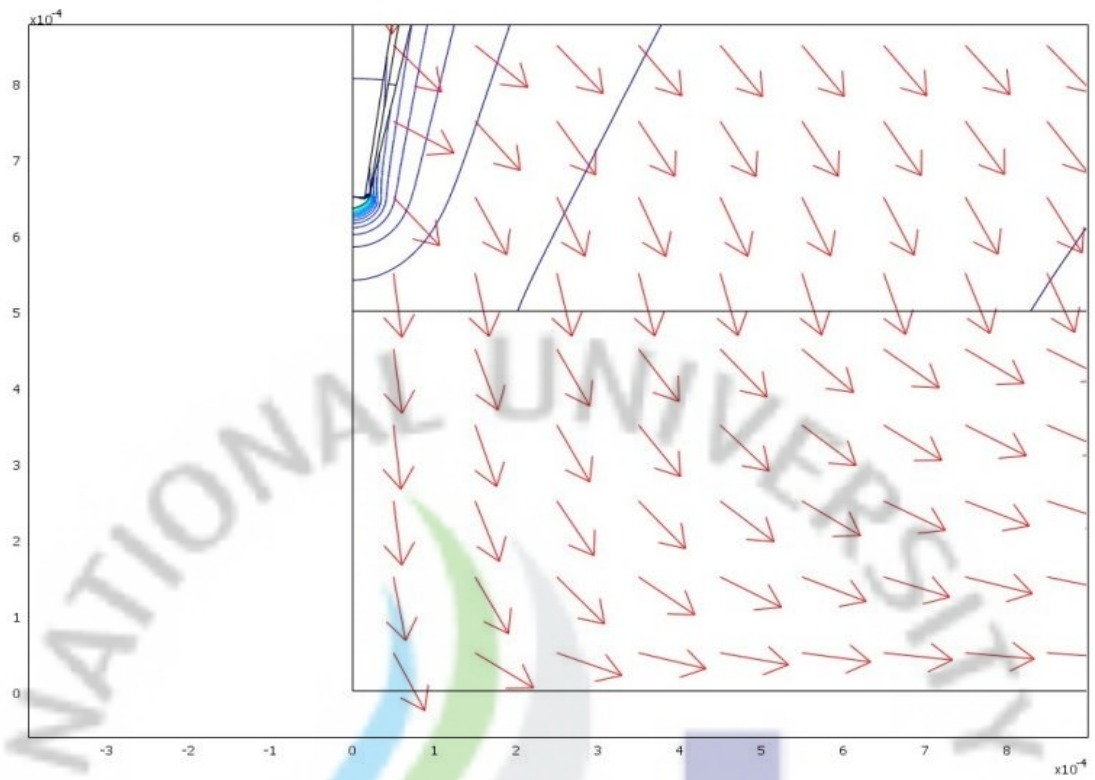
(e)



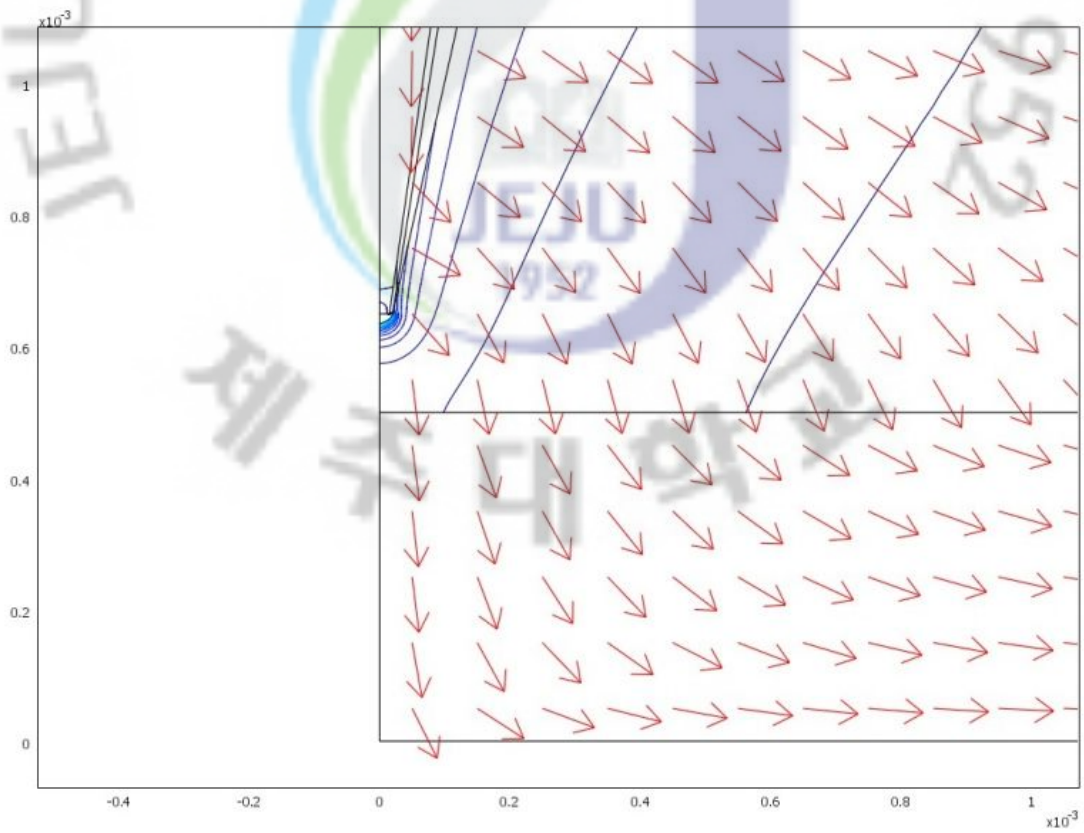
(f)

(continue)





(g)



(h)

(continue)

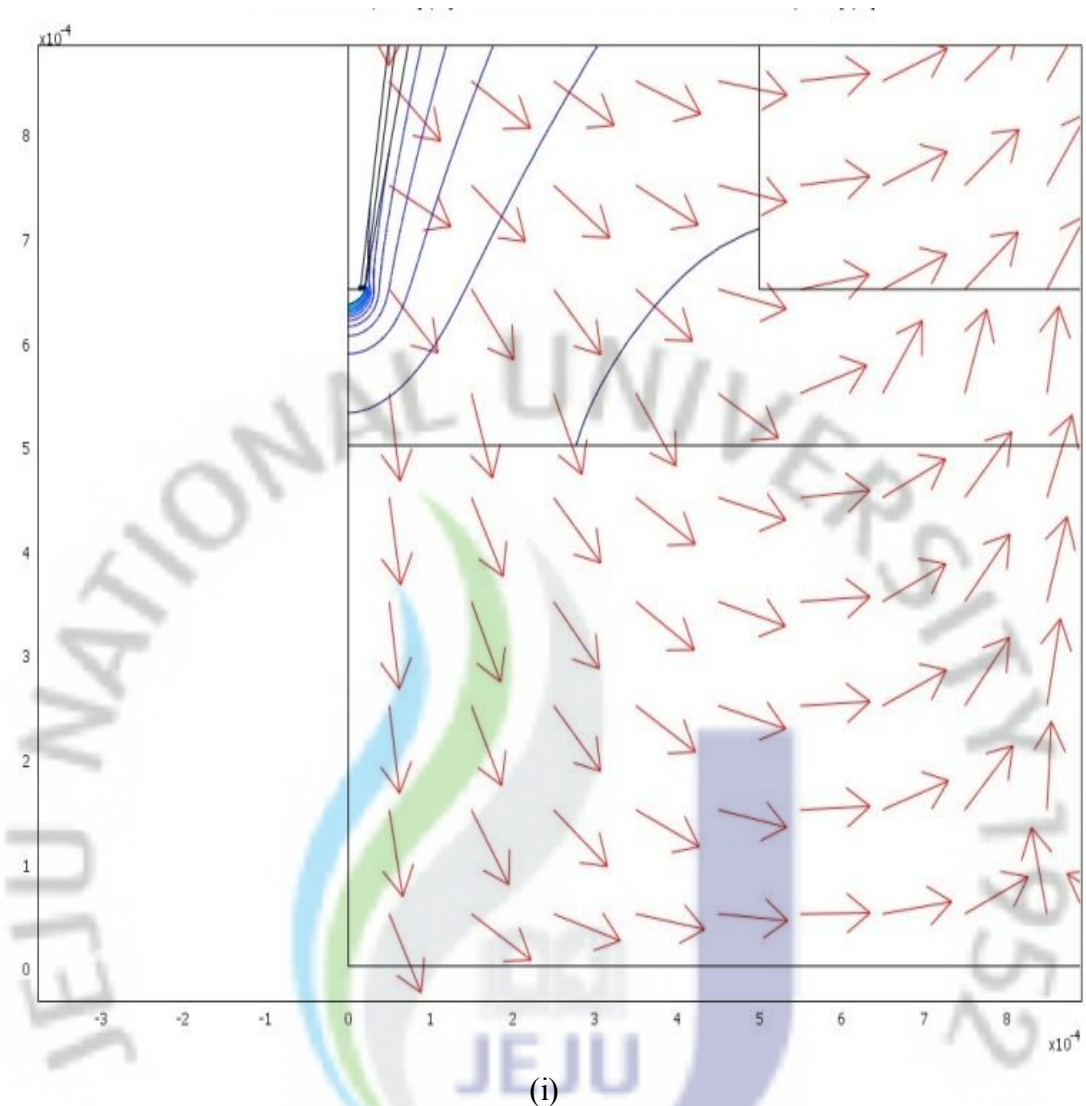


Figure 3.12: Response analysis at different cases and position of ground electrode at 5kV at nozzle tip (a) showing response of case 1, (b) response of case 2, (c) response of case 3, (d) response of case 4, (e) response of case 5, (f) response of case 6, (g) response of case 7, (h) response of case 8 and (i) response of case 9

And for the simulations, optimal positions of electrodes are found. Moreover, it found that minimum corona discharge and good contour of electric field was observed, when electrodes are away from the tip of the nozzle and also in radius. Due to the complex geometry inside electrostatic nozzle head it's difficult to model the meniscus shape and the extension in meniscus in detail here. Thus, for the evaluation of the electrode experiment is conducted.

### 3.4 Head Design

In this section head design, material selection and experiment is discussed.

#### 3.4.1 Head Design

For experiment, head is designed to analysis the above findings. The head design is showed in the Figure 3.13 (a), with the ability of moving ground terminal at different position. The head consist of metallic capillary, silica holder and ground. Figure 3.13 (b) shows the final model of developed head.

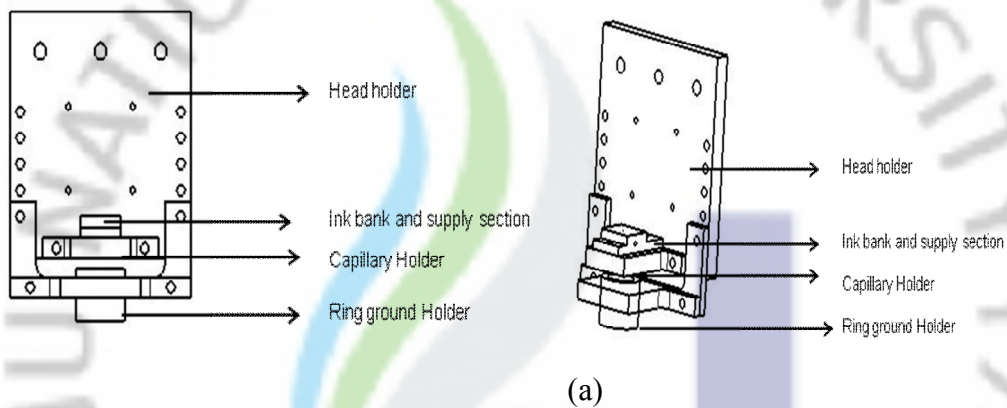
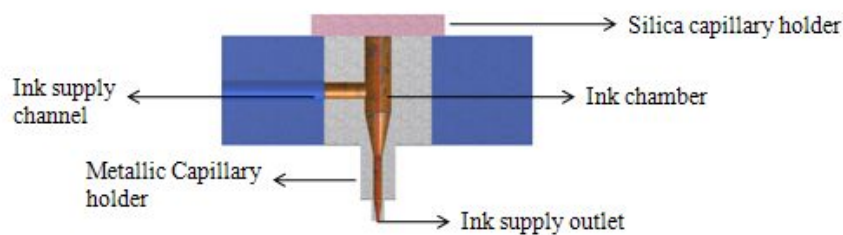


Figure 3.13: (a) Model diagram of head and (b) experimental model of head

### 3.4.2 Material Selection and Fabrication

The nozzle orifice section is kept metallic to give necessary electric field. But for the ink delivery a PDMS mold is used. Almost all material surfaces possess two distinctly different properties. They are either hydrophilic or hydrophobic or neutral. Hydrophilic grout will adhere more surfaces at the interface of where as hydrophobic grout will repel it and push it away and forms high contact angle than hydrophilic. The two type of high resolution nozzle heads used are with hydrophilic and hydrophobic properties respectively. The nozzle heads consist of three main components in structure namely: the nozzle and nozzle orifice, ink supply and reservoir and electrode holder. In this study, based on the trends, high precision structures such as nozzles, walls and electrodes, are designed. The head fabrication demands several new micromachining process and technology. The micromachining process of each nozzle head is given below:

For the nozzle design, metallic capillary is used. This has multi fold advantages. But main advantages include the homogenous electrification of the ink and control direction of electric filed. Metals are usually considered hydrophilic materials. So ink reservoir is designed in such a way that the system remains insulated from the outer hydrophilic layer. To minimize the effect of stress and interfacing between the ink and the sides of nozzle ink bank and channel, hydrophobic material is used. Hydrophobic properties are well known to be enhanced by an increased surface roughness and hydrophobic surfaces require appropriate surface roughness and low surface energy. For this study, Poly Di-Methyl Siloxane (PDMS) is used, which is hydrophobic in nature.



(a)

(continue)

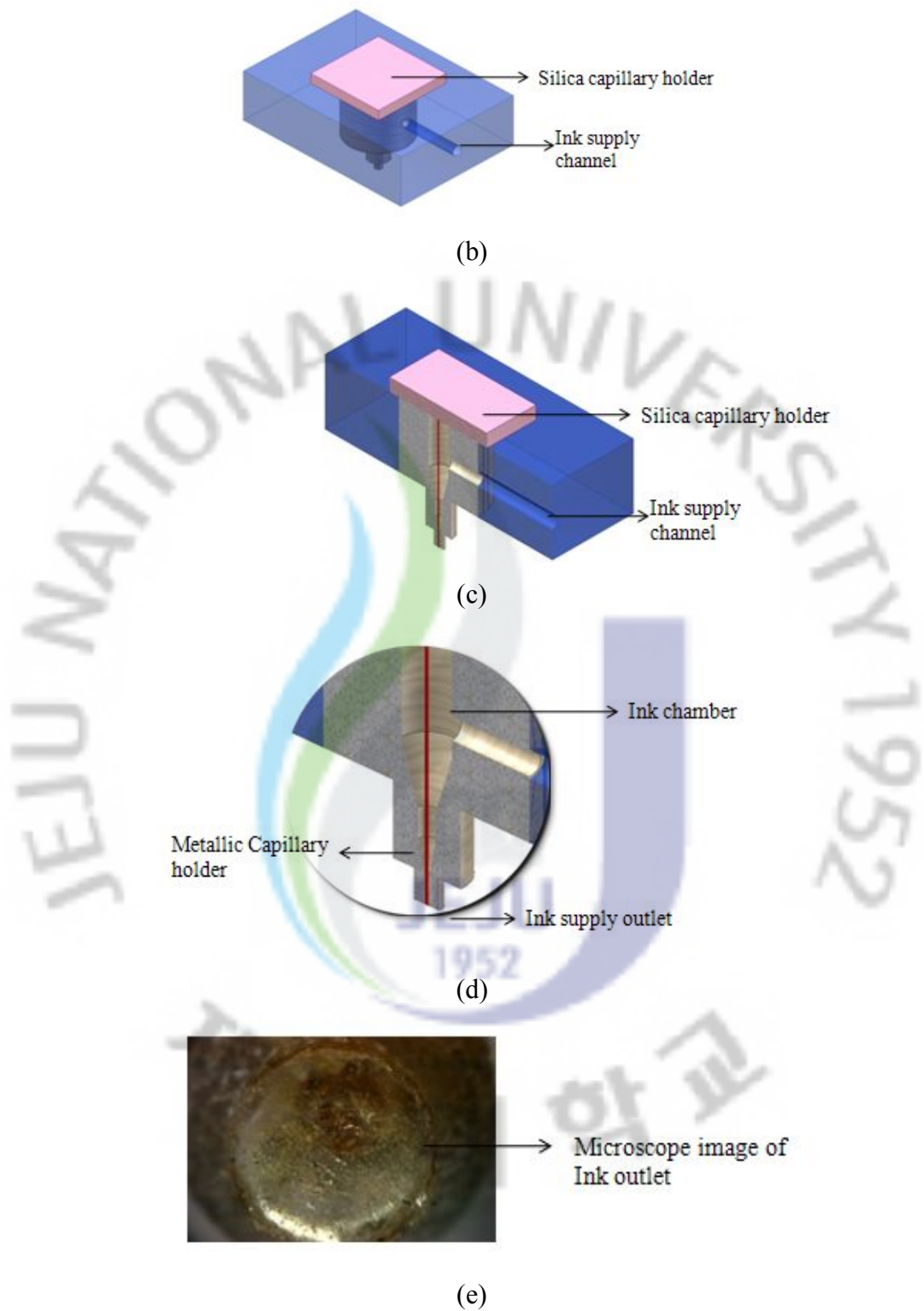


Figure 3.14: (a), (b), (c) and (d) show the schematic diagrams of the nozzle head and (e) shows the microscope image of the holder outlet

Micromachining fabrication steps and materials used are listed below; firstly the Sylgard 184 Silicon Elastomer base and Sylgard 184 Silicon Elastomer curing agent is mixed together in ratio of 10:1. And then mixed on shaker 70-90 rpm for 20 minutes or until bubbles removed from the mixture. Then its pour in the dye by making sure that no bubble generated inside the head dye. This stage is repeated until the bubble less dye is filled. Then its put for the curing in furnace at 80°C for 1 hour. After removing from the curing furnace the die assembly is dismantle and ink supply and power supply connection are attached; the head is tested for the blockage. The fabricated nozzle ink outlet head consists of OD 200 $\mu$ m. And For the final design of the head, both the PDMs mold and capillary is integrated. The voltage is applied on the metallic capillary. Figure 3.14 shows the final developed model.

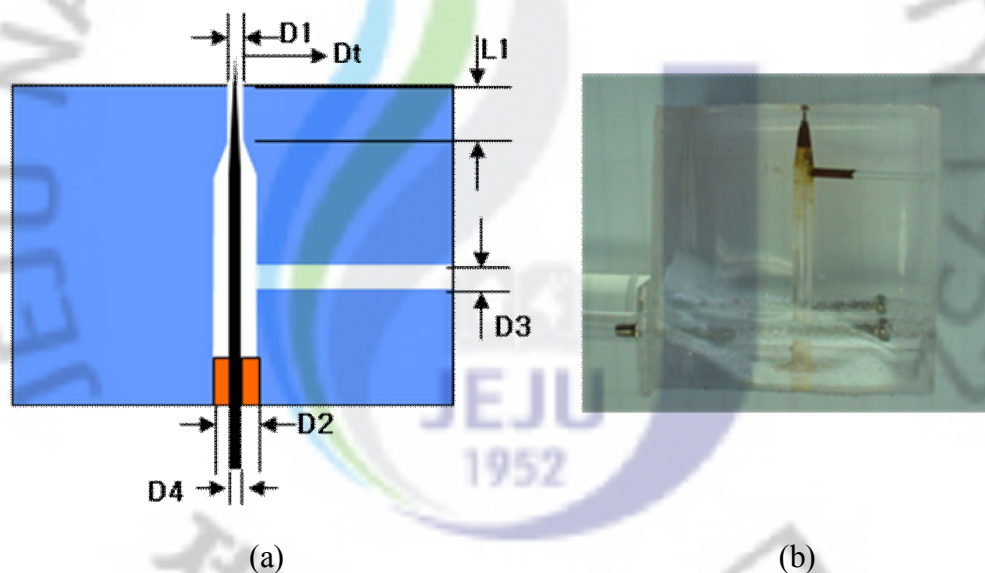


Figure 3.15 : (a) Showing the schematic diagram of the PDMS ink supply and silica holder and (b) showing the the final model of PDMS ink bank and silica holder mold

Ground is also fabricated using conductive material. The fabrication process is based on different processes, mentioned below; for the metallic composition of the hydrophilic thin metallic layer of metallic layer of copper (Cu) is less than 100  $\mu$ m is taken and baked with the insulator sheet having Teflon layer sheet between it for 150° C for 10 minutes. The final model is shown in the Figure 3.16.

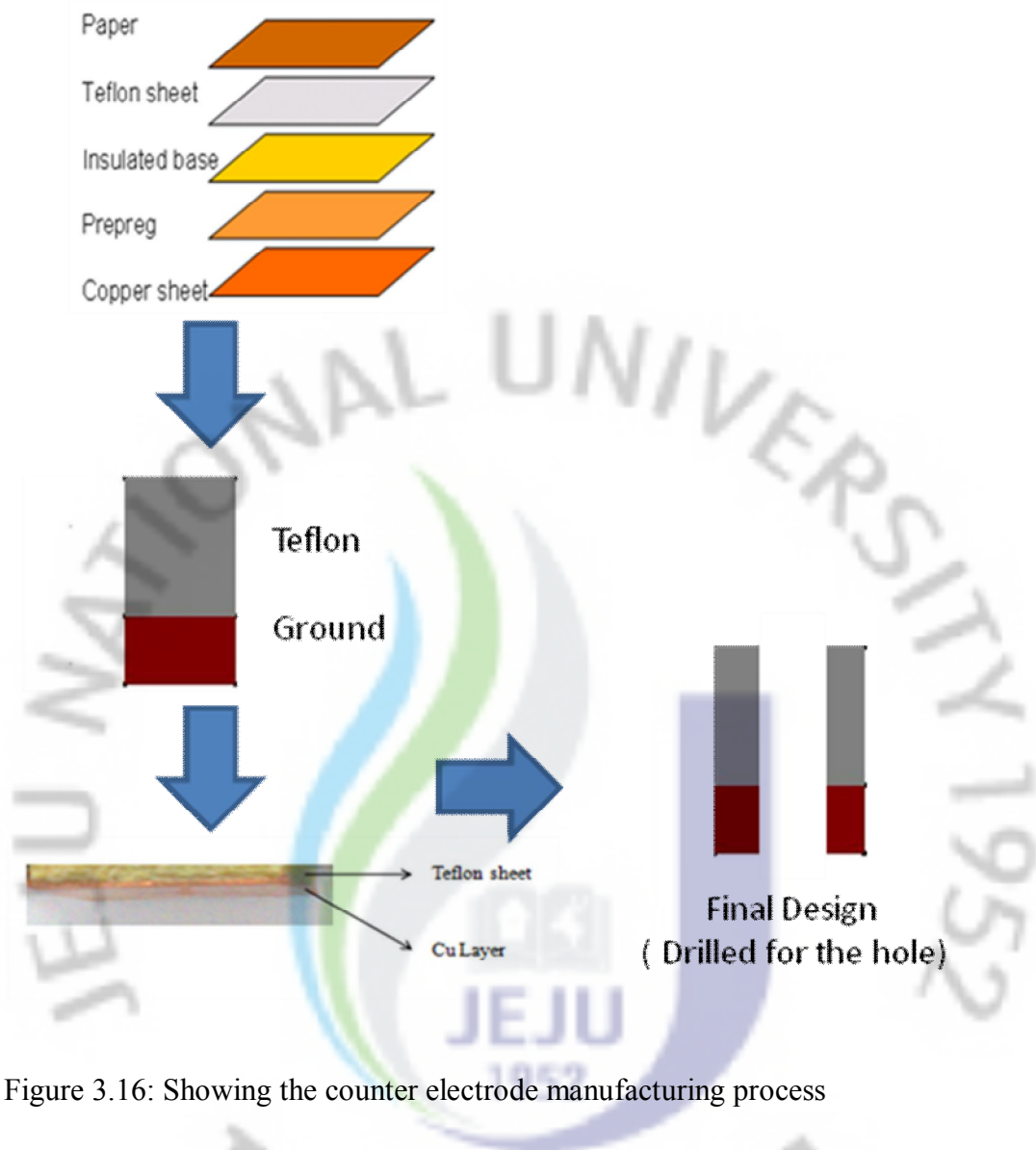


Figure 3.16: Showing the counter electrode manufacturing process

And to be usable as the counter electrode, a drill hole is done at the center of the ground plate. Then this assembly is mounted on the ground holder designed to be loaded on the nozzle holder as discussed earlier.

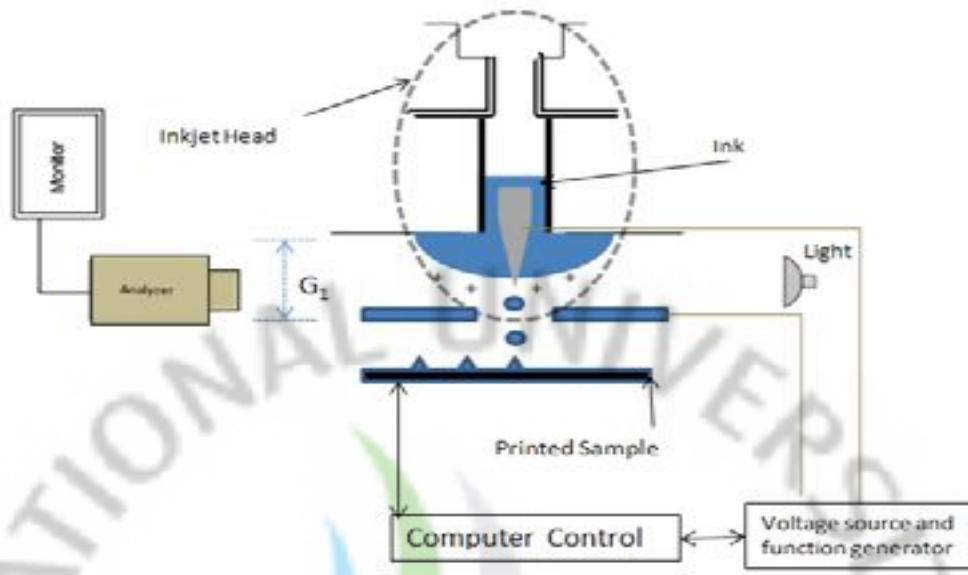
## 4. Results and Analysis

In the previous chapter head design and the different position of the head parameters are studied including the position of counter electrode, the flow rate, silica position, and voltage requirement on jetting. In this section the experiment setup and the behavior of the head on different substrate is studied and analysis. The head is also tested on the glass substrate for high aspect conductive pattern and nano-level with equilibrium spray deposition. And based on the findings introduce optimized model of I-Silica (integrated terminal silica capillary) head design for patterning supported by DOE techniques.

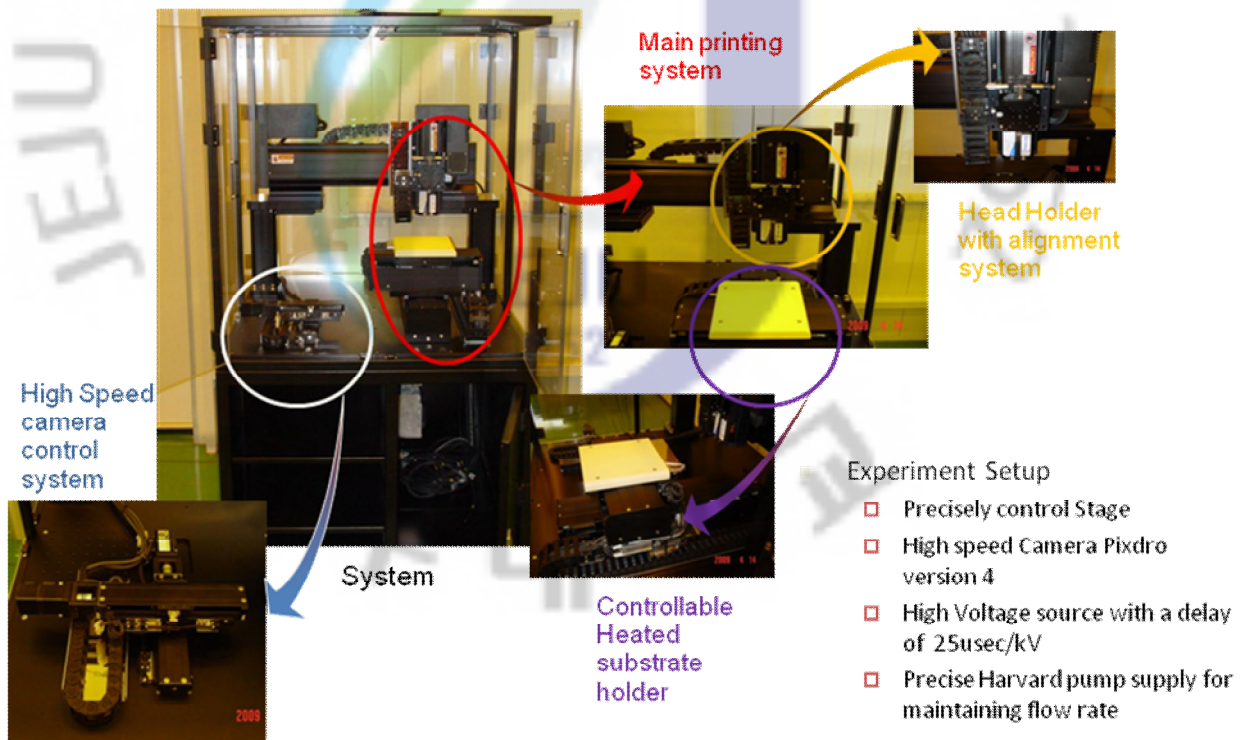
### 4.1. Experimental System and Methodology

The experiment setup and print head driven by on demand electrostatic forces specifically designed for this study, is shown in the Figure 4.1. The apparatus consist of X-Y stage, electrodes, a high voltage source, an observation system, ink supply system, and nozzle holder with Z-axis control. The positive potential is connected to nozzle head for activating the ink and providing the necessary potential to the ink for the drop extraction. The liquid pressure is controlled by using the pressure injection. The inlet flow rate is an important parameter to maintain the uniform static pressure in the ink chamber when the reservoir head is changing due to the ejection of ink during the printing process. By applying different flow rate the optimal flow rate is selected in such a way that drop generation slowdowns to dripping and kept system under this force for few minutes until the system get stabilized. Liquid is fed from a syringe to nozzle through Teflon tubing. After developing the meniscus, the result is analyzed to find the optimal values for the given nozzle. This is done by applying different voltages until optimal position of the voltage point is determine. For the application of valotage NanoNC power-supply is used, which can provide volatge upto 30kV. But in this resaerch the optenial is kept around 5kV. For observation purpose, Redlake N- series high speed camera having 5000 frames rate is used. The lens magnification is kept 10X.





(a)



(b)

Figure 4.1: Experiment setup (a) schematic diagram of the system and (b) physical system for the analysis of experiments

## 4.2 Experimental Analysis and Optimizing the Position of Silica

For experimental propose, jetting and spray behavior of the head is analyzed. The nozzle containing the silica is given positive potential and the ground is given negative potential. The nozzle and setup is shown in the Figure 4.2. Different dripping and jetting behavior are analyzed in are replicate in the Figure 4.2(b). For experiment, a commercial available conductive ink having viscosity 39 cps, surface tension 5 dyn/cm and number of nano particles 40% is used.

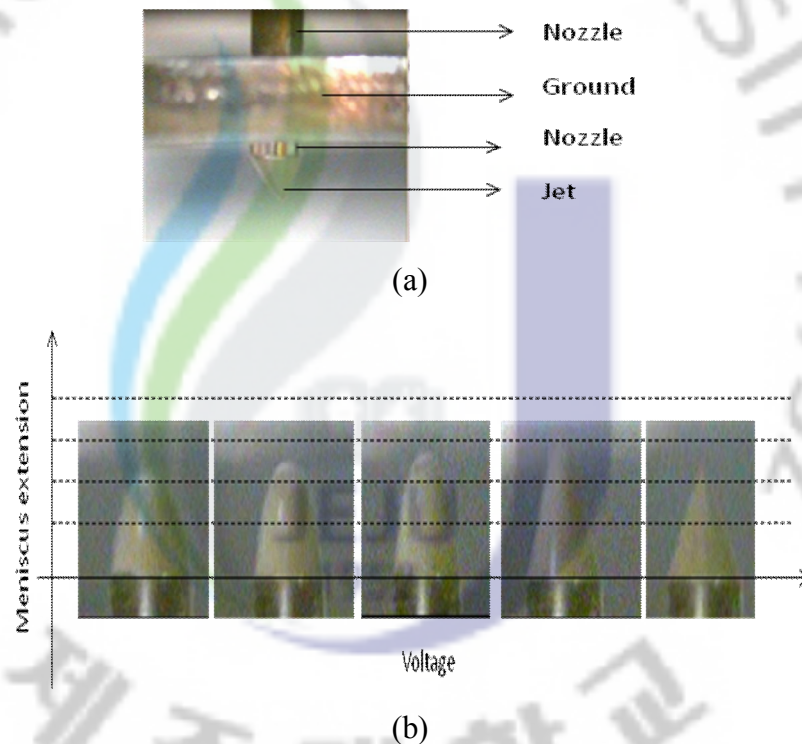


Figure 4.2: (a) Experiment setup and (b) the meniscus, dripping and jetting analysis of the head.

Experiments were repeated on different position of the silica in the head, to find the optimal position of the head. The Integrated terminal silica head (I-Silica Head) is tested on four different locations of the silica namely; at orifice (also used as zero position in literature rest of text), 500 um outside, 1000um outside and 1500 um outside the nozzle orifice. Its important to mention here that all experiment were run on case 1 as the best direction of the field was obtain at that potential.

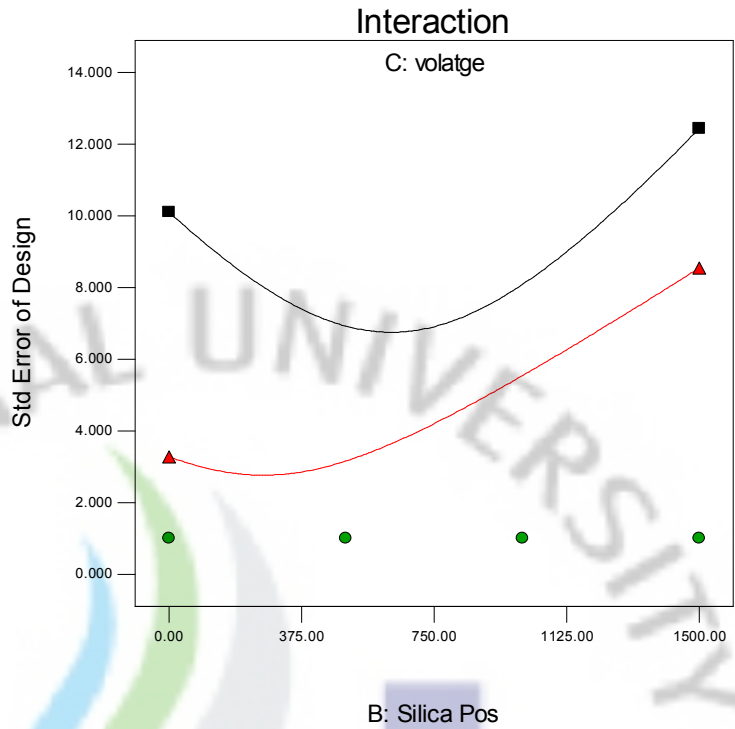
Design-Ease® Software  
 Factor Coding: Actual  
 Std Error of Design

● Design Points

X1 = B: Silica Pos  
 X2 = C: volatge

Actual Factor  
 A: flowrate = 25.00

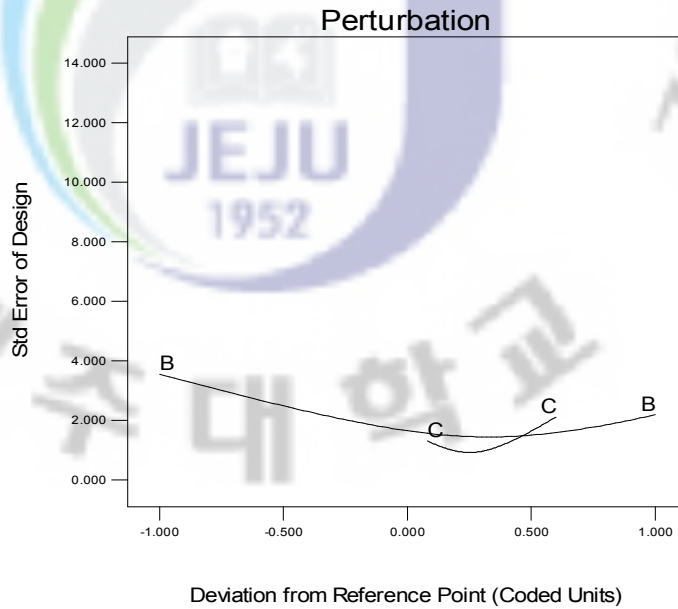
■ C- 0.00  
 ▲ C+ 5.00



(a)

Design-Ease® Software  
 Factor Coding: Actual  
 Std Error of Design

Actual Factors  
 \*A: flowrate = 25.00  
 B: Silica Pos = 750.00  
 C: volatge = 2.50

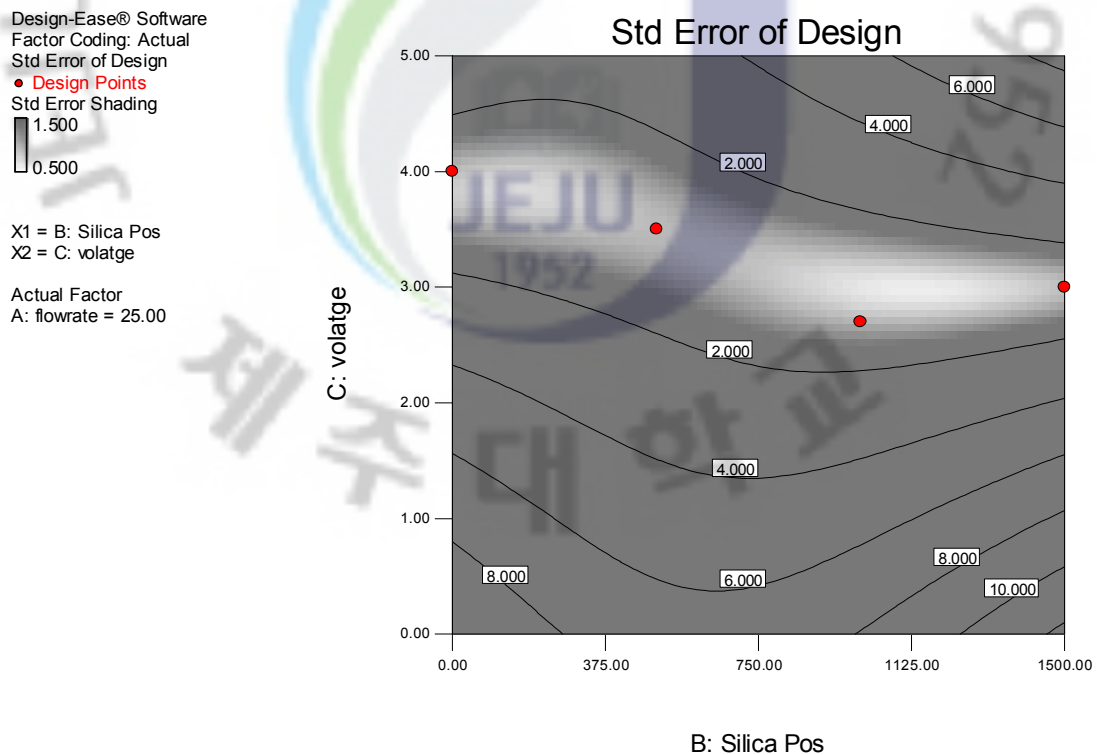


(b)

Figure 4.3: Showing (a) interaction and (b) perturbation graphs

To analysis the position of silica in the head, design of experiment techniques is used. The vectors of the electric field are not focused near the cone, which may cause instability in the cone jet or push positively charged droplets outward. Therefore optimized position of the silica is very important. Therefore, for deep investigation, design expert ® is used. The results of analysis are given below. For the initial analysis interaction and perturbation graphs are used. Different position of silica and voltage is analyzed and modified to find the response on different points. Moreover, with this graph the standard error of design are studied to optimize the parameters. The ground position is kept constant as already explained. The graphically obtained results are shown in the Figure 4.2.

To further analyze, the standard error design a 2D and 3D graphs are generated between voltage and silica capillary to reduce the instability in the cone jet or push positively charged droplets outward. The Figure 4.4 shows the analysis.



(a)

(continue)

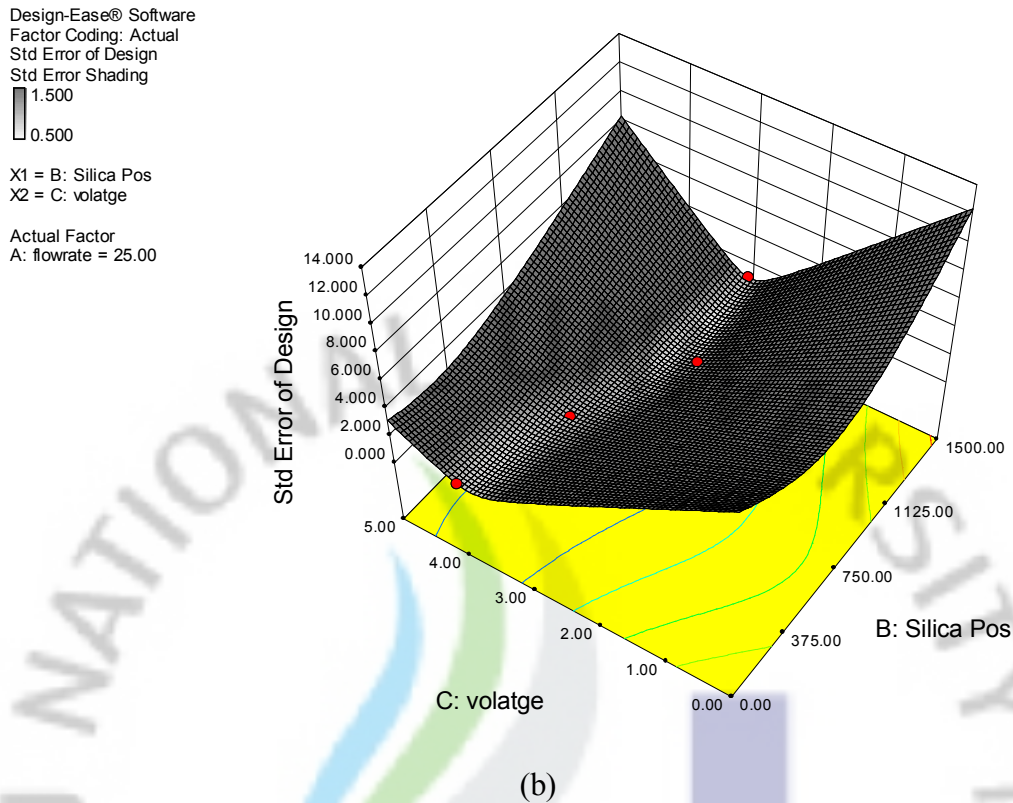


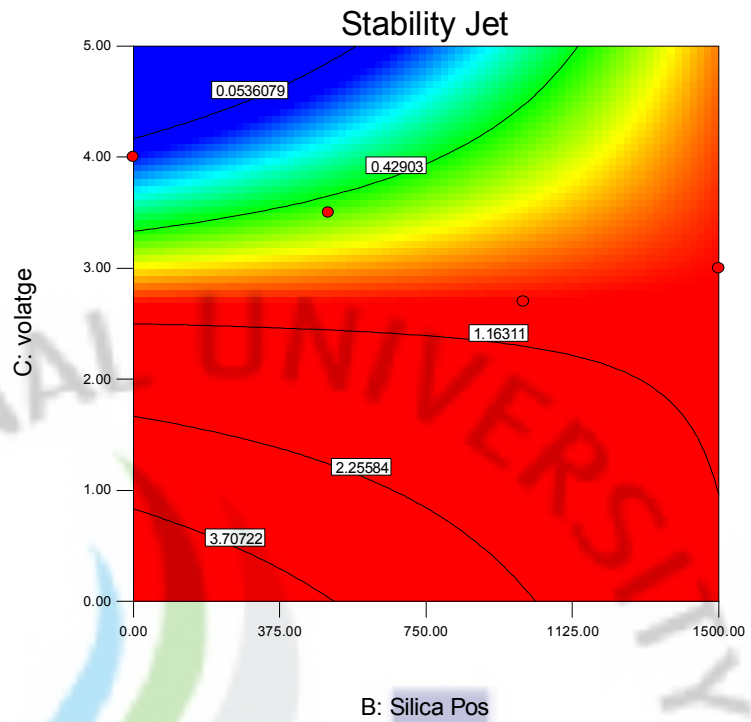
Figure 4.4: Standard error design between voltage and Silica pos at (a) 2D and (b) 3D graphs

From above analysis, region of jet stability is optimized. The graph is divided into different ranges where blue indicates the stable region for the jetting and red indicates unstable region for the jetting. The Figure 4.5(b) also shows the unstable and stable region of the jetting in 3D. And it can be seen that the head perform best when it's on the tip of the nozzle especially where meniscus is created. The most optimal position for the silica position is found to be around 500um where it breaks the meniscus. Therefore it's important to mention here that optimal range of the silica position is around the meniscus of the head. Silica inside and outside the head also generate the instabilities in the head. Therefore, in this section an optimal position of silica inside the head is analyzed while jetting in space. Next section will elaborate and analysis the jetting on substrate for further verification.

Design-Ease® Software  
 Factor Coding: Actual  
 Original Scale  
 Stability Jet  
 ● Design Points  
 1  
 0.1

X1 = B: Silica Pos  
 X2 = C: volatge

Actual Factor  
 A: flowrate = 25.00

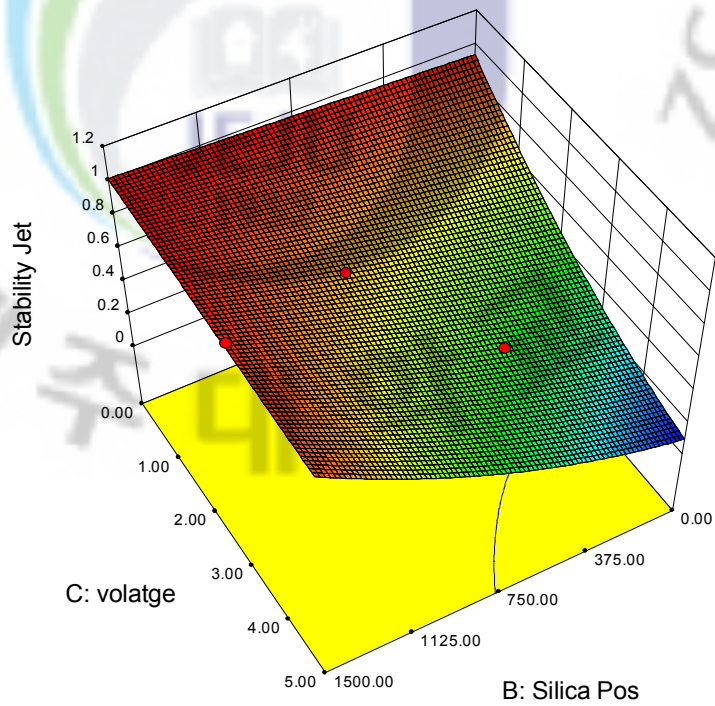


(a)

Design-Ease® Software  
 Factor Coding: Actual  
 Original Scale  
 Stability Jet  
 ● Design Points  
 1  
 0.1

X1 = B: Silica Pos  
 X2 = C: volatge

Actual Factor  
 A: flowrate = 25.00



(b)

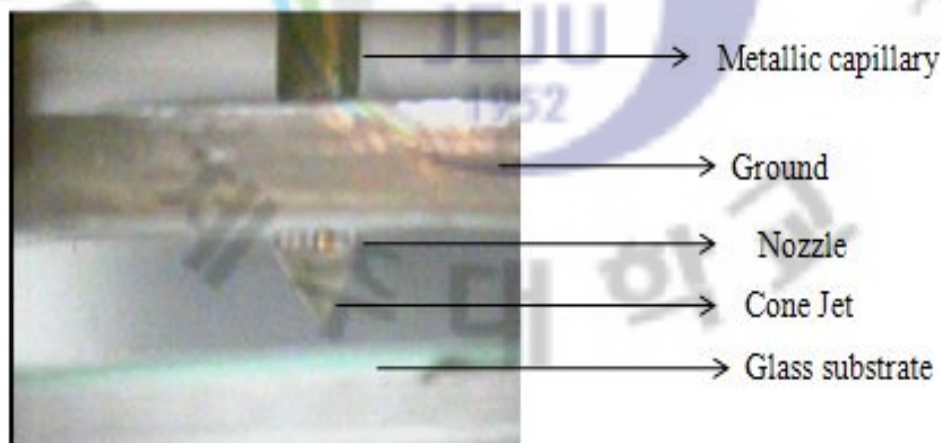
Figure 4.5: Region of stable and unstable jetting in (a) 2D and (b) 3D

### 4.3 Analysis of the Deposition Process on Substrate

To further analysis the head patterning and spray behavior of the head is studied on the substrate. For patterning and spray analysis glass substrate is used.

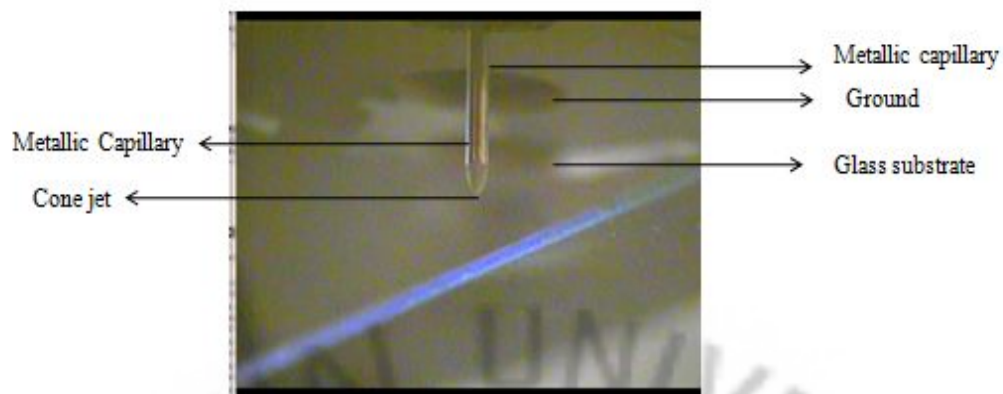
#### 4.3.1 Patterning Analysis

Patterning is very important aspect of printing. In printed electronics to connect and develop different printed electronics the connectors and the pattern line plays important role. Smooth patterning makes more reliable connections and more smooth circuit. Smooth printing also enhances the conductivity. To analysis the behavior of the head on glass substrate, experiments were done. For in detail analysis the high zoom camera is also used and the results are shown in the Figure 4.6. Figure 4.6 (a) showing image of printing on glass substrate through side camera, Figure 4.6 (b) showing the image from the camera under the substrate while jetting before printing and Figure 4.6 (c) show the pattern developed on glass substrate from the camera under the substrate.



(a)

(continue)



(b)



(c)

Figure 4.6: (a) Showing image of printing on glass substrate through side camera (b) showing the image from the camera under the substrate while jetting before printing and (c) show the pattern developed on glass substrate from the camera under the substrate.

The cone jet is analysis is also done to analysis the behavior while printing on the substrate. The stable cone jet graph is also shown in the Figure 4.7. The initial jetting was observed in case one around 3kV. The graph shows the optimal range of voltage and flow rate. Figure 4.8 shows the results of patterning on the glass substrate through microscope. It can be seen that even 20 um line can be obtain by using this configuration. The line length can be varied depending upon the silica orifice size, flow rate in the head.



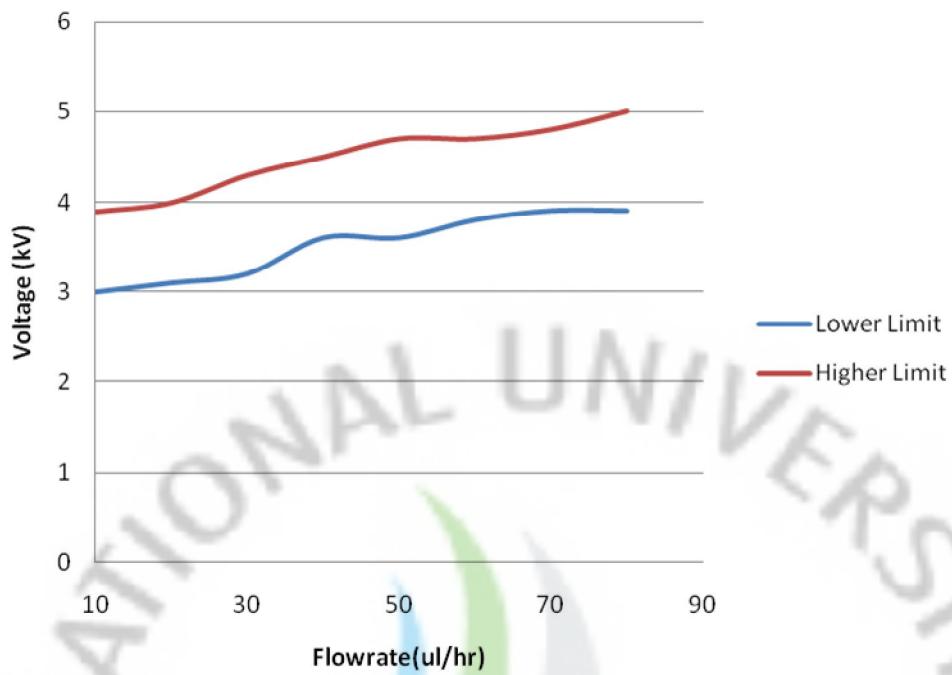


Figure 4.7: Optimal range of cone jet

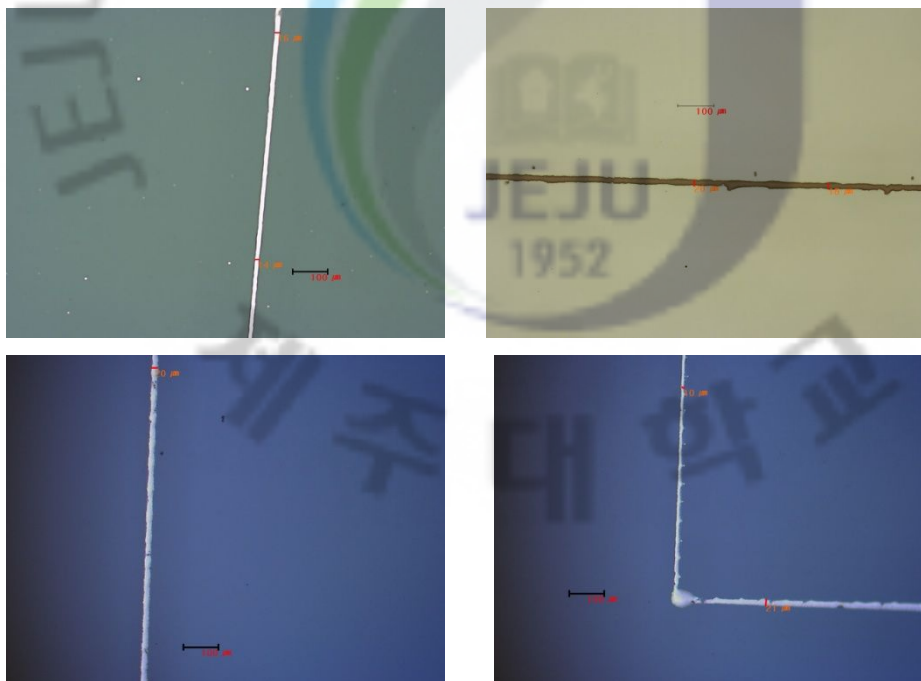


Figure 4.8: Different patterning results on the glass substrate through microscope.

### 4.3.2 Spray Deposition

Spray distribution refers to the density of flow of the scattered droplets at a given spray distance, measured along a cross-section of the spray pattern. Nozzle manufacturers have devised their own methods to measure flow distribution. One such method is to arrange containers on a level surface and to measure the level in each after spraying for a certain period of time. But in this research glass substrate is used to analysis the shape of the spray deposition in the substrate. Ink is sprayed on glass and characterized through different characterization the techniques (SEM and microscope).

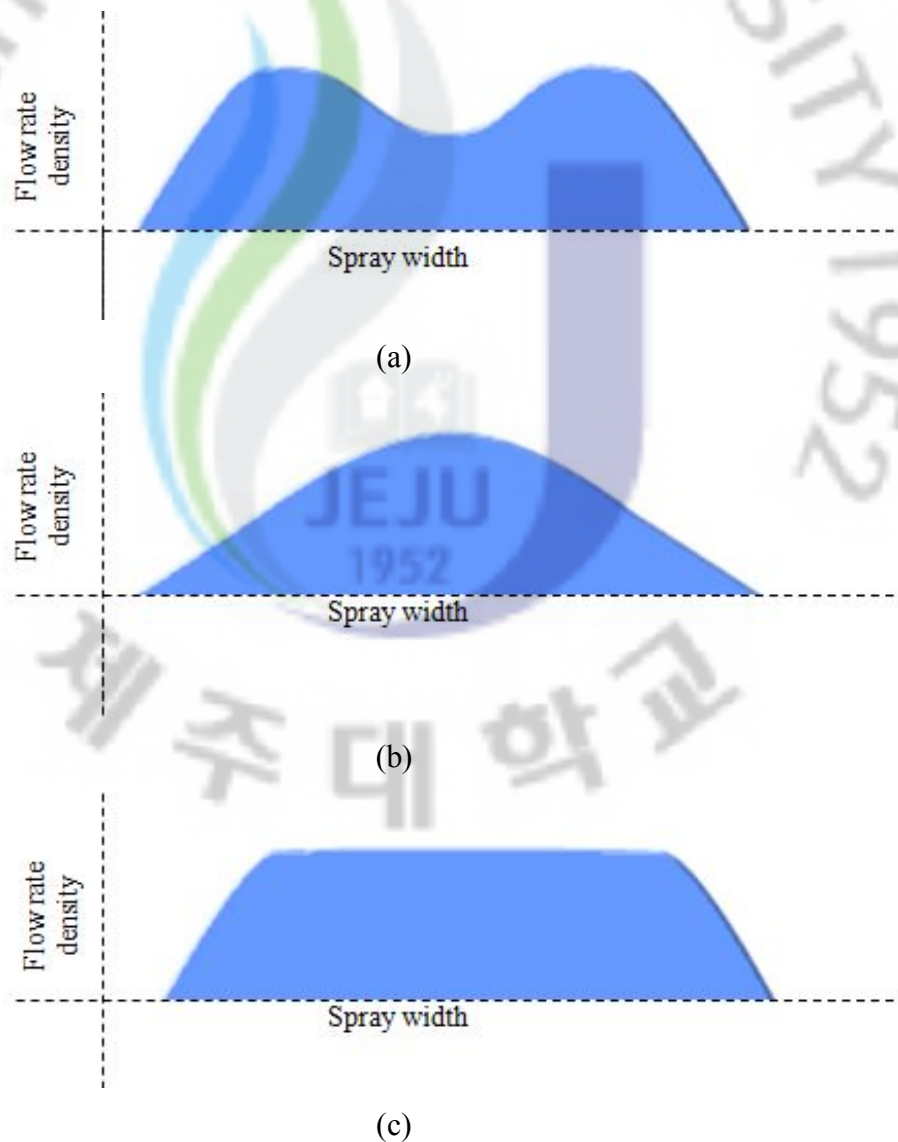


Figure 4.9: Flow distribution (a) concave, (b) convex, and (c) trapezoid

Flow distribution is classified into three types, concave, convex, and trapezoid, with the type of flow distribution varying according to the type of nozzle. Moreover, flow distribution readings vary from manufacturer to manufacturer. Normally, nozzle manufacturers standardize the flow distribution characteristics of their products according to nozzle. Spray distribution also refers to the distribution of the force of the spray as it comes into contact with the target. Spray impact and distribution vary according to a type of nozzle, pressure, flow rate and Fluid. The three type of distribution is given in Figure 4.9.

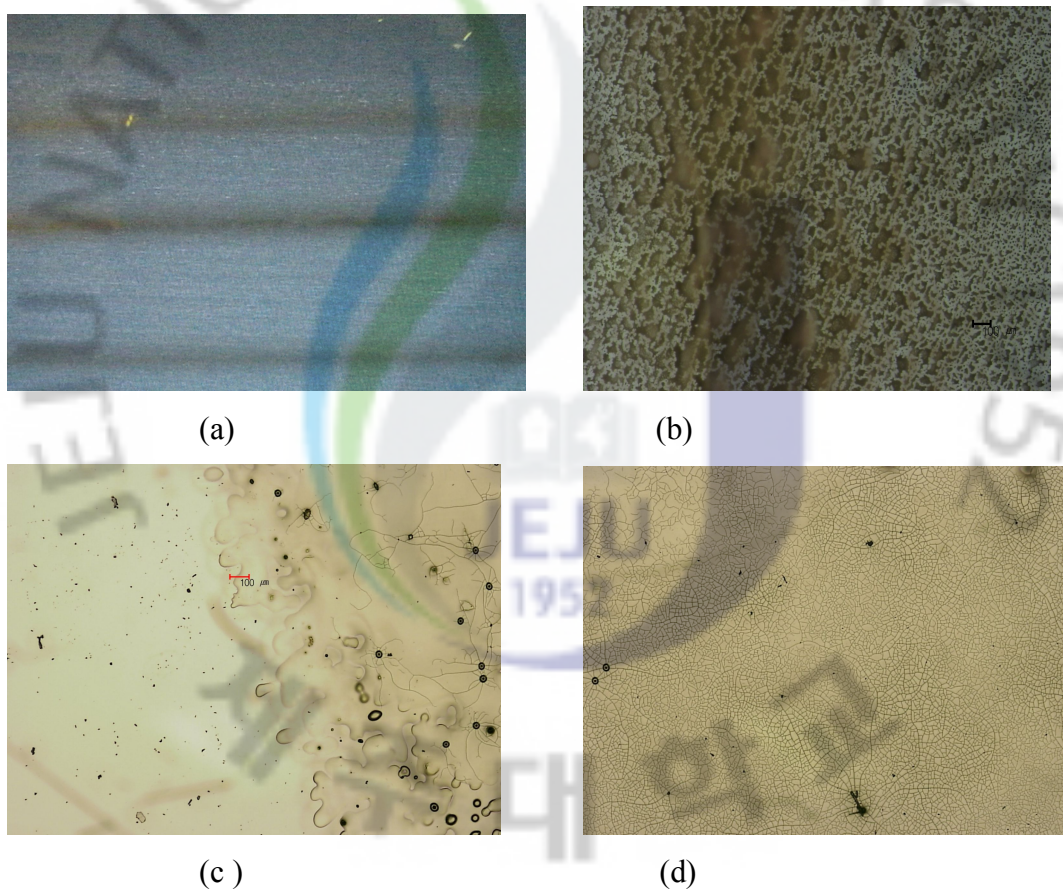
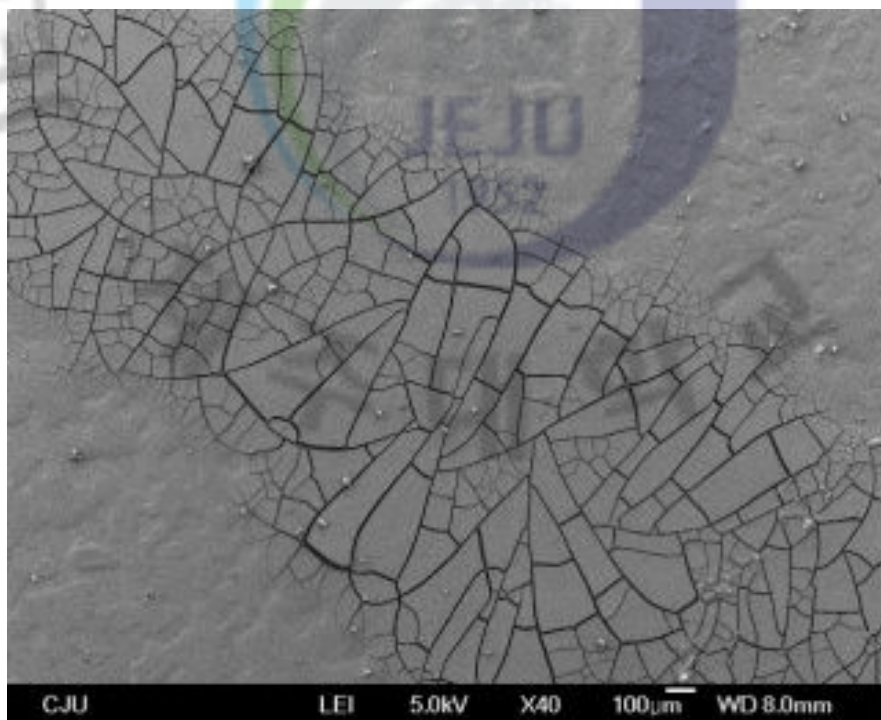


Figure 4.10: (a) Shows the spray image through camera eye (b) shows the spray results of commercially available Ag Ink (c) shows the results of TiO<sub>2</sub> results on edge and (d) shows the results in the center.

For the spray analysis of I-silica head experiments were conducted and results are analyzed on the glass substrate. The counter ground position and silica position is kept on the same parameter on which patterning except the distance of the substrate changed. For spray npk-2 ink and  $\text{TiO}_2$  is used. These experiments are done to analysis the behavior of the head on spray deposition. Figure 4.10 shows the spray results. Figure 4.10 (a) shows the spray image through camera and Figure 4.10 (b) shows the spray results of commercially available Ag Ink. And for further verification of  $\text{TiO}_2$  is used and results are shown in Figure 4.10 (c) and (d). Figure 4.10 (c) shows the results of  $\text{TiO}_2$  results on edge and Figure 4.10 (d) shows the results in the center.

Further in detail characterization and analysis is done to categories the spray on the glass substrate through the nozzle and it's found that by using Ag- conductive ink the spray was found to be convex while with  $\text{TiO}_2$  the spray was found to be more in trapezoid shape on optimal parameters. Figure 4.10 and 4.11 show the microscope image and SEM images of different results.



(a)

(continue)

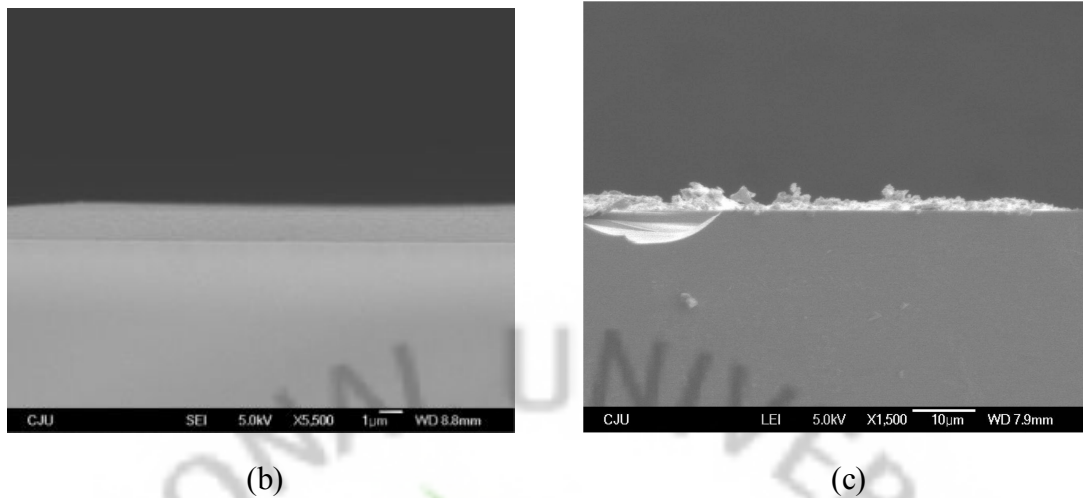


Figure 4.11: (a) Shows the overall SEM image of the TiO<sub>2</sub> layer (b) at center and (c) at side (edge)

#### 4.4 Comparison Analysis

For further analysis of the head, comparison with other existing technologies is performed. This comparison includes the voltage requirement analysis, jetting analysis and printing analysis. The comparison is performed though commercial available Ag ink. For the first case voltage requirement is analyzed. The comparison chart of the three counter electrodes studied in this study is shown in Figure 4.12.

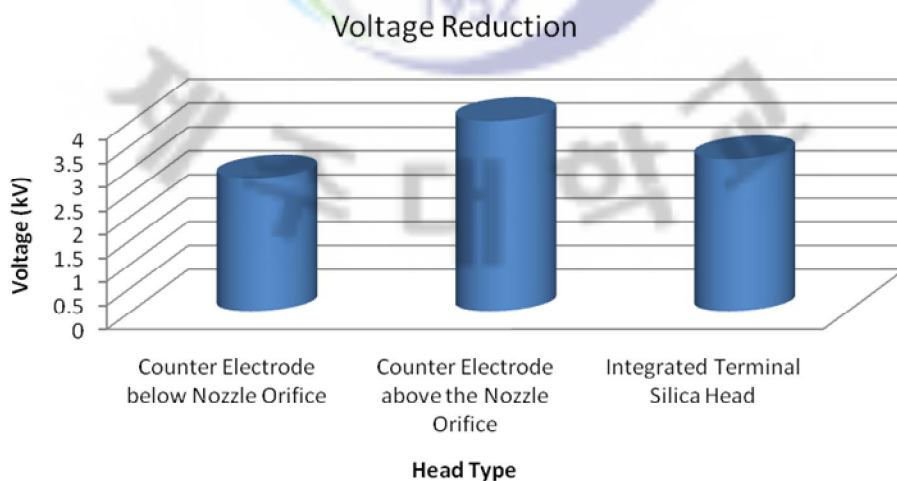


Figure 4.12: Voltage comparison chart

For voltage analysis, it's found that counter electrode below the nozzle orifice can deliver jetting at low potential as compared to the counter electrode above the nozzle. But it's also found that in integrated ground when silica is introduced the potential for producing jet also reduce. It's important to mention here that this jetting analysis in Figure 4.12 is in space. Therefore, for further analysis of printing, head's jetting behavior on glass substrate is studied. For applications for industrial purpose, Printed Electronics and better conductivity of line, stable printing, is very important factor. Therefore, the head is characterized on the basis of printing ability like shadowing effect and resolution. For industrial and Printed Electronics applications use, the trend in printing research is to achieve less shadowing effect and high resolution. Figure 4.13 and Figure 4.14 shows the comparison results of the head. And from the analysis it's found that even less potential is required to generate the jet when counter electrode is down the nozzle but more stable with high resolution results are obtain from the new proposed and optimized design.

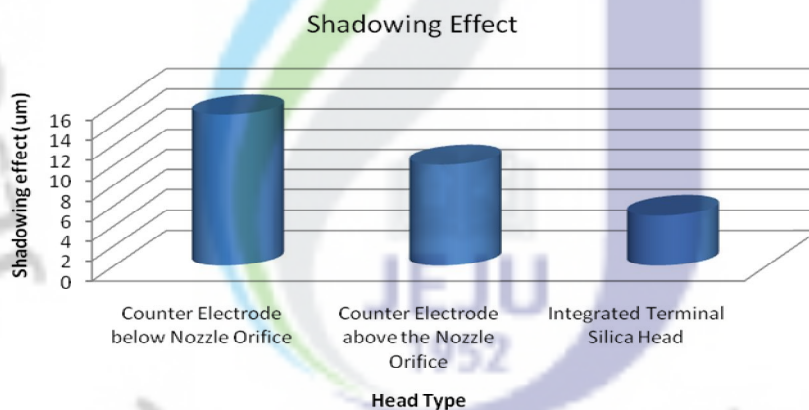


Figure 4.13: Comparison chart of shadowing effect

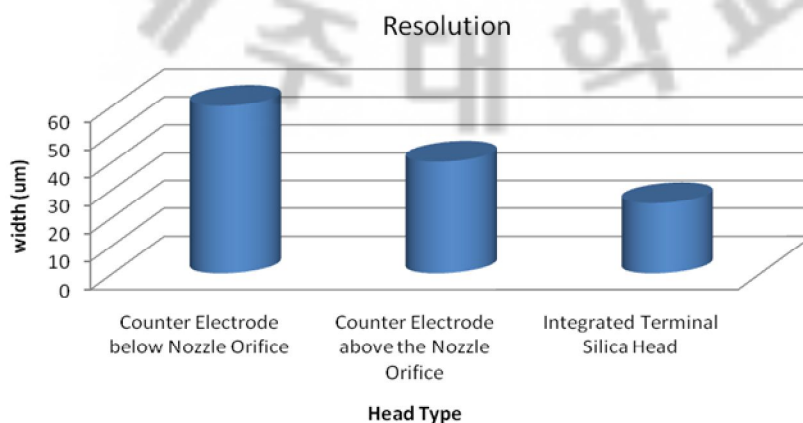


Figure 4.14: Resolution comparison chart

## 5. Literature Review and Fundamentals of Memristor

This chapter reviews fundamentals of Memristors. This chapter also includes different details of Memristors including historical point of view, equations to current state (HP developed) Memristors. And on the basis of literature survey, choose one model for printed Memristors.

### 5.1 Literature Survey

Within the last decade, the nanotechnology and nanodevice evolutions have been dominated by the aggressive scaling in the sub-100nm zone and the related cost-effectiveness of silicon technology. Today top-down nanolithography based approaches are challenged by bottom-up nanotechnology; atomic-scale technologies with nano-to-micro interface technologies and the possible extension of the Moore's law in the 3rd dimension for building systems are ultimate goals of the fabrication research and development. Presently, silicon top-down technology is the single recognized solution for reliable circuits and systems.

Bottom up nanotechnology is a unique opportunity for nanoelectronics to develop and exploit self-assembly approaches, which could offer unrivaled density of functionality beyond lithographic limits. In the this context, the exploration of both organic and inorganic materials, the nanowire and nanotubes growth and self-assembling techniques of these one dimensional structures, the possibility offered by semiconducting or metalized DNA technology and the controlled fabrication and exploitation of 0-dimensional structures (handout technology) are clear identified priority domains. In general, molecular electronic technologies that answer the computation, memory and interconnectivity challenges to build and serve for true scale systems, will be considered as future alternative of silicon CMOS, under the nanoelectronics umbrella.

On top of those, other realistic emerging fabrication techniques and related materials for large area electronics, where the global dimensionality of the system is completely different, such as direct printing techniques and ink-jetting (using

semiconducting and conducting inks based on nanoparticles), with applications in flexible electronics, or enabling advanced concepts as invisible or paint-able electronics, will be considered.

Novel devices and circuit architectures, truly exploiting the new emerging technology are key aspects of nano research because of their impact in all application domains and of the possibility to create unique know-how around the new concepts. While in the digital domain the world-wide research is dominated by the quests for the new quasi-ideal switch and the so-called universal memory (a memory concept that is non-volatile and able to integrate all the microprocessor memory hierarchy, including the slow external drive, on a single dense and high-speed memory platform).

A particularly important category is the bio-inspired devices and circuits; in this direction, priorities will be given to the increase of the local inter-connectivity of individual devices, such as in the neuron-inspired devices case and the processing of the information using principles other than the binary logic (analog or weighted multiple input approaches; neural-inspired circuits, in general). In the case of these architectures, the targeted performance factors will be not primarily related to high speed but rather parallel processing of information at extremely low power and 3D device and circuits architectures.

Universal memory device architectures and related addressing circuits is so far identified as a strategic research direction in micro/nanoelectronics; this is motivated by the fact that all the tera-system applications are requiring today huge amount of memory, as dense as possible and very high-speed. Moreover, today there is no clear winner in the quest for the universal memory; PCM/OUM (phase change/ovonic), FLASH, MRAM (magnetic RAM), FeRAM (Ferroelectric RAM), polymer memories, Millipede, etc., are all competing in an increasing market of non-volatile memories. Flexible electronics and applications in monitoring (security) and the medical field are expected to be supported by the category of flexible and large-area electronics. Ultra-thin film organic and non-organic materials (integrate-able on flexible substrate) with high carrier mobility, low voltage operation, the control of device lifetime and of the drift of characteristics of these devices, their processing



with ultra low temperature budget (less than 200C) and the co-integration of digital, analog, sensing, memory and communications functions on flexible substrates, all are challenges to be addressed in the future. Reliability and fault tolerance of future complex systems built with nanoscale electronic devices cannot be guaranteed using conventional measures, due to fundamental physical limitations such as process variability, excessive leakage, process costs as well as very high power densities. This observation calls for radical action on several fronts in order to ensure the continuity of the nanoelectronic systems integration paradigm.

Memristors are the strong candidate for future memory. In 2008 researchers at Hewlett-Packard announced the physical realization of the "memristor" which was theoretically predicted as a "fourth fundamental circuit element" by Leon Chua in 1971 (L. Chua. 1971). Since that time there have been numerous scientific papers applying the memristor theory to a wide range of thin film materials used for a new type of non-volatile memory called RRAM (resistive random-access memory). It has also been noted that the memristor theory is applicable to explain behavior of biological neurons and some research groups have developed circuit designs exploiting memristors as components of neuromorphic electronics. And also, it has the ability to be manufactured on different substrate and materials.

## **5.2 The Memristor as the Fourth Fundamental Circuit Element**

While the mathematical foundations of the memristor begins with papers published by Leon Chua and Sung Mo Kang in 1971 and 1976, examples of circuit elements having memristive characteristics actually predate the papers of Chua and Kang (1976). One important example is the similarly named "memistor" developed by Prof. Bernard Widrow of Stanford University in 1960 as a component of ADALINE (ADaptive LInear NEuron) (B. Widrow. 1960, Wikipedia). Although Widrow's memistor was a 3-terminal circuit element in contrast to Chua's 2-terminal memristor it shares the feature of storing the history of the voltage (or current) in the form of the electrical resistance. While Prof. Widrow did not develop a mathematical theory to explain the behavior of the memistor it is clear that a memistor is a memristor based on the description in a technical report published in

1961 entitled "Birth, Life, and Death in Microelectronics Systems" (B. Widrow 1961) . The top of page 23 of this report reads:

"Like the transistor, the memristor is a 3-terminal element. The conductance between two of the terminals is controlled by the time integral of the current in the third, rather than its instantaneous value as in the transistor. Reproducible elements have been made which are continuously variable (thousands of possible analog storage levels), and which typically vary in resistance from 100 ohms to 1 ohm, and cover this range in about 10 seconds with several milliamperes of plating current. Adaptation is accomplished by direct current while sensing the neuron logical structure is accomplished nondestructively by passing alternating currents through the arrays of memristor cells."

According to the memristor theory of Chua a memristor can basically be defined by the following coupled equations:

$$v = R(w)i \quad (5.1)$$

$$\frac{dw}{dt} = i \quad (5.2)$$

where  $v$  = voltage,  $i$  = current,  $w$  is a state variable,  $dw/dt$  is the time derivative of  $w$ , and  $R(w)$  is the memristance function.

In the above description of Widrow's memristor the conductance between two terminals is described to be controlled by the time integral of current. This can be expressed mathematically by the coupled equations:

$$i_1 = G(w) v \quad (5.3)$$

$$dw = i_2 dt \quad (5.4)$$

where  $v$  = voltage,  $i_1$  = current from the first to the second terminal,  $i_2$  = current in third terminal,  $w$  is a state variable which is the integral of current, and  $G(w)$  is the conductance which is a function of  $w$ . Given that resistance is the inverse of

conductance (i.e.  $R(w) = 1/G(w)$ ) it follows that the Memristors of Widrow are a 3-terminal equivalent of the memristor.

Thus while Chua and Kang's theory represents the fundamental mathematical basis for memory resistance circuit elements, it may have been inaccurate to characterize the memristor as a missing circuit element by Chua and (more recently) by HP Labs 2008 paper in Nature "The missing memristor found" (D. B. Strukov et al. 2008). More correctly it was the mathematical theory describing the memristor rather than the memristor itself which was missing in 1971. But in this study we will consider only two terminals (Chua memristor).

So, if memristors were physically realized back in 1960 why don't we have any memristor-based electronics today? At least a partial answer to that question can be found in the 1961 report entitled "Birth, Life, and Death in Microelectronics Systems." Page 1 of this report noted that:

"Even more elegant, although speculative, techniques have been proposed in which large numbers of components are formed en masse in thin film patterns on appropriate substrates by evaporative or ion-beam deposition or by electron-beam micromachining."

### **5.2.1 Memristors: Theory and Properties**

At the time of Chua's original paper and the later paper by Chua and Kang the memristor was considered a "fourth fundamental circuit element." The other three fundamental circuit elements are the resistor, the capacitor, and the inductor. The resistance of resistors is defined by a functional relationship between current and voltage. The capacitance of capacitors is defined by the functional relationship between charge and voltage. The inductance of an inductor is defined by the functional relationship between current and flux (the time integral of voltage). The mathematical justification for the existence of the memristor as a fourth fundamental circuit element was based on symmetry with the other three circuit elements in which a fourth functional relationship should exist between the electrical quantities of flux

and charge. Thus the mathematical functional relationship defining the four basic elements is as follows:

$$\text{Resistor : } v = R(i) \quad (5.5)$$

$$\text{Capacitor: } q = C(v) \quad (5.6)$$

$$\text{Inductor: } \phi = L(i) \quad (5.7)$$

$$\text{Memristor: } \phi = M(q) \quad (5.8)$$

where  $v$  = voltage,  $i$  = current,  $q$  = charge,  $\phi$  = flux

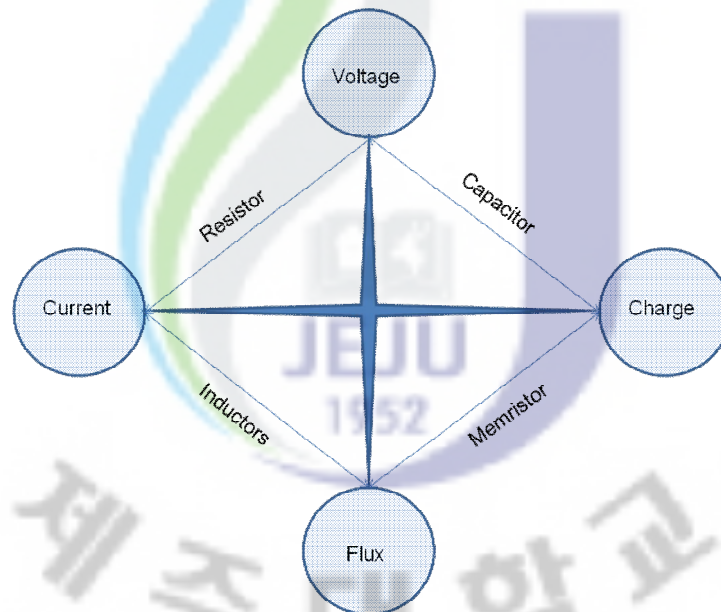


Figure 5.1: Relation between basic fundamental elements

A more recent reason for memristors to be considered as other than a fourth fundamental circuit element results from a recent 2009 publication entitled "Circuit elements with memory: memristors, memcapacitors, and meminductors" (Massimiliano Di Ventra. 2009). This paper generalizes the concept of memristive systems to include memcapacitors and meminductors. Assuming a time-invariant

system the mathematical equations defining memristive, memcapacitive, and meminductive systems are summarized as follows:

$$\text{Memristive system: } v = R(w,i) i \quad \frac{dw}{dt} = m(i,w) \quad (5.9)$$

$$\text{Memcapacitive system: } q = C(w,v) v \quad \frac{dw}{dt} = g(v,w) \quad (5.10)$$

$$\text{Meminductive system: } \phi = L(w,i) i \quad \frac{dw}{dt} = h(i,w) \quad (5.11)$$

where  $w$  is a state variable,  $dw/dt$  is the time derivative of the state variable, and  $m(i,w)$ ,  $g(v,w)$ , and  $h(i,w)$  are continuous functions of the respective variables. It is noted that these equations reduce to that of linear resistors, capacitors, and inductors provided that  $R(w,i) = R(w)$ ,  $C(w,v) = C(w)$ ,  $L(w,i) = L(w)$ , and  $dw/dt = 0$ .

Based on this interpretation it is more reasonable to consider devices having memristive effects as generalizations of the three basic elements of resistors, capacitors, and inductors rather than as a "fourth fundamental circuit element." However, this does not diminish the importance of memristive systems and may make them even more important since they represent a completely new paradigm of electronics which extends all of the basic circuit elements into the realm of dynamic circuit components. Such dynamic circuit components are more analogous to biological components which tend to have variable rather than static system characteristics and may be a critical component to future artificial intelligence systems.

The recent interest in the memristor theory of Chua and Kang was sparked by an article in the journal *Nature* published by researchers at HPLabs in 2008 reporting memristive effects in  $\text{TiO}_2$ . The title of the article was "The missing memristor found" in reflection of the title of Chua's original 1971 paper on the memristor theory which proposed the memristor as a "missing" circuit element. The HP Labs group did recognize that various materials exhibiting memristive characteristics were noted in the literature (see references 2-4 of the HP Labs *Nature*

article). It is also notable that incited work on  $\text{TiO}_2$  was performed in 1967 including substantially similar results (F.Argall. 1967). However, these prior publications did not recognize the connection between their scientific investigation and the theoretical work of Chua and Kang.

What the HP researchers accomplished in their article was to show that the memristor theory could be used to model the resistive switching effects found in a variety of thin film materials. A memristive systems model may be mathematically formulated as:

$$v = R(w) i \quad dw/dt = m(i) \quad (5.12)$$

where  $w$ = state variable,  $v$  = voltage,  $i$  = current,  $R(w)$ =memristance function,  $m(i)$  = rate of change of the state variable.

The HP researchers noted that the state parameter  $w$  could be equated with the ionic distribution within a thin insulative film. In this case the first equation of the memristive system  $v=R(w) i$  may be interpreted as defining the relationship between voltage and electron flow through the thin film at a particular ionic distribution while the second equation  $dw/dt = m(i)$  may be interpreted as defining the relationship between the ionic flow and the electron flow. In this respect I believe the HP researchers are correct. In the Nature paper they determine  $R(w)$  and  $m(i)$  as:

$$R(w) = R_{ON} (w/D) + R_{OFF} (1-w/D) \quad (5.13)$$

$$m(i) = u_v(R_{ON}/D) i \quad (5.14)$$

where  $D$  = the thickness of the thin film,  $u_v$ = the ionic mobility,  $R_{ON}$  = the on resistance,  $R_{OFF}$  = the off resistance.

Now that Hewlett Packard researchers have popularized the memristor theory of Chua and there are solid state examples of materials having memristive characteristics it is possible that neural computer designs similar to that of Bernard Widrow's 1960 memistor will be realized within the next few years. Ironically Moore's law, which has driven semiconductor-based electronics over the past several decades, may be viewed as a brief interruption in the development of memristive-based electronics in the future. DARPA is currently supporting a program called SYNAPSE in which IBM, Hewlett-Packard, and HRL are being funded to create neuromorphic circuitry in which memristive materials may play a role.

One may ask why memristive electronics would have any more effect on artificial intelligence than semiconductor-based microprocessors in which neural networks have been simulated in software. The use of software in artificial neural networks typically is based on a Von Neumann computer architecture which segregates memory storage and data processing. This segregation results in a limit to parallel processing of data which is one reason that pattern recognition and real-time responsiveness is limited in computer and robotic systems in comparison to biological systems. However, memristive systems integrate data storage and data processing capabilities in a single device which offers the potential to more closely emulate the capabilities of biological intelligence.

Of course it is unlikely that the development of memristive-based artificial intelligence or robotics achieving the capabilities of human beings will occur overnight. Since it has taken hundreds of millions of years of evolution to develop human-level intelligence it may take a while for a similar level to occur in autonomous memristive systems which model biological neurons (provided that such modeling was even possible). One way to short-circuit the amount of time necessary may be to use brain-computer interfaces to copy human brain patterns into memristive circuitry. Given the popularity of A.I. driven video games such as The Sims and Second Life and companies such as Emotiv and OCZ Technology, which develop brain-computer interfaces for video game applications, such developments may not be too far in the future.

## 6. EHD Printed Memristor Results and Analysis

Chapter explains the step by step development of Electrohydrodynamically Printed Memristor to authenticate the ability of spray and patterning of the head on glass substrate. Both dielectric ( $\text{TiO}_2$ ) and conductive ink used. This chapter also summarizes different steps needed for the development of the printed device by inkjet including device design, ink fabrication to optimization and analyzing techniques. To authenticate the results, 6 nibble and 2 byte printed memories are also developed.

### 6.1 Electrohydrodynamically Printed Memristor

After having necessary and excessive background research, first Electrohydrodynamically printed memristor device is developed. The device was printed after processing different steps. The step by step description of fabrication of printed memristor is given below:

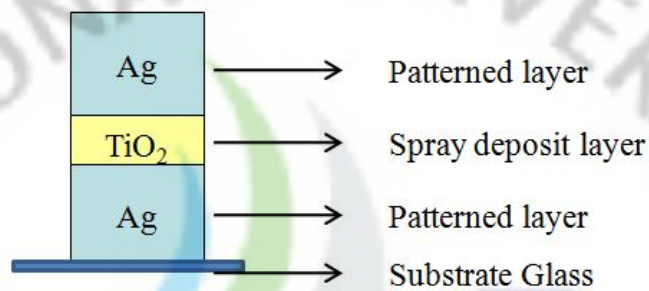
#### 6.1.1 Device Design

Memristor is a (minimum) three layer device. Firstly, a conductive layer is patterned on the substrate. Then for second layer oxide is deposit on the surface of the first patterned line. And then thirdly for last layer (in case of simple memristor), again conductive layer is deposit on the surface of the oxide layer, in such a way that deposit layer become sandwich between the two layers. For this study Ag-  $\text{TiO}_2$ - Ag will be used. The deposition mechanism is summarized in Table 6-1. Figure 6.1 (a) shows the single layer Memristors and Figure 6.1 (b) shows the printed structure of single layer memristors. This structure can be enhanced to multiple stack memory as shown in Figure 6.2. But in this study the single layer memristor will only be undertaken.

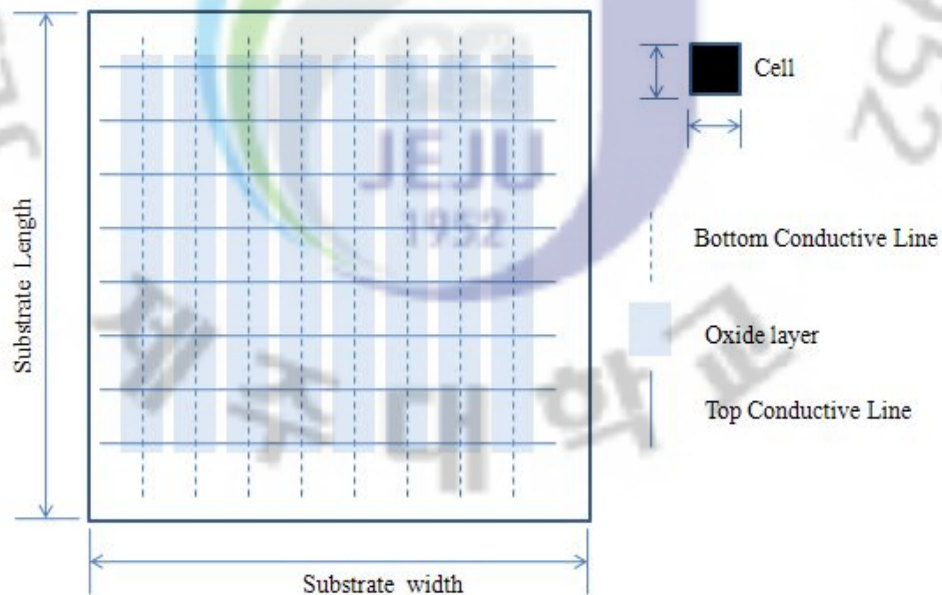


Table 6-1: Material and deposition mechanism for Memristor

S/n	Layer	Material	Procedure
1	Conductive	Ag	Patterning
2	Oxide	TiO <sub>2</sub>	Spray deposit
3	Conductive	Ag	Patterning



(a)



(b)

Figure 6.1: Single layer Memristors (a) the layer by layer configuration (b) device design on glass substrate

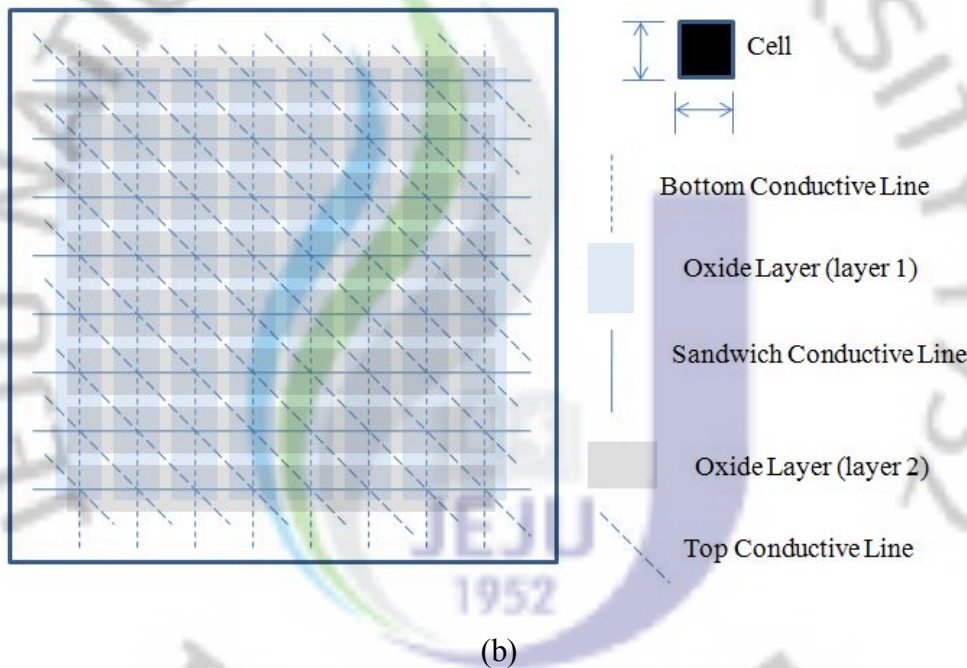
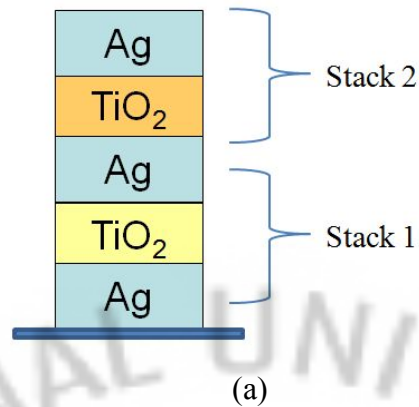


Figure 6.2: Multiple layer multiple stack memory (a) layer by layer (b) device design on glass substrate

### 6.1.2 Ink Status and Optimization for Electrohydrodynamics

Different materials combinations and different ways for the fabrication of memristors are under investigation. Here in research all inkjet printed memristor is fabricated and characterized. The memristors is printed by using electrohydrodynamic (EHD) head on glass substrate. The device is fabricated by using non contact nature of EHD head. The fabrication purpose silver-  $\text{TiO}_2$  -silver

combination is used. Nano particle based silver ink is used as the conductive connector to sandwich the TiO<sub>2</sub> layer. For silver ink, commercial available solution is used. And TiO<sub>2</sub> solution is developed in lab by using the sol gel technique and optimized for electrostatic inkjet from paper (Jin Young Kim et al. 2006). Different stages of ink are shown in the Figure 6.3.



Figure 6.3: TiO<sub>2</sub> synthesis process

### 6.1.3 Analysis of Ink Behavior on Substrate

For measuring surface and interfacial tension, herein pendant drop method is used. A proprietary edge tracing technology is employed to precisely capture and analyze the drop dimensions and profile characteristics in order to accurately calculate the surface tension of a liquid using the Young-Laplace equation as shown in Figure 6.4 (a) where  $D_s$ ,  $D_e$  showing upper and lower line lengths respectively. For the analysis the properties of the inks on substrate, contact angle is used. From contact angle system, surface tension of the used inks are also evaluated. It is found that surface tension of the TiO<sub>2</sub> is 161 mN/m as shown in Figure 6.4 (b). Moreover, conductivity of the ink is also measured and it is found out to be 95  $\mu$ S/m at 19 °C.

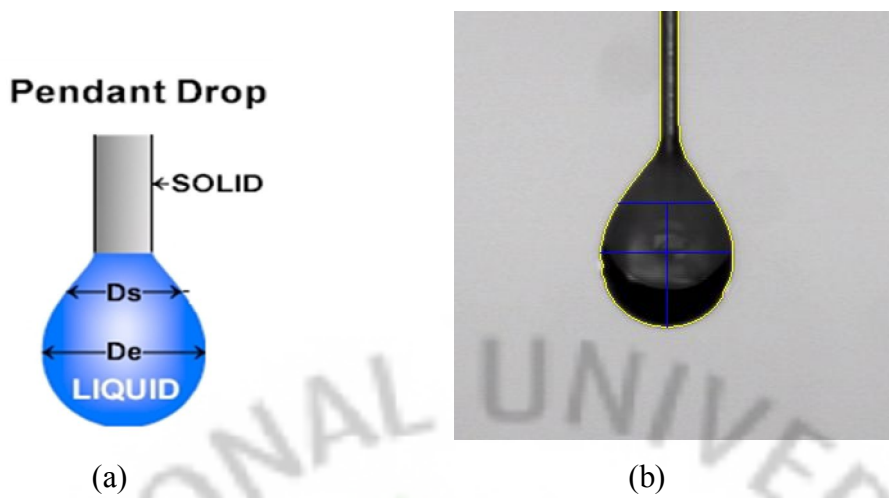


Figure 6.4: (a) Measuring technique used (b) measuring of surface tension of  $\text{TiO}_2$  through contact angle system

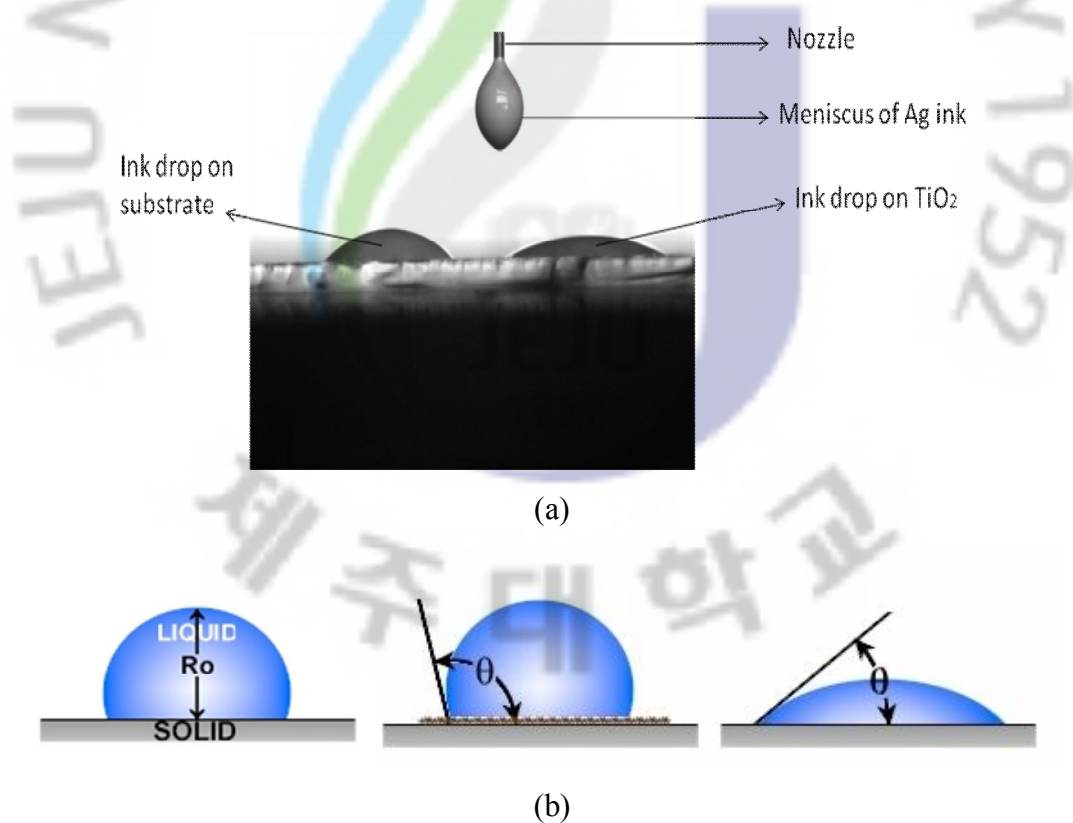
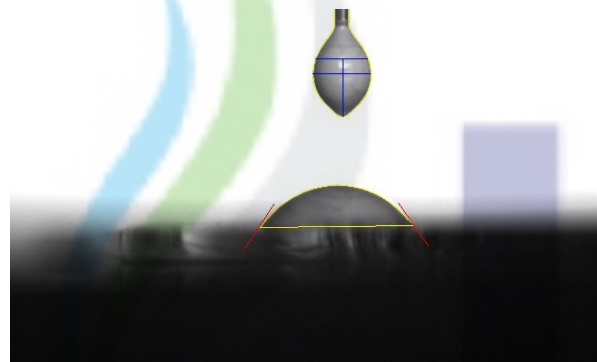
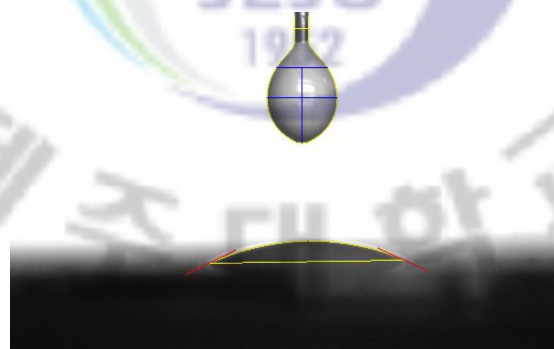


Figure 6.5: (a) Behavior of Ag ink on the glass and  $\text{TiO}_2$  deposit layer (b) showing the schematic diagram of the contact angle

Printing mechanism for device design by using ink (inkjet or printing mechanism) has inherent disadvantages like smooth layering and surfacing morphology. As we already know memristor is a (minimum) three layer device. Thus, herein, the contact angle of the patterned line on glass substrate and deposit layer (of  $\text{TiO}_2$ ) is analyzed. This will also help to analysis the area and cross-section each memory cell. Experiments were done to analysis the behavior of Ag ink's pendant and sessile behavior. Figure 6.6 (a) and (b) summarize the effects of Ag ink on glass substrate and the effects of Ag ink on  $\text{TiO}_2$  deposit on glass layer, respectively. All values are tested at 20 degree C. And Table 6-2 summarizes the resultant values.



(a)



(b)

Figure 6.6: (a) Behavior of Ag ink on the glass and (b) behavior of Ag ink on the  $\text{TiO}_2$  deposit layer

Table 6-2: Contact Angle measurements of Ag ink on glass and spray deposit  $\text{TiO}_2$

glass

S/n	Properties	Values of Ag ink on glass	Values of Ag ink on spray deposit TiO <sub>2</sub> layer
1	Contact Angle(Average)[degree]	56.4274868	23.564180
2	Left Angle[degree]	56.4274868	23.564180
3	Right Angle[degree]	56.4274868	23.564180
4	Height from Top to Base[mm]	0.906400	0.4429
5	Base Line Length[mm]	3.378651	4.244050
6	Base Area[mm <sup>2</sup> ]	8.965542	14.146560
7	Drop Volume[ul]	4.502207	1.664646
8	Wetting Energy[mN/m]	40.257931	66.729424
9	Spreading Conefficient[mN/m]	32.542080	6.070584
10	Work of Adhesion[mN/m]	113.057899	139.529404

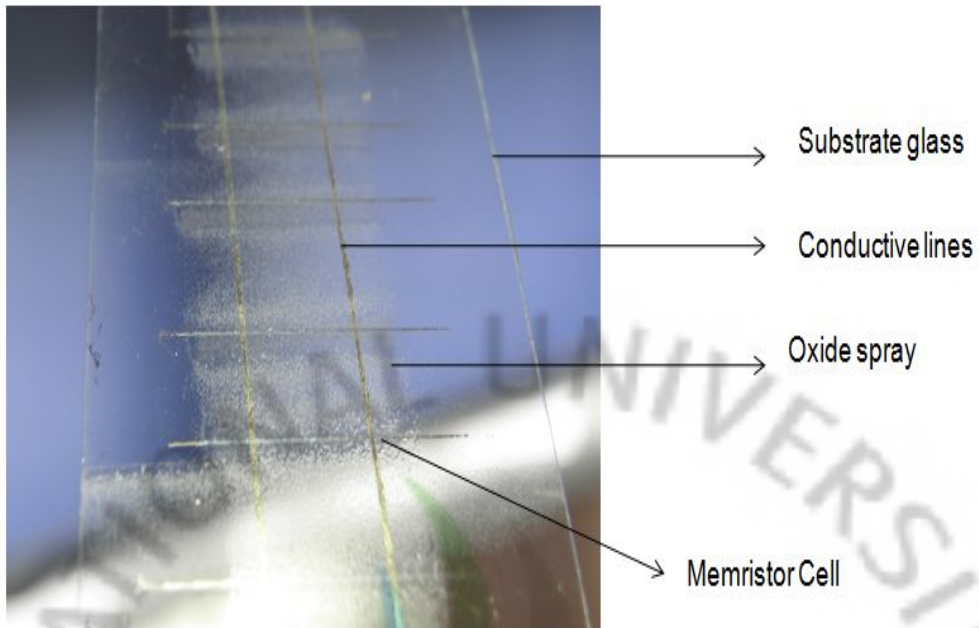
From the experiment it was found that Ag ink behavior was more hydrophobic on the surface of the glass and more hydrophilic on the surface of the TiO<sub>2</sub> layer. This indicates that the line aspect ratio will be more on the surface of the glass as compared to the glass containing TiO<sub>2</sub> layer. Thus, for device fabrication, bottom pattern lines can be patterned close to each other whereas the above cross lines should be patterned at a distance to avoid the conflict and overlapping. This also indicates that each memristor cell (probably) will not be in square shape until a different size nozzle orifice is used for patterning (larger size for bottom conductive line and smaller size nozzle for patterning on oxide layer).

#### 6.1.4 EHD Printed Memristor

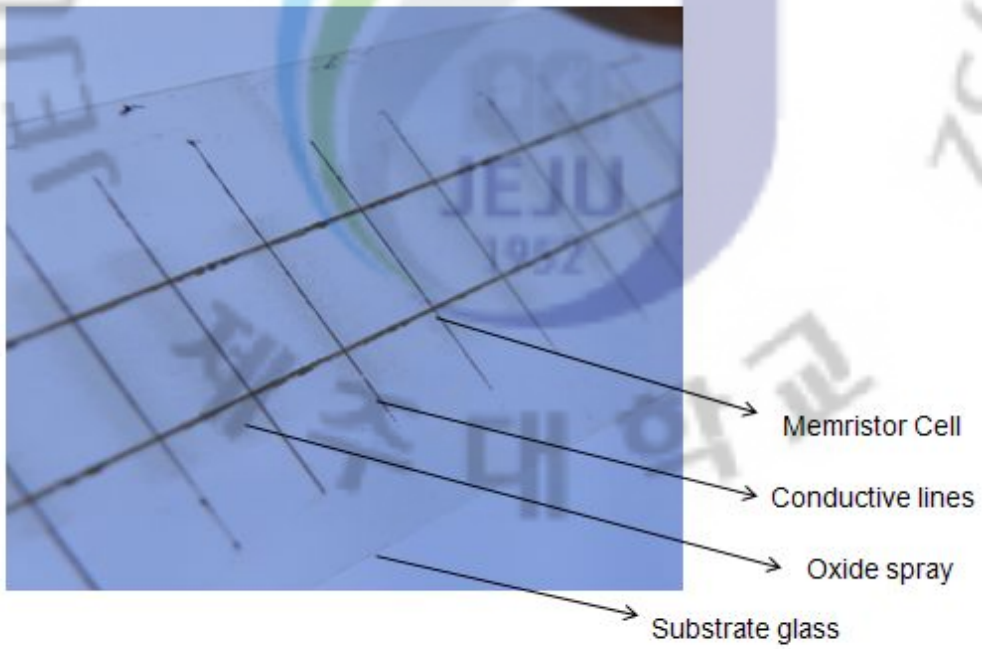
For the developing of the top and bottom conductive pattern of nano colloidal solution of Ag ink is used. The reason of using Ag ink is twofold: one reason is that Ag is more stable to oxides and secondly, Ag as ink is more stable than many of the other available conductors for electrostatic printing. For the oxide layer between two conductors TiO<sub>2</sub> is used. Glass is being used as substrate. Table 6-3 summarizes the values different steps used for the fabrication of the memristors. The steps can be summarized as: For the printing firstly, a conductive layer of Ag is deposit on the surface of the glass substrate. Then TiO<sub>2</sub> is electro-sprayed on the surface of glass and left for one hour for hydrolysis. And after that another layer of the Ag is deposit for making the top contact on the surface of the layer. The final results are shown in Figure 6.7. Figure 6.7 (b) shows 2 byte memory cells and Figure 6.7 (c) showing 6 nibble memory. And Figure 6.8 shows the microscope image of the printed cells.

Table 6-3: The general values of the printing materials

s/n	Materials and mechanism	Values and procedure
1	Substrate	Glass
2	Bottom conductor	Colloidal solution of Ag nano particle ink
3	Top conductor	Colloidal solution of Ag nano particle ink
4	Printing mechanism of the lower/bottom conductor	Electrohydrodynamic patterning
5	Printing mechanism of the top conductor	Electrohydrodynamic patterning
6	The oxide material used	Colloidal solution of TiO <sub>2</sub> nano particle ink
7	Oxide deposition mechanism	Electrohydrodynamic spray



(a)



(b)

(continue)



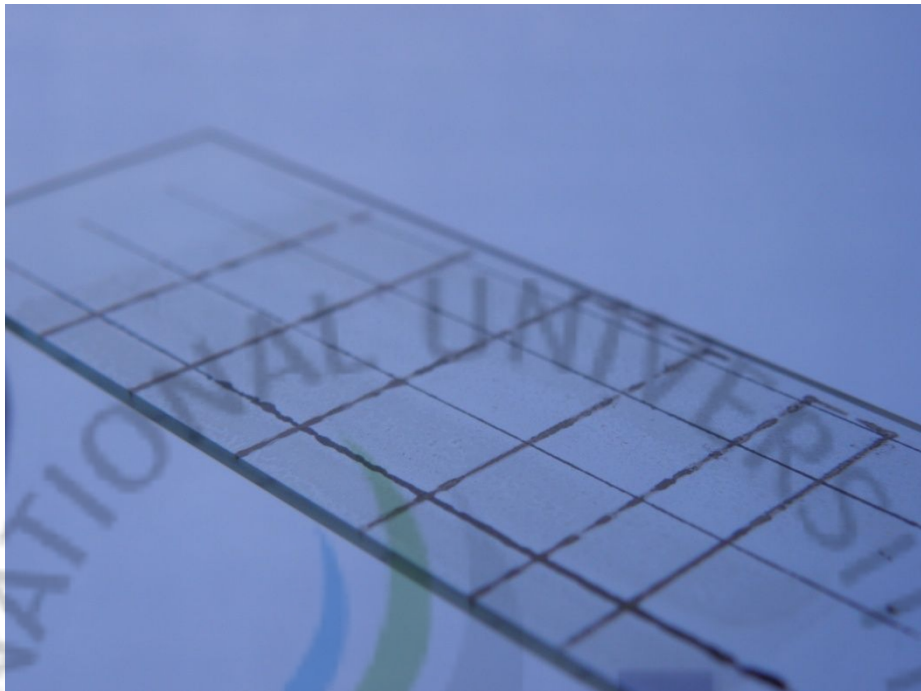
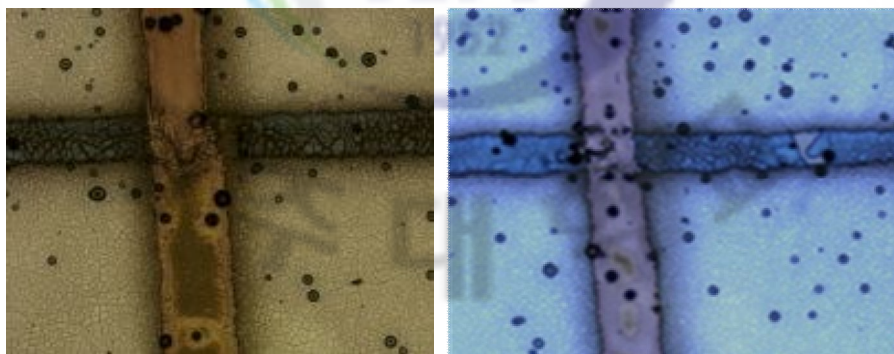


Figure 6.7: (a) Showing the printed memristors by using Electrohydrodynamic technique on glass substrate (b) showing 2 byte memory cells and (c) showing 6 nibble memory.



(a)

(b)

Figure 6.8: Shows microscope image of the printed memristor (a) and (b) shows shows the 40x40 um cell

### 6.1.5 Characterization

In this section, the electronic characterization of the device is studied. Firstly the method and techniques for the characterization of the memristors is summarize. Moreover, here is need to know the parameters we have to find. There are two things which we have to measure one is the current passing through it and second the state of the device. It's a two step process. So here is the technique to characterize the memristors is unfolded: Memristors are dynamic time dependent and highly non linear device (means time should be independent variable). Hence for analyzing IV curve chart, it's important to note the values of voltage versus time and current versus time and then we have to combine both for final IV curve chart. This is very important as both are derivative of time. And moreover, the new state depends upon the old state as it is contains memory (Nadine Gergel-Hackett. 2009). Hence, if old curve tracer is used then it will show oscillation, which drives one to wrong conclusions. A different characterization system is needed for the analysis. Moreover, we have to essentially measure the state of the device by collecting IV characteristics over range of voltage doing non protective base test. Then we have to apply one voltage and measure the state and perform it repeatedly for several voltages. Figure 6.9 shows the schematic diagram of the memristors with applied voltage and ammeter. Figure 6.9(a) shows the cross-sectional and Figure 6.9 (b) shows the characterization techniques printed memristors.

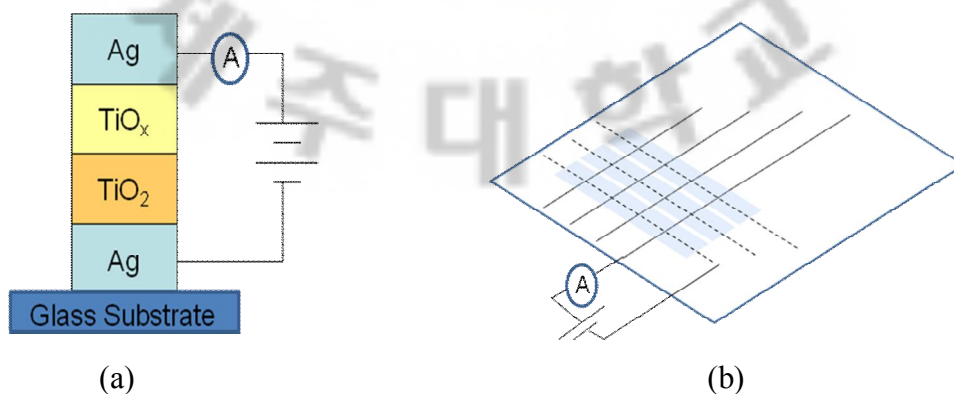


Figure 6.9: (a) Shows the schematic diagram of characterization of the memristors and (b) shows the schematic diagram of the characterization of the printed memristors

Mathematically, both voltage and time are function of time and depends upon the last state as given here:

$$V(t) = M(w, I, t)I(t) \quad (6.15)$$

Therefore, on each result it's important to measure respective voltage and current with same time reference. Thus Figure 6.10 summaries the results after applying the bias voltage. The graph in Figure 6.10 shows errors due to un-availability of precise characterization equipment, therefore some results are extrapolated. The state is a function of pervious state and current and time. So depending upon the pervious state the new state can be predicted. Figure 6.11 shows showing the memory read and write state through pinch hysterical loop. The other properties of the device are summarized in Table 6-4.

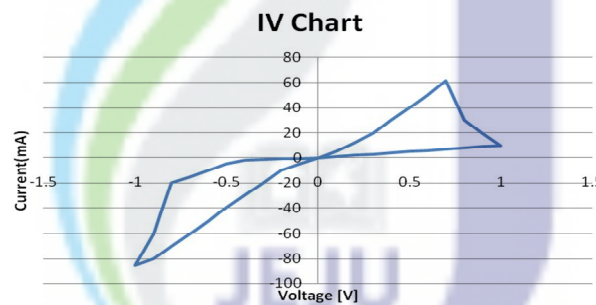


Figure 6.10: Shows pinch hysterical loop

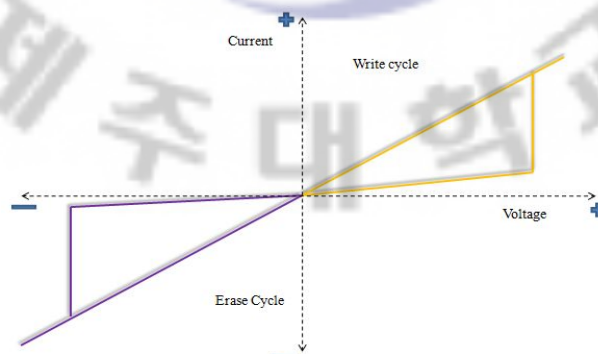


Figure 6.11: Memory write and erase through pinch hysterical loop

Table 6-4: Complete Data-sheet for EHD Printed Memristor

S/n	Properties	Values
Values of Ag ink on glass		
1	Contact Angle(Average)[degree]	56.4274868
2	Left Angle[degree]	56.4274868
3	Right Angle[degree]	56.4274868
4	Height from Top to Base[mm]	0.906400
5	Base Line Length[mm]	3.378651
6	Base Area[mm <sup>2</sup> ]	8.965542
7	Wetting Energy[mN/m]	40.257931
8	Spreading Conefficient[mN/m]	32.542080
9	Work of Adhesion[mN/m]	113.057899
Values of Ag ink on spray deposit TiO <sub>2</sub> layer		
10	Contact Angle(Average)[degree]	23.564180
11	Left Angle[degree]	23.564180
12	Right Angle[degree]	23.564180
13	Height from Top to Base[mm]	0.4429
14	Base Line Length[mm]	4.244050
15	Base Area[mm <sup>2</sup> ]	14.146560
16	Wetting Energy[mN/m]	66.729424
17	Spreading Conefficient[mN/m]	6.070584
18	Work of Adhesion[mN/m]	139.529404
Cell Size		
21	Cell size [um]	~40
Materials		
22	Conductors	Sliver
23	Oxide	TiO <sub>2</sub>
24	Substrate	Glass

## 6.2 Comparison Analysis

In this section, a comparison study related to printed and HP's fabricated Memristors is done. Even it's highly difficult to compare these technologies with each others as one is (HP fabricated Memristors) is made by highly developed technology and the other is (printed Memristors) are in its stage of infancy. The attraction of printing technology for the fabrication of electronics mainly results from the possibility to prepare stacks of micro-structured layers (and thereby thin-film devices) in a much more simple and cost-effective way compared to conventional electronics. Beside this, also the possibility to implement new or improved functionalities (e.g. mechanical flexibility) plays a role. The selection of used printing methods is determined by requirements concerning printed layers, by properties of printed materials as well as economic and technical considerations in terms of printed products. The properties are summarized and shown in the Table 6-5.

Table 6-5: Comparison Analysis

S/n	Properties	Printed Device Values	Conventional Device Values
Cell Size			
1	Cell size [ $\mu\text{m}$ ]	$\sim 40 \times 40$	$5 \times 5$ and $0.05 \times 0.05$
Materials			
4	Conductors	Ag	Pt
5	Oxide	$\text{TiO}_2$	$\text{TiO}_2$
Advantages			
6	Remarks	All Printed, Cost	Faster, Smaller

It's found that in case of printed Memristors long switching times and low integration density is visible due to size ( $40 \times 40 \mu\text{m}$ ) and depositing mechanism. And in the case of HP fabricated Memristors are extremely small (in nanometer scale) which has extremely short switching time and extremely high integration density. The HP Memristor is fabricated conventional substrate while in this case the printing is done on bear glass which also increases the resistance and increase the hoping process due to non uniformity of printing as compared to lithography technique.

Therefore, it's been concluded and quite evident from above discussion that the device fabricated by using conventional electronics is much faster, much smaller and have more integration density than the printed device. But printed device has the intrinsic advantages of cost effectiveness, simplicity and independency of substrate. Moreover, this research will help to transfigure discrete electronics in the world of printed electronics.



## 7. Conclusion

This chapter summarizes the approach, results and overall achievement of the work listed in this manuscript. And at the end of chapter, also list some suggestions and directions for future work.

### 7.1 Concluding Remarks

This dissertation presented a theoretical and experimental study of electrohydrodynamic head design and summarizes an approach for printing conductive and dielectric ink with different aspect ratio for printed electronics and to generate different types of micro and nano electronics structures through experiment and simulation analysis. The main achievements of the manuscript are summarized below:

- For the completion of this research, the design requirements for an electrohydrodynamic inkjet were introduced, based on which several prototypes were fabricated.
- A series of prototypes with various designs was selected to evaluate the effect of geometrical parameters on the performance. The ring counter electrode is kept above the nozzle orifice. Patterning is done by maneuvering contour of electric field in such a way that even with the smaller length of jet, stable printing can be done. This technique also helps to reduce the dependency on substrate.
- For the formation and stabilization of electrohydrodynamics jet printing, a non conductive silica capillary enclosed by metallic capillary is used. The silica capillary is used to control electric double layer distribution and the black flow in liquid meniscus. This also allows ink circulation mechanism to be applied to uncharged particles. The above factors also helped to reduce the potential needed to obtain cone-jet mode and stabilizing the patterning. This factor also helps to decrease surface tension and enabling the system to use high surface tension inks.

- The head is also tested on the glass substrate and a high aspect conductive pattern and nano with equilibrium spray deposition. And to authenticate these results Electrohydrodynamically Memristors are printed.
- Moreover, first time all printed Memristor is developed. Printed Memristors will help to revolutionize discrete electronics in the world of printed electronics.

## 7.2. Future Work

The major recommendation for future work on this study is to reduce the uncertainty involved with the experimental results and to improve the life of the head. The main sources of uncertainty seen in the results are believed to be impurity molecules in the working liquid and microscopic differences existing in the electrode structure. To address the issues, it is worthwhile to consider the following recommendations:

- Although all the electrodes were visually inspected before being tested, but there was no way to detect and control microscopic defects. Those microscopic defects are to be blamed for much of the uncertainty. Batch-fabrication of the electrodes is therefore recommended to lowering the uncertainty.
- The second most important source of uncertainty was the impurity molecules entering the system from outside during liquid charging process, or the impurity molecules detaching from the electrode surface and entering the liquid.
- Another factor responsible for the uncertainty of the results was the gradual degradation of the electrodes. Therefore, its recommend that on different material based electrodes should be tested.
- Memristors are newly developed device, and advance characterization is still in developing stage. Therefore, new techniques should be evaluated for the characterization of this device. Moreover, different materials should be tested for more reliable configuration of the Memristors.



## References

- Ahsan Rahman, Adnan Ali, B. S. Yang, S. Khan, D.S.Kim, Y.H. Doh and K. H. Choi, Analysis of different dripping behavior in electrostatic integrated deposition Inkjet head, at ICMDT 2009, Jeju Island, Korea, June 25-26, 2009. pp 30.
- Ahsan Rahman, Adnan Ali, Khalid Rahman, Hyung Chan Kim, Yang Hoi Doh, D.S.Kim, K. H. Choi, Influence of Electrode Position and Electrostatic Forces on the Generation of Meniscus in Dielectric Ink, J.Jap. Appl. Phys 49 (2010). DOI: 10.1143/JJAP.49.05EC02.
- Ahsan Rahman, J.B. Kho, Y.H. Doh, K. Rahman, A. Rehmani and K. H. Choi: 5th Int. Conf. Adv. Material and Processing, Harbin, 2008.
- Ahsan Rahman, J.B. Ko, K. Rehman, M. A. Ali Rehmani, Y.H. Doh, K.H. Choi, Study of Droplet Generation through Drop on Demand Electrostatic Inkjet for printed Electronics, 1<sup>st</sup> International Conference on R2R Printed Electronics Apr 30-May 2, 2008 in Konkuk University, Seoul, Korea.
- Ahsan Rahman, J.B. Ko, K. Rehman, M. A. Ali Rehmani, Y.H. Doh, K.H. Choi, Study of Droplet Generation through Drop on Demand Electrostatic Inkjet for printed Electronics, 1<sup>st</sup> International Conference on R2R Printed Electronics Apr 30-May 2, 2008 in Konkuk University, Seoul, Korea.
- B.Widrow, An adaptive “Adaline” Neuraon Using chemical “Memistors”, Technical report No 1553-2, Oct 17, 1960
- B.Widrow, W.H. Pierce, J.B. Angell, Birth, Life and Detah in microelectronics systems, Technical Report no. 1552-2/1851-1, 1961
- Bruce R. Munson, Donald F. Young, Theodore H. Okiishi, “Fundamentals of Fluid Mechanics”, John Wiley & Sons, 2002.
- Castellanos, A., 1991, “Coulomb-driven Convection in Electrohydrodynamics,” IEEE Transactions on Electrical Insulations, 26(6): 1201-1215.

- Castellanos, A., 1998, *Electrohydrodynamics*, New York, Springer-Verlag.
- Coatanéa, E., Kantola, V., Kulovesi, J., Lahti, L., Lin, R., & Zavodchikova, M. (2009). Printed Electronics, Now and Future. In Neuvo, Y., & Ylönen, S. (eds.), *Bit Bang – Rays to the Future*. Helsinki University of Technology (TKK), MIDE, Helsinki University Print, Helsinki, Finland, 63-102.
- Crowley, J. M., Wright, G. S., and Chato, J.C., 1990, “Selecting a Working Fluid to Increase the Efficiency and Flow Rate of an EHD Pump,” *IEEE Transactions on Industry Applications*, 26(1): 42-49.
- Crowley, J. M., Wright, G. S., and Chato, J.C., 1990, “Selecting a Working Fluid to Increase the Efficiency and Flow Rate of an EHD Pump,” *IEEE Transactions on Industry Applications*, 26(1): 42-49.
- D. Y. Lee, Y. S. Shin, S. E. Park, T. U. Yu and J. Hwang: *Appl. Phys. Lett.* 90 (2007) 081905.
- D.B. Chrisey: *Science* 289 (2000) 879.
- Darabi, J., 1999, “Micro and Macro Scale Electrohydrodynamic Enhancement of Thin-Film Evaporation,” Ph.D. Dissertation, University of Maryland, College Park, USA
- Dmitri B. Strukov, Gregory S. Snider, Duncan R. Stewart & R. Stanley Williams, The missing memristor found, *Nature*, Vol 453, 2008, doi:10.1038/nature06932
- Esinenco D, Codreanu I, Rebigan R (2006) Design of inkjet printing head, based on electrowetting effect, for printable electronics applications. *International Semiconductor Conference* 2:443–446
- F.Argall, *Switching Phenomena in Titanium Oxide Thin Films*, *Solid-State Electronics Pergamon Press* 1968. Vol. 11, pp. 535-541.

Ford, Martin, *the Lights in the Tunnel: Automation, Accelerating Technology and the Economy of the Future*, Acculant Publishing, 2009, ISBN 978-1448659814.

Gamota D, Brazis P, Kalyanasundaram K & Zhang J (2004) *Printed organic and molecular electronics*. Kluwer Academic Publishers.

H. P. Le, *Progress and trends in ink-jet printing technology*, *Journal of Imaging Science and Technology*, 42(1), JIMTE6; ISSN: 1062-3701, 1998

H.F. Poon: Dr. Thesis, Princeton University, Princeton (2002).

H.-K. Roth et al., *Materialwissenschaft und Werkstofftechnik* 32 (2001) 789.

Haus, H. A., and Melcher J. R., 1998, 6.013 *Electromagnetism*, Chapter 7.7., [http://web.mit.edu/6.013\\_book/www/book.html](http://web.mit.edu/6.013_book/www/book.html).

Hind AM (1935) *An introduction to a history of woodcut*. Houghton Mifflin Co.

IEEE-DEIS-EHD Technical Committee, 2003, "Recommended International Standard for Dimensionless Parameters Used in Electrohydrodynamics," *IEEE Transactions on Dielectrics & Electrical Insulation*, 10(1): 3-6.

J. Heinzl and C. H. Hertz: *Adv. Electron. Electron Phys.* 65 (1985) 91.

J. S. Lee, S.Y. Kim, Y.J. Kim, J. Park, Y. Kim, J. Hwang and Y.J. Kim: *Appl. Phys. Lett.* 93 (2008) 243114.

Jin Young Kim, sun Hee Kim, Hyun-Ho Lee, Kwanghee Lee, Wanli Ma, Xiong Gong and Alan J. Heeger, *New Architecture for high efficiency Polymer Photovoltaic cells using Solution based Titanium Oxide as an optic Spacer*, Doi: 10.1002/adma.200501825

Jun Zeng: *ASME Int. Mech. Engg. Congress & Exposition*, 2009.

K. H. Choi, A. Rahman, J. B. Ko, A. Rehmani, A. Ali, Y. .H. Doh and D. S. Kim: to be published in Int. J. Adv. Manuf. Technol. Int. J. Adv. Manuf. Technol., Volume 48, Issue 1 (2010), Page 165.

Kahng, Andrew B., Scaling : More than Morre's Law, IEEE Circuits and Systems Society IEEE Computer Society, May-June 2010

Khan B (2006) Advances in printed batteris and photovoltaics. Pira International.

Krahenbuhl, F., Bernstein, B., Danikas, M., Densley, J., Kadotani, K., Kahle, M., Kosaki, M., Mitsui, H., Nagao, M., Smit, J, and Tanaka, T., 1994, "Properties of Electrical Insulating Materials at Cryogenic Temperatures: a Literature Review," IEEE Electrical Insulation Magazine, 10(4): 10-22.

Kurzweil, Ray (2005). The Singularity is Near. Penguin Books.

Kyung Hyun Choi & Ahsan Rahman & J. B. Ko & Asif Rehmani & Adnan Ali & Y. H. Doh & D. S. Kim, Development and Ejection Behavior of Different Material Based Electrostatic Inkjet Heads, Int. J. Adv. Manuf. Technol., Volume 48, Issue 1 (2010), Page 165.

L. Chua, Memristor-The missing circuit element, Circuit Theory, IEEE Transactions, 1971, Vol. 18 Issue:5, page(s): 507 – 519, ISSN: 0018-9324

L.O.Chua and Sung Mo Kang, Memristive devices and systems, Proceedings of the IEEE, 1976, Vol. 64 Issue:2, page(s): 209 – 223, ISSN: 0018-9219

Malone, Michael S. Silicon Insider: Welcome to Moore's WarABC News, 27 March 2003

Massimiliano Di Ventra, Yuriy Pershin, and Leon Chua, Circuit elements with memory: memristors, memcapacitors, and meminductors, 2009

Melcher, J. R., 1981, Continuum Electromechanics, Cambridge, Mass., MIT Press.

Melcher, J. R., and Taylor, G. I., 1969, "Electrohydrodynamics: A Review of the Role of Interfacial Shear Stresses," Annual Review of Fluid Mechanics, 1: 111-146.

Nadine Gergel-Hackett, Behrang Hamadani, Barbara Dunlap, John Suehle, Curt Richter, Christina Hacker and David Gundlach. "Flexible Solution-Processed Memristor", IEEE Electron Device Letters, Vol. 30, No. 7, July 2009

Ohadi, M.M., Darabi, J., and Roget, B., 2001, "Electrode Design, Fabrication, and Materials Science for EHD-Enhanced Heat and Mass Transport," Annual Review of Heat Transfer, 11: 563-623.

Panofsky W. K. H., and Phillips, M., 1962, Classical Electricity and Magnetism, Addison-Wesley Publishing Company.

Parisa Foroughi, "Design and characterization of an electrohydrodynamic (ehd) micropump for cryogenic spot cooling applications", ph.d. Dissertation, 2008

R. J. Melcher, "Continuum Electromechanics", MIT Press, Cambridge, 1981.

Rao. R. Tummala, Moore's Law Meets its Match, in IEEE spectrum, June 2006

Ray Kurzweil (2001-03-07). The Law of Accelerating Returns. KurzweilAI.net. Retrieved 2006-06-24.

Schmidt, W. F., 1997, Liquid State Electronics of Insulating Liquids, New York, CRC Press.

Shooshtari, A., 2004, "Experimental and Computational Analysis of an Electrohydrodynamic Mesopump for Spot Cooling Applications," Ph.D. Dissertation, University of Maryland, College Park, USA.

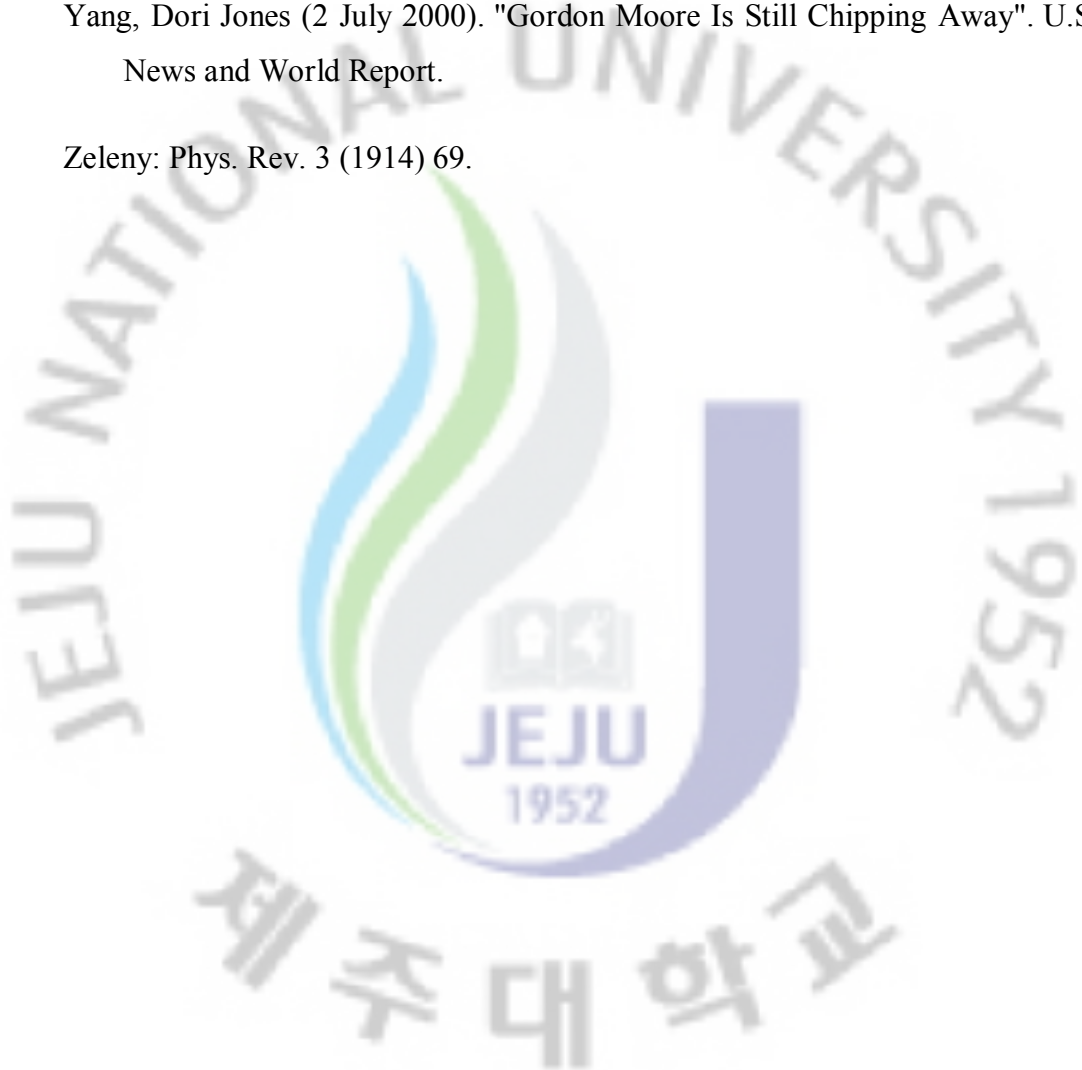
Stratton, J. A., 1941, Electromagnetic Theory, New York, London, McGraw-Hill Book Company, Inc.

Taylor: Proc. R. Soc. London, Ser. A 280 (1964) 383.

Wikipedia

Yang, Dori Jones (2 July 2000). "Gordon Moore Is Still Chipping Away". U.S. News and World Report.

Zeleny: Phys. Rev. 3 (1914) 69.



# Curriculum Vitae

Ahsan Rahman

Date of birth: August 08, 1981

Place of birth: Lahore, Pakistan

## Education:

- Mar 08 ~ Dec 2010     **Jeju National University**     *Jeju, Korea*  
Ph.D., College of Engineering, School of Mechanical and System Engineering  
Course work: CGPA 4.21/4.30.  
Thesis area/topic: Development of Non-Contact Universal Platform Printing Technology for Micro-Electronics Structures
- Aug 04 ~ Aug 07     **Air University**     *Islamabad, Pakistan*  
M.S. (with major in Electronics & Control), Faculty of Engineering, Department of Mechatronics Engineering  
Course work: CGPA 3.86/4.00 with distinction (Silver Medal)  
Thesis: Vibration Control of Large Scale Flexible Structures at Excitation
- Mar 99 ~ Mar 04     **Quaid-e-Awam University of Engineering, Sciences and Technology (QUEST)**     *Nawabshah, Pakistan*  
Bachelor of Engineering(B.E), Department of Computer System Engineering  
Course work: 89.03% with distinction (2<sup>nd</sup> Position)  
Thesis: System Designing for Engendering & Transformation of Stem Cell.

**Patents:** Total- 4; Register-1; Pending -3

1. (Granted) “Multi Array integrated electrostatic inkjet mechanism”, Registration number 10-2009-0047644.
2. (Pending) “Electrostatic inkjet system with ink circulation mechanism”.
3. (Pending) “Meniscus less electrostatic integrated inkjet system with ink circulation mechanism”.
4. (Pending) “Patterning through cone jet by maneuvering contour of electric field in integrated electrostatic inkjet head”.

**Articles:** “Drop on demand electrostatic inkjet system for printed electronics”, K.H. Choi, Ahsan Rahman, J.B.Ko, D.S. Kim at R2R printing process technology published by KIMM.

**Publications List and Status:**

**Refereed Articles: Total-8; In Progress-2, Published-6**

**In Progress:**

1. (Under review) “Electrostatic Deposition Mechanism Of Particle And Non-Particle Solution Containing Nano Silver Conductive Pigments For Printed Electronics”, Ahsan Rahman, Adnan Ali, Khalid Rahman, Y.H. Doh, D.S. Kim, K.H. Choi at The Journal of Electrostatic 2010.
2. (Accepted) “Direct Patterning and Electrospray Deposition through EHD for fabrication of Printed Thin Film Transistors” by Saleem Khan, Yang Hoi Doh, Arshad Khan, Ahsan Rahman, Kyung Hyun Choi and Dong Soo Kim in current Applied Physics



**Published:**

3. “Electrode Configuration Effects on Electrification and Voltage Variation in Electrostatic Inkjet Printing Head”, K.H. Choi, Adnan Ali, Ahsan Rahman, Nauman Malik Mohammad, D.S.Kim at J. MICROMECH MICROENG 2010.
4. “Influence of Electrode Position and Electrostatic Forces on the Generation of Meniscus in Dielectric Ink”, Ahsan Rahman, Adnan Ali, Khalid Rahman, Hyung Chan Kim, Yang Hoi Doh, D.S.Kim, K. H. Choi, at J.Jap. Appl. Phys 49 (2010).
5. “Printed Patterns Adhesion dependency on Contact Angle of Ink on Substrate”, Adnan Ali, Ahsan Rahman, Khalid Rahman, Nauman Malik Muhammad, Arshad Khan, J.B. Ko, Saleem Khan, B.S. Yang, H.C.Kim, Y.H. Doh, D.S. Kim, K.H. Choi at IJET-IJENS, Vol. 10 No. 01, 2010, pp 95~100.
6. “Drop on Demand Non-contact Hydrophilic Electrostatic Deposition Head”, Ahsan Rahman, J.B. Ko, Adnan Ali, Saleem Khan, Khalid Rahman, B.S. Yang, H.C.Kim, Y.H. Doh, D.S. Kim, K.H. Choi at IJET-IJENS, Vol. 10 No. 01, 2010, pp 61~69.
7. “Development and Ejection Behavior of Different Material Based Electrostatic Inkjet Heads”, Kyung H Choi, Ahsan Rahman, J B Kho, Asif Rehmani, Adnan Ali, Y H Doh, D.S. Kim, at Int. J. Adv. Manuf. Technol., Volume 48, Issue 1 (2010), Page 165.
8. “Anticipation and Avoidance of Electro-Spray in the Printed Conductive Lines Using Electrostatic Inkjet Head with Conductive Ink”, Ahsan Rahman, J.B. Ko, Khalid Rehman, M. Asif Ali Rehmani, H.C. Kim, B.S. Yang, Adnan Ali, S.J. Kim, Y.H. Doh, K.H. Choi, Inst. Adv. Tech. jour., Vol. 19, pp65~72, 2008.

### Conferences:

1. “Meniscus Control and Optimization of Electrodes in Electro-Staticly Driven Integrated Inkjet Head “, Ahsan Rahman, Adnan Ali, Khalid Rahman, Yang-Hoi Doh, Dong-Soo Kim and Kyung-Hyun Choi at Mechatronics 2010, June 28 – 30, Swiss Federal Institute of Technology ETH, Zurich, Switzerland.
2. “Analysis of meniscus less electrohydrodynamics-patterning of metallic ink through standard tapered tip needle”, K.H. Choi, Ahsan Rahman, Saleem khan, H.C. Kim, J.B. Ko, Yang-Hoi Doh and Dong-Soo Kim at Proceeding of Korean society of Precision Engineering , May 27, 2010, pp 591.
3. “Comparison and analysis of patterning based on different ground configurations for polyimide substrate”, Saleem Khan, Ahsan Rahman, Adnan Ali, Arshad Khan, H.C. Kim, J.B. Ko, Y.H Doh, D. S. Kim, K.H Choi at Proceeding of Korean society of Mechanical Engineers, April 22, 2010.pp 192-193.
4. “Development and analysis of inkjet printing head by introducing Ring shaped electrode”, Adnan Ali, Khalid Rahmani, Ahsan Rahman, Arshad Khan, H.C. Kim, J.B. Ko, Saleem Khan, Y.H Doh, D. S. Kim, K.H Choi at Proceeding of Korean society of Mechanical Engineers, April 22, 2010.pp 194-195.
5. “Analysis Of Ink Droplet On Substrate And Its Effect On Printed Patterns”, Kyung Hyun Choi, Adnan Ali, Ahsan Rahman, B.S. Yang, D.S.Kim at International conference on flexible and printed electronics, November 11 to 13, 2009, Jeju, Korea.
6. “Influence of Electrode Position and Electrostatic Forces on the Generation of Meniscus in Dielectric Ink”, Kyung Hyun Choi, Ahsan Rahman, Adnan Ali, Khalid Rahman, Hyung Chan Kim,

Yang Hoi Doh, D.S.Kim at International conference on flexible and printed electronics, November 11 to 13, 2009, Jeju, Korea.

7. "Printed Patterns Life dependency on Contact Angle of Ink on Substrate", Adnan Ali, Ahsan Rahman, Saleem Khan and K. H. Choi, at Proceeding of Korean society of Precision Engineering, October 28, 2009. pp 753-754.
8. "Analysis of the Effect of Different Ground Hole Size on Stable Meniscus in Electrostatic Integrated Deposition Inkjet Head", K. H. Choi, Ahsan Rahman, Adnan Ali, B. S. Yang, D.S.Kim, Y.H. Doh at 2009 IEEE International Symposium on Assembly and Manufacturing (IEEE ISAM 2009) in Seoul, Korea, November 17 - 20, 2009. pp 159-164.
9. "Analysis and design of Electrostatic inkjet System", K. Rahman, Ahsan Rahman, Adnan Ali, Saleem Khan, J.B. Ko, Bong Su, Y.H. Doh and Kyung Hyun Choi at LOPE-C, May 4, 2009.
10. "Analysis of different dripping behavior in electrostatic integrated deposition Inkjet head", Ahsan Rahman, A. Ali, B. S. Yang, S. Khan, N.N. Han, Y.H. Doh and K. H. Choi, at ICMDT2009, Jeju Island, Korea, June 25-26, 2009. pp 30.
11. "Drop on Demand Analysis of Electrostatic Inkjet Considering Ground Position Effects" Ahsan Rahman, B. S. Yang, Adnan Ali, Y.H. Doh and K. H. Choi at Proceeding of Korean society of Precision Engineering, April 30, 2009.
12. "Interface Attach-ability Analysis of Printed Patterns through Electrostatic Inkjet System ", Adnan Ali, Ahsan Rahman, Kyung Hyun Choi, at 4th International Conference on Advanced Research in Virtual and Rapid Prototyping, Leiria, Portugal 6th-10th October 2009. pp 377-380.

13. "Effect Of Flow Rate In The Generation Of Printed Line In Electrostatic Inkjet System", Ahsan Rahman, J.B. Kho, Khalid Rahman, M. Asif Ali Rehmani, Y.H. Doh and Kyung Hyun Choi, at Proceeding of Korean Society of Manufacturing Process Engineers Autumn Conference 2008. pp 272-276.
14. "Fabrication of Non-MEMS based Electrostatic Nozzle Design For Electrostatic Inkjet System", Ahsan Rahman, J.B. Ko, K. Rahman, M. A. Ali Rehmani, K.H. Choi, D.S. Kim, Y.H. Doh, at Proceeding of Korean society of Precision Engineering, Nov 12-14, 2008. pp 729-730.
15. "Effect of Electrostatic Stricture On The Droplet Generation By Drop On Demand Electrostatic Inkjet System", Ahsan Rahman, J.B. Ko, Khalid Rahman, M. Asif Ali Rehmani, Y.H. Doh and Kyung Hyun Choi at 1st International Symposium on Hybrid Materials and Processing (HyMaP), Oct 27-29, 2008.
16. "Droplet Generation Process In Conductive Ink Under The Influence Of Electrostatic Forces", Ahsan Rahman, J.B. Kho, Y.H. Doh, Khalid Rehman, M. Asif Ali Rehmani And Kyung Hyun Choi, at 5th International Conference on Advanced Materials and Processing (ICAMP-5) Harbin, China, Sep 2-5, 2008. pp 399.
17. "Study of Inkjet Printing Process for printed electronics", J.B. Ko, Ahsan Rahman, K. Rehman, S.J. Kim, D.S. Kim, K.H. Choi, Y.H. Doh at Korean society for Precision Engineering. Cheju, Korea. pp: 959~960.
18. "Fabrication And Design Of Hybrid Printed Electronics", Ahsan Rahman, J.B. Ko, K. Rehman, M. A. Ali Rehmani, Y.H. Doh, K.H. Choi at The 10th Joint Symposium of Cheju National University and Nagasaki University on Science and Technology, at Cheju National university, Korea, June4-6, 2008. pp: 52~55.

19. "Simulation and experimental verification of Electrostatic behavior of Drop on Demand Inkjet system for Printing Electronics", Ahsan Rahman, J.B. Ko , K. Rehman, Su-Jin Kim, Hyung-Chan Kim, Kyung-Hyun Choi, Yang-Hoi Doh, at Materials Research Society of Korea, Seoul, Korea.
20. "Study of Droplet Generation through Drop on Demand Electrostatic Inkjet for printed Electronics", Ahsan Rahman, J.B. Ko, K. Rehman, M. A. Ali Rehmani, Y.H. Doh, K.H. Choi at 1<sup>st</sup> International Conference on R2R Printed Electronics Apr 30-May 2, 2008 in Konkuk University, Seoul, Korea.
21. "PID Based Controller for High Rise Buildings under Earthquake Excitation", Ahsan Rahman and L.A. Khan, International Conference on Advance Sciences and Technology (IBCAST), Islamabad, Pakistan, January 2007.
22. "Effect of Force on Finite Element in Vivo Skin Model", Ahsan Rahman and Dr. Umar Hayat Khan, in the Second International conference on Emerging Technologies, Peshawar, Pakistan, November 2006, pp 727-734.
23. "Cultivation & Transformation of Stem cell stem into the body through Embedded System Design / Virtual Vivacity", Ahsan Rahman, NIE-Seminar/ES/04; of IEE (UK), Pakistan Chapter; on Embedded System held at the National Institute of Electronics, Islamabad, Pakistan, November 2005, pp 45-52.